ENERGY DISSIPATION IN EIGHTEEN-FOOT BROKEN-BACK CULVERTS USING LABORATORY MODELS

FINAL REPORT ~ FHWA-OK-12-05

ODOT SP&R ITEM NUMBER 2234

Submitted to:
John R. Bowman, P.E.
Planning & Research Division Engineer
Oklahoma Department of Transportation

Submitted by:
Avdhesh K. Tyagi, Ph.D., P.E.
Principal Investigator
Abdelfatah Ali
Nicholas Johnson
Mariazel Rios Motte
Taylor Davis
Graduate Research Associates
Oklahoma Infrastructure Consortium
School of Civil and Environmental Engineering
Oklahoma State University
Stillwater, OK 74078

September 2012

TECHNICAL REPORT DOCUMENTATION PAGE

REPORT NO. FHWA-OK-12-05	2.GOVERNMENT ACCESSION NO.	3. RECIPIENTS CATALOG NO.
4. TITLE AND SUBTITLE ENERGY DISSIPATION IN EIGHTEEN-FOOT BROKEN-BACK CULVERTS USING LABORATORY MODELS		5. REPORT DATE September 2012 6. PERFORMING ORGANIZATION CODE
7. AUTHOR(S): Avdhesh Tyagi, Ph.D., P.E., Abdelfatah Ali, Nicholas Johnson, Mariazel Rios Motte, and Taylor Davis		8. PERFORMING ORGANIZATION REPORT
9. PERFORMING ORGANIZATION NAME AND ADDRESS Oklahoma Infrastructure Consortium School of Civil & Environmental Engineering Oklahoma State University 207 Engineering South Stillwater, OK 74078		10. WORK UNIT NO. 11. CONTRACT OR GRANT NO. ODOT SP&R Item Number 2234
12. SPONSORING AGENCY NAME AND ADDRESS Oklahoma Department of Transportation Planning and Research Division 200 N.E. 21st Street, Room 3A7 Oklahoma City, OK 73105		13. TYPE OF REPORT AND PERIOD COVERED Final Report October 2011 –September 2012 14. SPONSORING AGENCY CODE
15. SUPPLEMENTARY NOTES Oklahoma Transportation Center		

16. ABSTRACT : This report represents Phase III of broken-back culverts with a drop of 18 feet. The first phase of this research was performed for a drop of 24 feet and the second phase of this research was carried out for a drop of 6 feet. This research investigates the reduction in scour downstream of a broken-back culvert by forming a hydraulic jump inside the culvert. A broken-back culvert is used in areas of high relief and steep topography as it has one or more breaks in profile slope. A broken-back culvert in the laboratory represents a 1 (vertical) to 2 (horizontal) slope after the upstream inlet and then continuing 114 feet at a 1 percent slope in the flat part of the culvert to the downstream outlet. Also, in this project, two other slopes, 0.6 and 0.3 percent, were simulated. The prototypes for these experiments were either a two barrel 10-foot by 10-foot, or a two barrel 10-foot by 20-foot reinforced concrete. The drop between inlet and outlet is selected as 18 feet. Three flow conditions were simulated, consisting of 0.8, 1.0 and 1.2 times the culvert depth.

The Froude number (F_{r1}) of the hydraulic jump created in the flat part of the culvert ranges between 2.5 and 4.12. This F_{r1} classifies the jump as an oscillating jump. The jump in experiments began nearly at the toe by placing sills in the flat part. For new culvert construction, the best option to maximize energy dissipation under open channel flow conditions is to use one 5-foot sill located 43.3 feet from the outlet. The maximum length of the culvert can be reduced by 30 feet to 43.3 feet. In pressure flow conditions, The optimal location was determined at a distance of 62 feet from the outlet for 2.5-foot sill and at distance of 45 feet from the outlet of face of the culvert for 3.3-foot sill. The length of the culvert can be reduced by 40 feet to 45 feet. Such a scenario is important where right-of-way problems exist for culvert construction.

The sills contain two small orifices at the bottom to allow the culvert to completely drain. The impact of friction blocks was found to be minimal. No friction blocks were used to further dissipate the energy. The change of slope in the Broken-Back culvert does not significantly affect to the efficiency of the hydraulic jump.

17. KEY WORDS Hydraulic jump, broken-back culvert, energy dissipation, pressure flow, open-channel flow	18. DISTRIBUTION STATEMENT No restrictions. This publication is available from the Planning and Research Division, Oklahoma DOT.		
19. SECURITY CLASSIF. (OF THIS REPORT) unclassified	20. SECURITY CLASSIF. (OF THIS PAGE) unclassified	21. NO. OF PAGES 120 pages	22. PRICE N/A

ACKNOWLEDGMENTS

This project was funded by the Federal Highway Administration and sponsored by the Oklahoma Department of Transportation. We would like to thank Mr. Robert Rusch, P.E., Bridge Division Engineer, Oklahoma Department of Transportation for his active participation in incorporating ideas to make this research more practical to field conditions.

In addition, Dr. Greg Hanson, P.E., Dr. Sherry Hunt, and Kem Kadavy, P.E., Hydraulic Engineers of the U.S. Department of Agriculture, Agricultural Research Service each contributed their ideas in the early stages of this project regarding ways to improve physical construction of the model.

DISCLAIMER

The contents of this report reflect the views of the author(s) who is responsible for the facts and the accuracy of the data presented herein. The contents do not necessarily reflect the views of the Oklahoma Department of Transportation or the Federal Highway Administration. This report does not constitute a standard, specification, or regulation. While trade names may be used in this report, it is not intended as an endorsement of any machine, contractor, process, or product.

SI* (MODERN METRIC) CONVERSION FACTORS

APPROXIMATE CONVERSIONS TO SI UNITS				
SYMBOL	**WHEN YOU KNOW**	**MULTIPLY BY**	**TO FIND**	**SYMBOL**
LENGTH				
in	inches	25.4	millimeters	mm
ft	feet	0.305	meters	m
yd	yards	0.914	meters	m
mi	miles	1.61	kilometers	km
AREA				
in^2	square inches	645.2	square millimeters	mm^2
ft^2	square feet	0.093	square meters	m^2
yd^2	square yard	0.836	square meters	m^2
ac	acres	0.405	hectares	ha
mi^2	square miles	2.59	square kilometers	km^2
VOLUME				
fl oz	fluid ounces	29.57	milliliters	mL
gal	gallons	3.785	liters	L
ft^3	cubic feet	0.028	cubic meters	m^3
yd^3	cubic yards	0.765	cubic meters	m^3
NOTE: volumes greater than 1000 L shall be shown in m^3				
MASS				
oz	ounces	28.35	grams	g
lb	pounds	0.454	kilograms	kg
T	short tons (2000 lb)	0.907	megagrams (or "metric ton")	Mg (or "t")
TEMPERATURE (exact degrees)				
^oF	Fahrenheit	5 (F-32)/9 or (F-32)/1.8	Celsius	^oC
ILLUMINATION				
fc	foot-candles	10.76	lux	lx
fl	foot-Lamberts	3.426	candela/m^2	cd/m^2
FORCE and PRESSURE or STRESS				
lbf	poundforce	4.45	newtons	N
lbf/in^2	poundforce per square inch	6.89	kilopascals	kPa

APPROXIMATE CONVERSIONS FROM SI UNITS				
SYMBOL	**WHEN YOU KNOW**	**MULTIPLY BY**	**TO FIND**	**SYMBOL**
LENGTH				
mm	millimeters	0.039	inches	in
m	meters	3.28	feet	ft
m	meters	1.09	yards	yd
km	kilometers	0.621	miles	mi
AREA				
mm^2	square millimeters	0.0016	square inches	in^2
m^2	square meters	10.764	square feet	ft^2
m^2	square meters	1.195	square yards	yd^2
ha	hectares	2.47	acres	ac
km^2	square kilometers	0.386	square miles	mi^2
VOLUME				
mL	milliliters	0.034	fluid ounces	fl oz
L	liters	0.264	gallons	gal
m^3	cubic meters	35.314	cubic feet	ft^3
m^3	cubic meters	1.307	cubic yards	yd^3
MASS				
g	grams	0.035	ounces	oz
kg	kilograms	2.202	pounds	lb
Mg (or "t")	megagrams (or "metric ton")	1.103	short tons (2000 lb)	T
TEMPERATURE (exact degrees)				
^oC	Celsius	1.8C+32	Fahrenheit	^oF
ILLUMINATION				
lx	lux	0.0929	foot-candles	fc
cd/m^2	$candela/m^2$	0.2919	foot-Lamberts	fl
FORCE and PRESSURE or STRESS				
N	newtons	0.225	poundforce	lbf
kPa	kilopascals	0.145	poundforce per square inch	lbf/in^2

*SI is the symbol for the International System of Units. Appropriate rounding should be made to comply with Section 4 of ASTM E380.

(Revised March 2003)

TABLE OF CONTENTS

List of Tables

LIST OF FIGURES

EXECUTIVE SUMMARY

This research investigates the reduction in scour downstream of a broken-back culvert by forming a hydraulic jump inside the culvert. A broken-back culvert is used in areas of high relief and steep topography as it has one or more breaks in profile slope. A broken-back culvert in the laboratory represents a 1 (vertical) to 2 (horizontal) slope after the upstream inlet and then continues 114 feet at a 1 percent slope in the flat part of the culvert to the downstream outlet. Also, in this project, two other slopes, 0.6 and 0.3 percent, were simulated. The prototype for these experiments was either a two barrel 10-foot by 10-foot, or a two barrel 10-foot by 20-foot reinforced concrete culvert. The drop between inlet and outlet was selected as 18 feet. Three flow conditions were simulated, consisting of 0.8, 1.0 and 1.2 times the culvert depth.

The Froude number of the hydraulic jump created in the flat part of the culvert ranges between 2.5 and 4.12. This Froude number classifies the jump as an oscillating jump. The jump in the experiments began nearly at the toe by placing sills in the flat part. For new culvert construction, the best option to maximize energy dissipation under open channel flow conditions is to use one 5-foot sill located 43.3 feet from the outlet. The maximum length of the culvert can be reduced by 30 feet to 43.3 feet. In pressure flow conditions, the optimal location was determined at a distance of 62 feet from the outlet for 2.5-foot sill and at distance of 45 feet from the outlet face of the culvert for 3.3-foot sill. The length of the culvert can be reduced by 40 to 45 feet. Such a scenario is important where right-of-way problems exist for culvert construction.

The sills contain two small orifices at the bottom to allow the culvert to completely drain. The impact of friction blocks was found to be minimal. No friction blocks were used to further dissipate the energy. The change of slope in the Broken-Back culvert does not significantly affect the efficiency of the hydraulic jump.

1 INTRODUCTION

A recent research study conducted by the Oklahoma Transportation Center at Oklahoma State University indicated that there are 121 scour-critical culverts on the Interstate System (ISTAT), the National Highway System (NHS), and the State Transportation Program (STP) in Oklahoma (Tyagi, 2002). The average replacement cost of these culverts is about $121M. A survey of culverts in Oklahoma indicates that the drop in flowline between upstream and downstream ends ranges between 6 and 24 feet. Tyagi et al. (2009, 2011) carried out two phases of these projects; the first phase of this research was performed for a drop of 24 feet and the second phase of this research was performed for a drop of 6 feet.

This report represents Phase III of broken-back culverts with a drop of 18 feet. A drop of 18 feet was used in the laboratory model because it is close to the middle limit. Results of this research could maximize the energy loss within the culvert, thus minimizing the scour around the culvert and decreasing the degradation in the downstream channel. This reduces the construction and rehabilitation costs of culverts in Oklahoma. The project is supported by the Bridge Division, Oklahoma Department of Transportation (ODOT).

The purpose of this project is to develop a methodology to analyze broken-back culverts in Oklahoma such that the energy is mostly dissipated within the culverts to minimize the degradation downstream. The purpose of a culvert is to safely pass water underneath the roadways constructed in hilly topography or on the side of a relatively steep hill. A broken-back culvert is used in areas of high relief and steep topography as

it has one or more breaks in profile slope. This project investigates culverts with a vertical drop of 6 feet that may result in effective energy dissipation inside the culvert and consequently minimize the scour downstream of broken-back culverts. Culvert dimensions and hydraulic parameters for the scale model were provided by the Bridge Division, ODOT (personal communication with R. Rusch, 2007).

The research investigation includes the following tasks: 1) to obtain and review existing research currently available for characterizing the hydraulic jump in culverts; 2) to build a scale model to represent a prototype of a broken-back culvert 150 feet long, with two barrels of 10 X 10 feet, and a vertical drop of 18 feet; 3) to simulate different flow conditions for 0.8, 1.0 and 1.2 times the culvert depth (d) in the scale model constructed in Task 2; 4) to evaluate the energy dissipation between upstream and downstream ends of the broken-back culvert with and without friction blocks of different shapes; 5) to observe in physical experiments the efficiency of the hydraulic jump with and without friction blocks between upstream and downstream ends of the culvert and the location of the hydraulic jump from the toe of the drop in the culvert; 6) to simulate different slopes of the flat part of the Broken-Back culvert; and 7) to prepare a final report incorporating analysis of the hydraulic jump and devices to create the jump and energy loss. These tasks are presented in the following sections.

2 LITERATURE REVIEW

The literature search was performed for hydraulic jump and Acoustic Doppler Velocimeter and the results are discussed in the following sections.

2.1 Hydraulic Jump

The hydraulic jump is a natural phenomenon of a sudden rise in water level due to change from supercritical flow to subcritical flow, i.e., when there is a sudden decrease in velocity of the flow. This sudden change in velocity causes considerable turbulence and loss of energy. Consequently, the hydraulic jump has been recognized as an effective method for energy dissipation for many years. There have been many studies carried out to explain the characteristics of the hydraulic jump. Some of these studies are summarized in the following paragraphs.

Ohtsu et al. (1996) evaluated incipient hydraulic jump conditions on flows over vertical sills. They identified two methods of obtaining an incipient jump: (1) increasing the sill height, or (2) increasing the tailwater depth until a surface roller forms upstream of the sill. For wide channels, predicted and experimental data were in agreement, but in the case of narrow channels, incipient jump was affected by channel width.

Mignot and Cienfuegos (2010) focused on an experimental investigation of energy dissipation and turbulence production in weak hydraulic jumps. Froude numbers ranged from 1.34 to 1.99. Mignot and Cienfuegos observed two peak turbulence production regions for the partially developed inflow jump, one in the upper shear layer and the other in the near-wall region. The energy dissipation distribution in the jumps was measured and revealed a similar longitudinal decay of energy dissipation, which was integrated over the flow sections and the maximum turbulence production values from the intermediate jump region towards its downstream section. It was found that the energy dissipation and the turbulence production were strongly affected by the inflow

development. Turbulence production showed a common behavior for all measured jumps. It appeared that the elevation of maximum Turbulent Kinetic Energy (TKE) and turbulence production in the shear layer were similar.

Alikhani et al. (2010) conducted many experiments to evaluate the effects of a continuous vertical end sill in a stilling basin. They measured the effects of sill position on the depth and length of a hydraulic jump without considering the tailwater depth. In the experiments, they used five different sill heights placed at three separate longitudinal distances in their 1:30 scaled model. The characteristics of the hydraulic jump were measured and compared with the classic hydraulic jump under varied discharges. They proposed a new relationship between sill height and position, and sequent depth to basin length ratio. The study concluded that a 30% reduction in basin length could be accomplished by efficiently controlling the hydraulic jump length through sill height.

Finnemore et al. (2002) stated that the characteristics of the hydraulic jump depend on its Froude number (F_{r1}). The Froude number is the ratio between inertia force and gravity force. They added that in order for the hydraulic jump to occur, the flow must be supercritical, i.e. a jump can occur only when the Froude number is greater than 1.0. The hydraulic jump is classified according to its Froude number. When F_{r1} is between 1.7 and 2.5, the flow is classified as a weak jump and will have a smooth rise in the water surface with less energy dissipation. A F_{r1} between 2.5 and 4.5 results in an oscillating jump with 15-45% energy dissipation. A steady jump will occur when F_{r1}

ranges from 4.5 to 9.0, and results in energy dissipation from 45% to 70%. When F_{r1} is above 9.0, a strong jump will occur with energy losses ranging from 70% to 85%.

Ohtsu et al (2001) investigated undular hydraulic jump conditions in a smooth rectangular horizontal channel. They found that the formation of an undular jump depends only on the inflow Froude number and the boundary-layer development at the toe of the jump. At its Froude number ranges, they found that the effects of the aspect ratio and the Reynolds number on the flow characteristics were negligible. Under experimental investigation, it was found that the upper limits of the Froude numbers range between 1.3 and 2.3 at the inflow. Furthermore, a Froude number of 1.7 was found to be the critical velocity point at which inflow was fully developed. They obtained the ratio thickness of the boundary layer to the depth of the toe of the jump to be 0.45 to 1.0, which agreed with predicted values from experimental results.

Bhutto et al. (1989) provided analytical solutions for computing sequent depth and relative energy loss for a free hydraulic jump in horizontal and sloping rectangular channels from their experimental studies. They used the ratio of jump length to jump depth and the Froude number to compute the length of the free jump on a horizontal bed. Jump factor and shape factor were evaluated experimentally for the free jump on a sloping bed. To check the efficiency of the jump, they made comparisons with previous solutions by Ludin, Bakhmateff, Silvester and Chertoussove and found that the equations they derived could be used instead of their equations.

Gharanglk and Chaudhry (1991) present three models for the numerical simulation of hydraulic jumps in a rectangular channel while factoring in the

considerable effect of nonhydrostatic pressure distribution. The one-dimensional Boussinesq equations are solved in time subject to appropriate boundary conditions which numerically simulate the hydraulic jump. The results were compared to experimental data which indicates that four-order models with or without Boussinesq terms give similar results for all Froude numbers tested. The Froude numbers ranged from 2.3 to 7.0. The MacCormack scheme and a dissipative two-four scheme were used to solve the governing equations subject to specified end conditions until a steady state was achieved.

Hotchkiss and Donahoo (2001) report that the Broken-back Culvert Analysis Program (BCAP) is a simple but powerful analysis tool for the analysis of broken-back culverts and hydraulic jumps. The program is easy to understand, explain, and document, and is based on the energy equation and momentum equation for classical jumps. It is able to plot rating curves for the headwater, outlet depth and outlet velocity. Hotchkiss and Donahoo described a computer code capable of analyzing hydraulic jumps in the broken-back culvert.

Hotchkiss et al. (2003) describe the available predictive tools for hydraulic jumps, the performance of the Broken-Back Culvert Analysis Program (BCAP) in analyzing the hydraulics of a broken-back culvert, and the current applications and distribution of BCAP. They conducted tests on the Broken-Back culvert made of Plexiglas® to assess the performance of BCAP in predicting headwater rating curves, the locations of hydraulic jumps, and the lengths of hydraulic jumps. Hotchkiss et al. concluded that accounting for the losses within the jumps because of friction in corrugated metal pipes

and more accurately predicting the locations of hydraulic jumps may both be improved by predictions of flow hydraulics within the culvert barrel.

The Utah Department of Transportation (UDOT) addresses aspects of broken-back culverts and hydraulic jumps in the state's *Manual of Instruction – Roadway Drainage (US Customary units), Culverts (2004)*. This manual illustrates steps for the design of broken-back culverts which include: 1) Establishing a flow-line profile, 2) sizing the culvert, 3) beginning to calculate a supercritical profile, 4) completing profile calculations, and 5) considering hydraulic jump cautions. Section F of Appendix 9 of the manual covers aspects of hydraulic jumps in culverts, including: cause and effect, momentum friction, comparison of momentum and specific energy curves, and the potential occurrence of hydraulic jumps. The manual also takes into account the sequent depth of jump for rectangular conduits, circular conduits, and conduits of other shapes.

Larson, (2004), in her Master's thesis entitled *Energy Dissipation in Culverts by Forcing a Hydraulic Jump at the Outlet,* suggests forcing hydraulic jumps to reduce the outlet energy. She considered two design examples to create a hydraulic jump within a culvert barrel: (1) a rectangular weir placed on a flat apron and (2) a vertical drop along with a rectangular weir. These two designs were used to study the energy reduction in the energy of the flow at the outlet. From these experiments, she found that both designs were effective in the reduction of outlet velocity, momentum, and energy. These reductions would decrease the need for downstream scour mitigation.

Hotchkiss et al. (2005) proposed that by controlling the water at the outlet of a culvert, water scour around the culvert can be reduced. The effectiveness of a simple weir near the culvert outlet is compared to that of a culvert having a weir with a drop upstream in the culvert barrel. These two designs are intended to reduce the specific energy of the water at the outlet by inducing a hydraulic jump within the culvert barrel, without the aid of tailwater. The design procedure was proposed after studying the geometry and effectiveness of each jump type in energy reduction. In this research, they found the Froude number ranged from 2.6 to 6.0. It was determined that both forms of outlets are effective in reducing the velocity of water; hence the energy and momentum thus reduced the need for downstream scour mitigation.

The *Hydraulic Design of Energy Dissipators for Culverts and Channels* (July, 2006), from the Federal Highway Administration, provides design information for analyzing and mitigating problems associated with the energy dissipation at culvert outlets and in open channels. It recommends the use of the broken-back culvert design as an internal energy dissipator. The proposed design for a broken-back culvert is limited to the following conditions: 1) the slope of the steep section must be less than or equal to 1.4:1 (V: H) and 2) the hydraulic jump must be completed within the culvert barrel.

According to this report, for situations where the runout section is too short and/or there is insufficient tailwater for a jump to be completed within the barrel, modifications may be made to the outlet that will induce a jump. The design procedure

for stilling basins, streambed level dissipaters, riprap basins and aprons, drop structures and stilling wells is also discussed.

Pagliara et al. (2008) analyzed the hydraulic jump that occurs in homogeneous and nonhomogeneous rough bed channels. They investigated the sequent flow depth and the length of the jump which are the influence parameters of the hydraulic jump. In this research, they drew on the general jump equation to analyze the jump phenomenon. In analyzing the rough bed data, they were able to formulate a representative equation to explain the phenomenon. The equations found in their study may be used to design stilling basins downstream of hydraulic structures.

Hotchkiss et al. (2008) analyzed the accuracy of the following seven programs on culvert hydraulics: HY-8, FishXing, Broken-back Culvert Analysis Program (BCAP), Hydraflow Express, CulvertMaster, Culvert, and Hydrologic Engineering Center River Analysis System (HEC-RAS). The software was tested on the accuracy of three calculations: headwater depths, flow control, and outlet velocities. The software comparison was made between software output values and hand calculations, not from laboratory experimental data. The hand calculations used were derived from laboratory experiments done by the National Bureau of Standards (NBS). Hotchkiss et al. concluded HEC-RAS is the most comprehensive program for both accuracy and features for culverts affected by upstream structures.

Tyagi et al. (2009) investigated hydraulic jump under pressure and open channel flow conditions in a broken-back culvert with a 24 foot drop. It was found that for pressure flow, a two-sill solution induced the most desirable jump, and for open channel

a single sill close to the middle of the culvert was most desirable. The investigation was funded by the Oklahoma Transportation Center, Research and Innovative Technology Administration, Federal Highway Administration, and Oklahoma Department of Transportation.

Tyagi et al. (2010a) performed many experiments for open channel culvert conditions. Optimum energy dissipation was achieved by placing one sill at 40 feet from the outlet. Friction blocks and other modifications to the sill arrangement were not as effective.

Tyagi et al. (2010b) carried out many experiments to optimize flow condition and energy dissipation in a broken-back culvert under pressure flow. It was found that two sills, the first 5 feet high at 25 feet from the outlet and the second 3.34 feet high at 45 feet from the outlet, gave the best results. The culvert could not be shortened since it was full under the tested conditions.

2.2 Effect of friction blocks and sill in Broken-Back culvert

Eloubaidy et al. (1999) found that in order to provide a better stability and after running multiple series of tests to determine which floor block dissipates the most energy, the curved blocks work the best. Different experiments tested various sizes, curvatures, and locations of the blocks. By choosing these blocks, optimum flow conditions are created having a lower capacity for erosion of the downstream bed. The curved blocks range from 3.2% to 33.3% more effective in dissipating excessive kinetic energy.

Bessaih and Rezak (2002) tried to determine how to shorten the length of a hydraulic jump; experiments were run with different cut ratios of baffled blocks. The blocks shapes will create strong vortices, which then shorten the lengths of the jumps. After completing the tests, it was shown that baffle blocks with a sloping face reduce the length of a jump up to 48% relative to the free jump, as well as up to 18% relative to USBR basin II. However, only a 5% decrease in length is observed when adding a second row, therefore adding an additional row is not very effective.

Oosterholt (1947) found that the total amount of heat generated and the decrease of the energy transport deviated greatly between them. The surface roller dissipates the most energy in the lower part; energy dissipation also takes place in the upper part of the main stream. As one continues downstream, the energy dissipation slowly decreases. The surface roller's upper part only contributes to a small amount of the energy dissipation. The bottom friction also makes only a small contribution to energy dissipation.

According to Habibzadeh et al. (2012), the deflected surface jet and the reattaching wall jet were the two flow regimes that were observed during the study. In order to get the best results, various block arrangements and submerged factors were tested, as well as a wide range of different Froude numbers. In order to determine the maximum submergence factor (S_1) and minimum submergence factor (S_2), empirical equations were derived; using the empirical equations that were developed it was found that 85% of the time the flow regime was able to be predicted. It was found also that adding more blocks and adjusting their heights did not play a strong role in the energy

dissipation. In order to create energy dissipation from baffle blocks, one needs to make sure that the flow is in the deflected surface jet regime.

According to Baylar et al. (2011), Stepped chutes have become more popular over the years and are being used for gabion weirs, river training, and storm waterways. Not only are they low-cost but they have a speedy construction process. It was observed that aeration efficiency increases with the increasing energy-loss ratio. Nappe flow regime leads to greater aeration efficiency and has higher energy dissipation than the skimming flow regime. From their results came the conclusion that using the genetic expression programming method will result in a high rate when predicting aeration efficiency.

Meselhe and Hebert (2007) stated that culverts are very useful and common when trying to control hydraulic systems. In order to collect water level and discharge measurements a laboratory apparatus was used to simulate flow through culverts. In conducting the experiments Meselhe and Hebert used circular culvert barrels, as well as square culvert barrels. While measuring the stage-discharge relationship and the rising and receding limbs of a hydrograph, a noticeable difference was observed.

Jamshidnia et al. (2010) used a three-dimensional acoustic doppler velocimeter to investigate the effect of an intermediate standing baffle in a rectangular open channel. In the upstream baffle region, a peak structure was observed after analyzing the spaced-averaged power spectra of stream velocity. They also observed that a peak structure existed both up and downstream of the baffle.

Noshi (1999) determined that spillways, regulating structures, and outlet works often require stilling basins in order to achieve energy dissipation. His study estimates the maximum downstream velocity for near the bed, which is vital to know before construction in order to know what materials are needed and how much is needed. For the flow conditions that were investigated, Noshi concluded that a sill height of .15 the tailwater depth can improve energy dissipation. It was concluded that using a greater end-sill height does not increase energy dissipation. The recirculation length is estimated to be about 2.3 times that of the water depth.

Varol et al. (2009) investigated hydraulic jumps in horizontal channels and the effects a water jet has. During the experiments, five different water jet discharges were used as well as Froude numbers ranging from 3.43 to 4.83. A high-speed SVHS camera was used to analyze the jumps with jets and the free jumps. According to their findings, whenever the water jet flow increased this caused the hydraulic jump to move farther upstream. They also observed an increase in downstream depth (y_2) and energy loss when they increased the water jet discharge. Furthermore, roller length increased with increased water jet discharge. It was found that forced hydraulic jumps initiated by water jets had higher energy losses than free jumps.

Habibzadeh et al. (2011) conducted a preliminary study of the effects baffle blocks and walls have on submerged jumps. When testing the baffle block series, a range of submerged factors and five Froude numbers were tested on one configuration of baffle blocks. They found that the maximum energy dissipation efficiency of submerged jumps was greater than that of the free jump efficiency.

Debabeche and Achour (2007) researched the effect of placing a sill in a horizontal symmetrical triangular channel of 90° central angle. Using various flow conditions they investigated the sill-controlled jump and the minimum-B jump using either a thin-crested or a broad-crested sill. In order to detect the effect of the inflow Froude number relative to the sill height, the data was fitted to empirical relations. They concluded that a reduced length is needed and a lower tailwater level is required when comparing it to a triangular jump basin.

2.3 Effect of slopes in Broken-Back culvert

Numerous studies have observed the characteristics of the hydraulic jump in sloping open channels. Husain et al. (1994) performed many experiments on the sloping floor of open rectangular channels with negative and positive step to predict the length and depth of hydraulic jump and to analyze the sequent depth ratio. They found that the negative step has advantages over the positive with respect to the stability and compactness of hydraulic jump. They developed a set of non-dimensional equations in terms of profile coefficient, and they used multiple linear regression analyses on jumps with or without a step. Using Froude numbers between 4 to 12 and slope, S, between 1 and 10 percent, the length and sequent depth ratio can accurately be predicted.

Defina and Susin (2003) investigated the stability of a stationary hydraulic jump situated over a lane with sloping topography in a rectangular channel of uniform width with assuming inviscid flow conditions. On the upslope flow, it was found that the hydraulic jump is unstable and if the jump is slightly displaced from its stationary point, it will move further away in the same direction. In the channel with adverse slope, they

indicated that a stationary jump can be produced. Defina and Susin calculated the ratio of bed to friction slope such as energy dissipation per unit weight and unit length, and the result was quite large. Authors found that the equilibrium state is weakly perturbed when the theoretical stability condition was inferred in terms of the speed adopted by the jump.

Li (1995) studied how to find the location and length of the hydraulic jump in 1^o through 5^o slopes of rectangular channels. He carried out many experimental laboratory models to get the relationship between upstream flow Froude numbers and ratios of jump length and sequent after jump L/y_2. Li used the HEC-2 software to locate the heel of a hydraulic jump to get the length of the jump and toe of the jump. The scale between the models and the prototypes was 1:65. Researchers concluded that an estimation of sequent depth for a hydraulic jump had to take the channel bed slope into account if the bed slope was greater than 3^o. He found out that y_2/y_1 and F_{r1} had linear relation and could be used to estimate the sequent depth. Also, Li recommended some rules such as using a solid triangular sill which could be arranged at the end of the basin apron to lift the water and reduce the scour from the leaving flow. He stated that if the Fr_1 ranged between 4.5 and 9, the tailwater depth was lowered by 5% of the sequent water depth.

2.4 Acoustic Doppler Velocimeter

Acoustic Doppler Velocimeter (ADV) is a sonar device which tracks suspended solids (particles) in a fluid medium to determine an instantaneous velocity of the particles in a sampling volume. In general, ADV devices have one transmitter head and two to four receiver heads. Since their introduction in 1993, ADVs have quickly become

valuable tools for laboratory and field investigations of flow in rivers, canals, reservoirs, oceans, around hydraulic structures and in laboratory scale models (Sontek, 2001).

Wahl (2000) discusses methods for filtering raw ADV data using a software application called WinADV. Wahl suggests that ADV data present unique requirements compared to traditional current-metering equipment, due to the types of data obtained, the analyses that are possible, and the need to filter the data to ensure that any technical limitations of ADV do not adversely affect the quality of the results. According to Wahl, the WinADV program is a valuable tool for filtering, analyzing, and processing data collected from ADV. Further, this program can be used to analyze ADV files recorded using the real time data acquisition programs provided by ADV manufacturers.

Goring and Nikora (2002) formulated a new post processing method for despiking raw ADV data. The method combines three concepts, including:

1. That differentiation of the data enhances the high frequency portion of a signal which is desirable in sonar measurements.
2. That the expected maximum of a random series is given by the Universal threshold function.
3. That good data clusters are a dense cloud in phase space maps

These concepts are used to construct an ellipsoid in three-dimensional phase space, while points lying outside the ellipsoid are designated as spikes (bad data). The new method has superior performance over various other methods with the added advantage of requiring no parameters. Several methods for replacing sequences of

spurious data are presented. A polynomial fitted to good data on either side of the spike event, then interpolated across the event, is preferred by Goring and Nikora.

Mori et al. (2007) investigates measuring velocities in aerated flows using ADV techniques. ADV measurements are useful and powerful for measurements of mean and turbulent components of fluids in both hydraulic experimental facilities and fields. However, it is difficult to use the ADV in bubbly flows because air bubbles generate spike noise in the ADV velocity data. This study describes the validity of the ADV measurements in bubbly flows. The true three-dimensional phase space method is significantly useful for eliminating the spike noise of ADV recorded data in bubbly flow as compared to the classical low correlation method (Goring and Nikora, 2002). The results of the data analysis suggest that:

1. There is no clear relationship between velocity and ADV's correlation/signal-to-noise ratio in bubbly flow.
2. Spike noise filtering methods based on low correlation and signal-to-noise ratio are not adequate for bubbly flow.
3. The true 3D phase space method significantly removes spike noise of ADV velocity in comparison with the original 3D phase space method.

In addition the study found that ADV velocity measurements can be valid for 1% to 3% air void flows. The limitations of the ADV velocity measurements for high void fractions were not studied.

Chanson et al. (2008) investigated the use of ADVs to determine the velocity in turbulent open channel flow conditions in both laboratory and field experiments. They demonstrated that the ADV is a competent device to measure velocity in steady and unsteady turbulent open channel flows. However, in order to accurately measure velocity, the ADV raw data must be processed and the unit must be calibrated to the suspended sediment concentrations. Accurately processing your ADV data requires practical knowledge and experience with the device's capabilities and limitations. Chanson concluded that turbulence properties should not be derived from unprocessed ADV signals and that some despiking methods were not directly applicable to many field and laboratory applications.

3 HYDRAULIC SIMILITUDE THEORY

Similarity between a hydraulic model and a prototype may be achieved through three basic forms: a) geometric similarity, b) kinematic similarity, and c) dynamic similarity (Chow, 1959).

3.1 BROKEN-BACK CULVERT SIMILARITIES

a. Geometric similarity implies similarity of physical form. The model is a geometric reduction of the prototype and is accomplished by maintaining a fixed ratio for all homologous lengths between the physical quantities involved in geometric similarity: length (L), area (A), and volume (Vol). To keep the homologous lengths in the prototype (p) and the model (m) at a constant ratio (r), they may be expressed as:

$$\frac{L_p}{L_m} = L_r$$

An area (A), is the product of two homologous lengths; hence, the ratio of the homologous area is also a constant given as:

$$\frac{A_p}{A_m} = \frac{L_p^2}{L_m^2} = L_r^2$$

A volume (Vol.) is the product of three homologous lengths; the ratio of the homologous volume can be represented as:

$$\frac{Vol_p}{Vol_m} = \frac{L_p^3}{L_m^3} = L_r^3$$

b. Kinematic similarity implies similarity of motion. Kinematic similarity between the model and the prototype is attained if the homologous moving particles have the same velocity ratio along geometrically similar paths. This similarity involves the scale of time and length. The ratio of times required for homologous particles to travel homologous distances in a model and prototype is given by:

$$\frac{T_p}{T_m} = T_r$$

The velocity (V) is defined as distance per unit time; thus, the ratio of velocities may be expressed as:

$$\frac{V_p}{V_m} = \frac{\left(L_p/T_p\right)}{\left(L_m/T_m\right)} = \frac{L_r}{T_r}$$

The flow (Q) is expressed as volume per unit time and may be given by:

$$\frac{Q_p}{Q_m} = \frac{\left(L_p^3/T_p\right)}{L_m^3/T_m} = \frac{L_r^3}{T_r}$$

c. Dynamic similarity implies similarity in forces involved in motion. In broken-back culverts, inertial force and gravitational (g) force are considered dominant forces in fluid motion. The Froude number is defined as:

$$F_r = \frac{\left[V_p \Big/ \left(g_p L_p\right)^{1/2}\right]}{\left[V_m \Big/ \left(g_m L_m\right)^{1/2}\right]} = 1$$

As g_p and g_m are the same in a model and the prototype, these cancel in Equation 7, yielding:

$$\frac{V_r}{\left(L_r\right)^{1/2}} = 1$$

$$V_r = \frac{V_p}{V_m} = \left(L_r\right)^{1/2}$$

$$V_p = V_m \left(L_r\right)^{1/2}$$

Using the three similarities, a variable of interest can be extrapolated from the model to the prototype broken-back culvert.

4 LABORATORY MODEL

During the initial period of discussion regarding the construction of a scale model representing a 150 feet long broken-back culvert with 2-10'x10' to 2-10'x20' and a vertical drop of 18 feet, the research group visited the USDA Agricultural Research Service Hydraulic Engineering Research Laboratory in Stillwater, Oklahoma. This was the facility at which testing was done. The group visited with facility personnel and inspected the equipment that would be used to conduct tests. Physical dimensions of the flume that would be used were noted, as well as the flow capacity of the system.

Two scales were considered for the model. A scale of either 1:10 or 1:20 would allow for geometric similitude in a model that could easily be produced. The 1:20 scale was adopted due to space limitations at the testing facility and in consideration of the potential need to expand the model depending on where the hydraulic jump occurred. If the hydraulic jump did not form within the model, the smaller scale would leave room to double the length of the culvert. In addition, a lower flow rate would be required during testing if a smaller scale were used.

Other considerations included what materials to use in building the model, and what construction methods would be best. The materials considered were wood and Plexiglas®. Plexiglas® was found preferable because it offered visibility as well as durability, and a surface which would closely simulate the surface being modeled (Figures 1 through 7). The Manning's roughness value for Plexiglas® is 0.010 which is very close to the roughness of finished concrete at 0.012. The thickness of the Plexiglas® was decided based on weight, rigidity, workability, and the ease with which

the material would fit into scale. Half-inch Plexiglas® proved to be sturdy and was thick enough to allow connection hardware to be installed in the edges of the plates. This material also fit well into the proposed scale of 1 to 20 which equated 0.50 inch in the model to one foot in the prototype. The construction methods included constructing the model completely at the Oklahoma State University campus and moving it to the test facility, creating sections of the model at the university and assembling them at the test facility, or contracting with the testing facility to construct the model. It was decided that the model would be constructed at the test facility. During the course of the test runs, it became apparent that a flow straightener would have to be installed inside the reservoir in order to calm the inlet flow. A sealed plywood divider was constructed with a series of openings covered with coarse mesh (Figure 15).

In addition to the Plexiglas® model of the culvert, a reservoir was constructed upstream of the model to collect and calm the fluid entering the model. The reservoir was constructed with plywood because it was not necessary to observe the behavior of the fluid at that stage (Figure 8 and 9). Within the reservoir, wing walls at an angle of 60 degrees were constructed to channel flow into the model opening. The base of the wingwalls was constructed with plywood and the exposed wingwall models were formed with Plexiglas®. The same design was used for the outlet structure of the culvert.

The objective of the test was to determine the effect of sill and friction blocks on the hydraulic jump within the prototype, therefore the model was constructed so that different arrangements of sill and friction blocks could be placed and observed within the model. Friction blocks were mounted in different arrangements on a sheet of

Plexiglas® the same width as the barrels, and placed in the barrels (Figure 12). The friction block shape selected was a regular flat faced Friction block (Figure 11). Sills were located only on the horizontal portion of the mode (Figure 10).

Two sections were constructed and added to the model for several experiments. These sections served two purposes. During initial experimentation, it was observed that the original design was under pressure and that a theoretical hydraulic jump would occur above the confines of the existing culvert ceiling. The additional sections were inverted and mounted to the top of the original model, making a culvert with 2 barrels 6 inches wide by 12 inches high and the original length of 68.4 inches (Figure 13). Access holes were cut into the top of these sections to allow for the placement of a velocity meter when used as a cover for the expanded height. Figure 14 shows the downstream channel made from plywood, and it connected with wingwall. Figure 16 shows the point gauge that was used to correct height of the three flow conditions consisting 0.8, 1.0, and 1.2 times the culvert depth. The Acoustic Doppler Velomtere (ADV) can be plugged in the culvert model and connected with the computer as shown in Figure 17. Figure 18 shows the Pitot Tube plugged in the culvert model and more picture in the appendix illustrate the place where to measure the velocity in the upstream and downstream. More pictures in the appendix illustrate how to measure the velocity in the upstream and downstream.

Three dimensional laboratory model. Scale 1:20 All measurements in inches

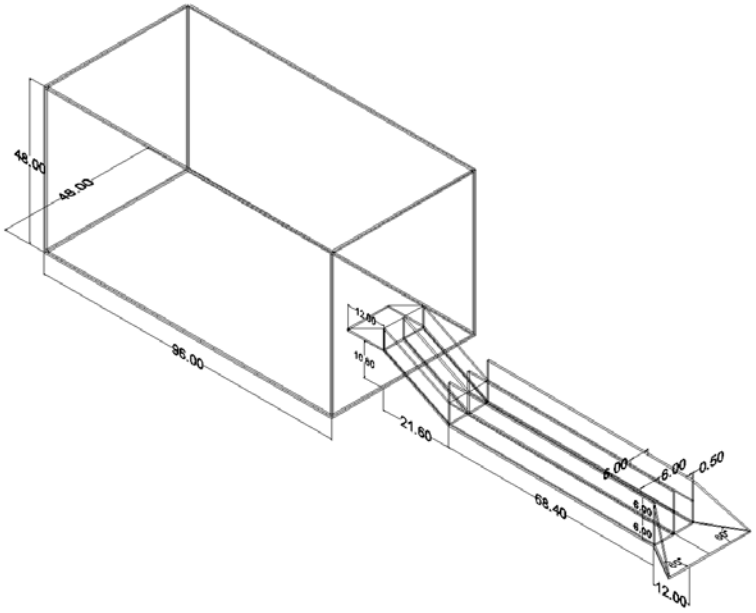

Figure 1-1. Model A: Open Channel Flow

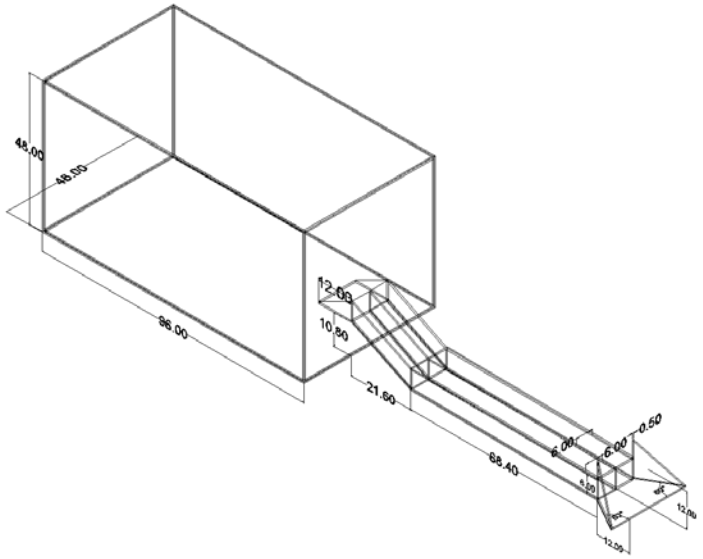

Figure 1-2. Model B: Pressure Flow

Open Channel Laboratory Model. Scale 1:20

All measurements in inches

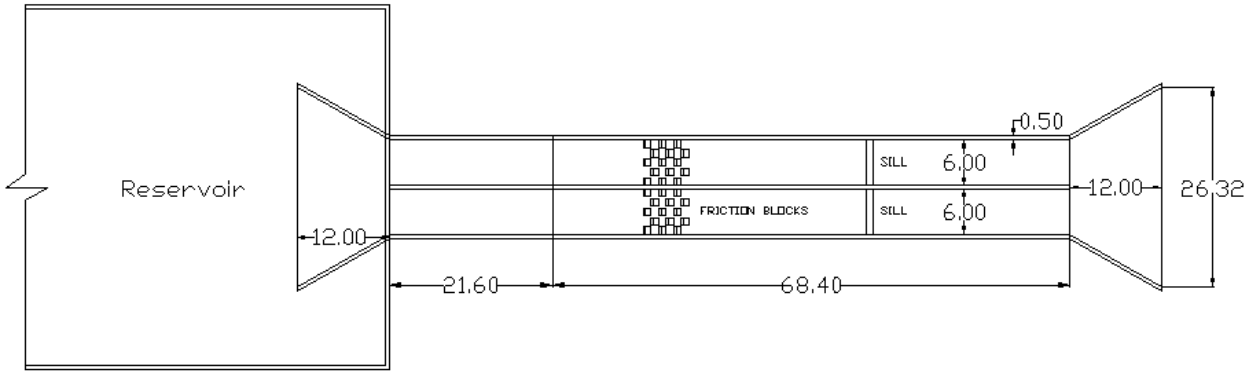

Figure 2. Plan View of model

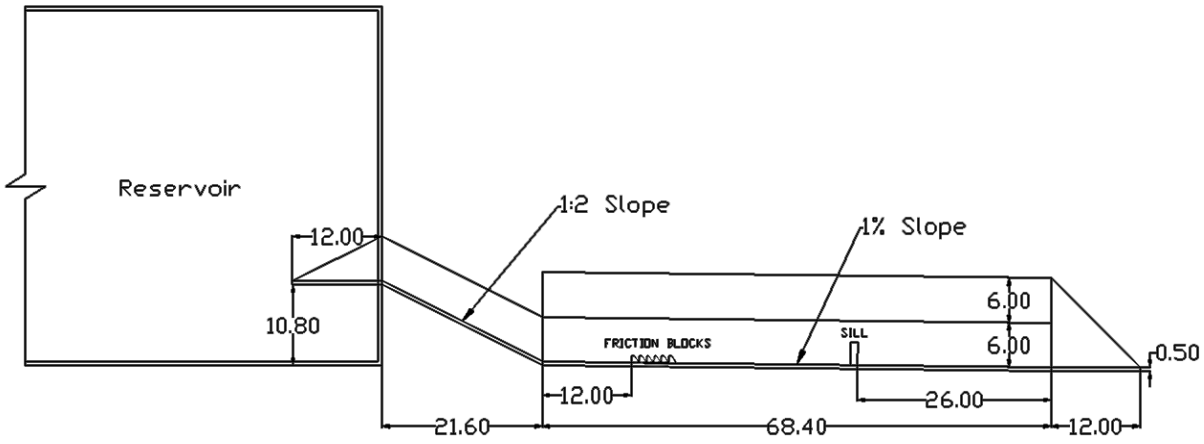

Figure 3. Profile View of 1% slope model

Open Channel Laboratory Model Scale 1:20

All measurements in inches

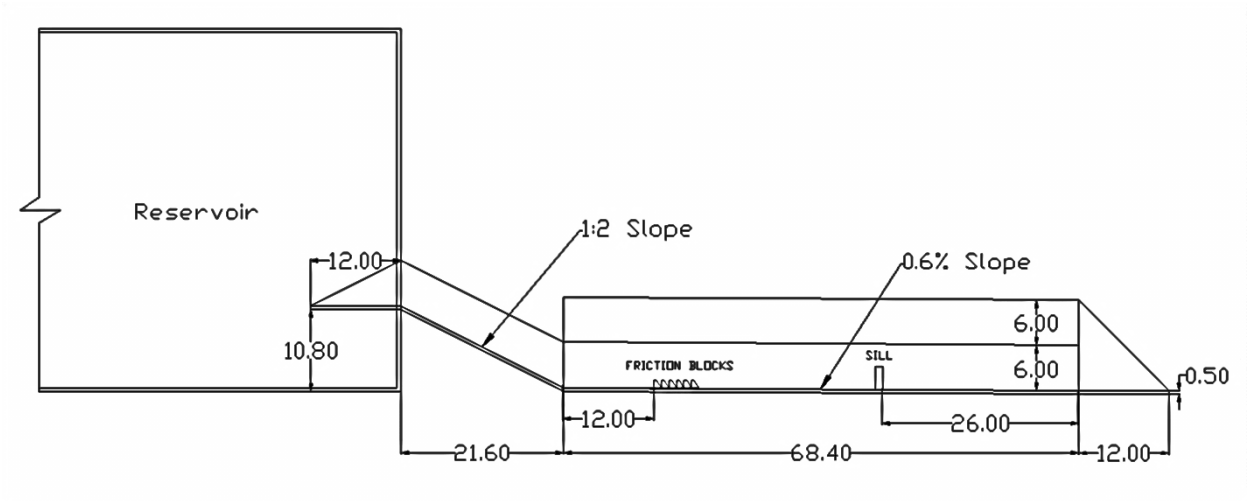

Figure 4. Profile View of 0.6% slope model

Laboratory Model Scale 1:20

All measurements in inches

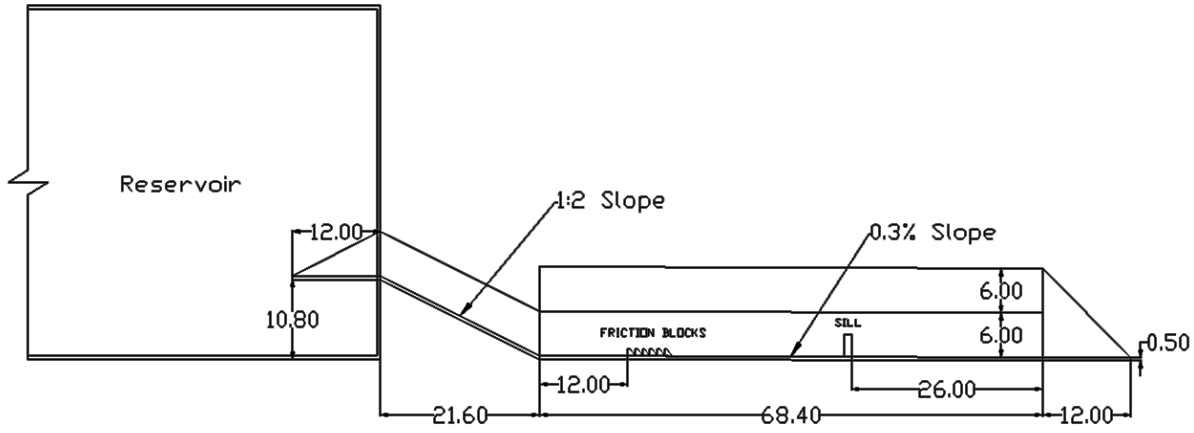

Figure 5. Profile View of 0.3% slope model

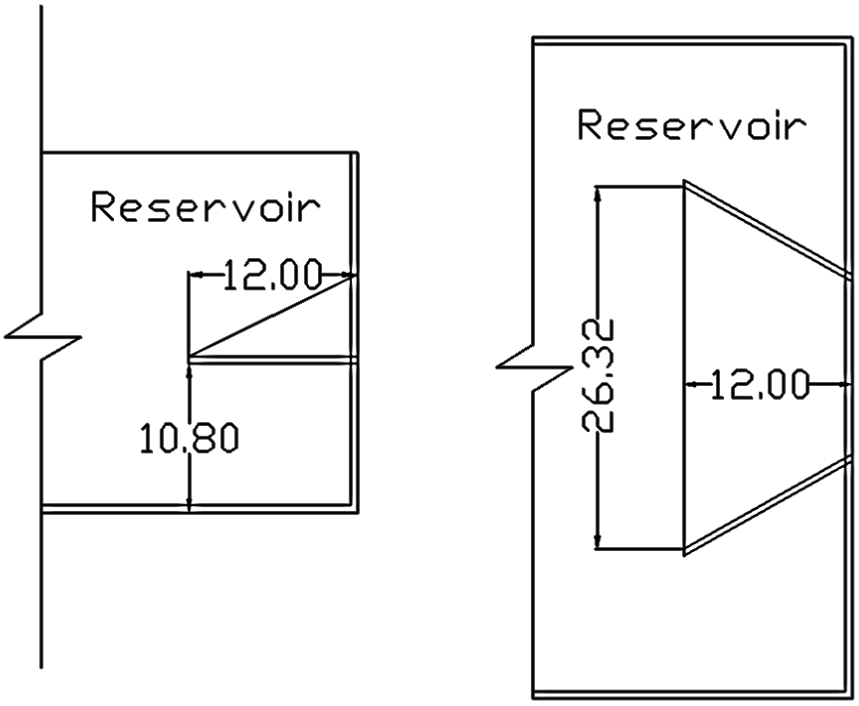

Figure 6. Profile and Plan View of Reservoir Inlet (Upstream)

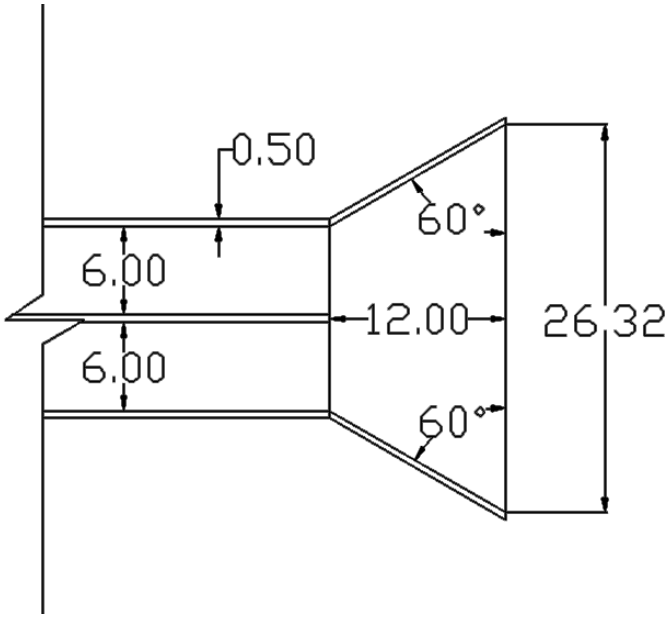

Figure 7. Plan View of Reservoir Outlet (Downstream)

Figure 8. Front View of laboratory model

Figure 9. Side view of laboratory model

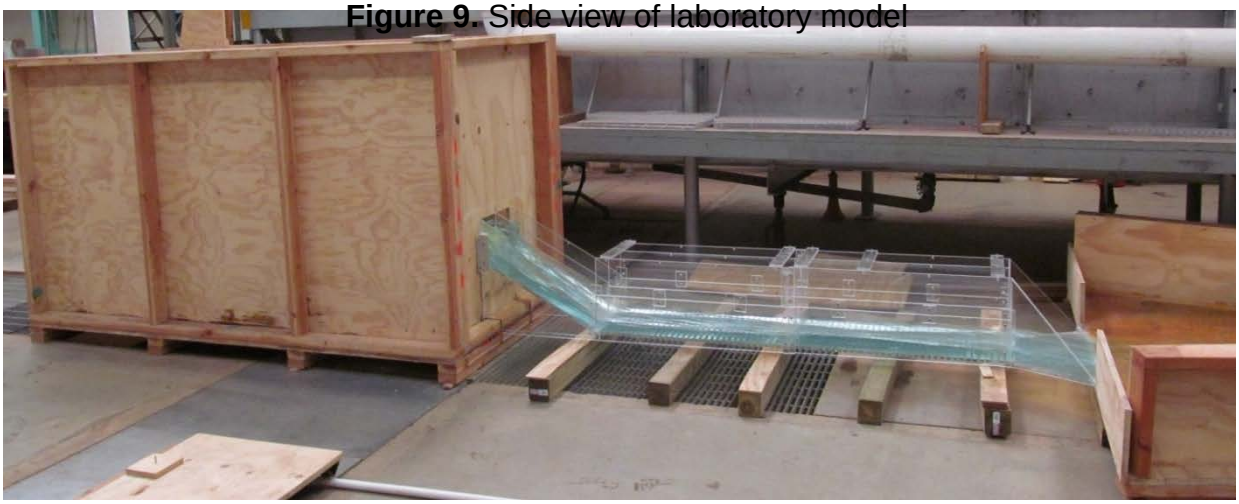

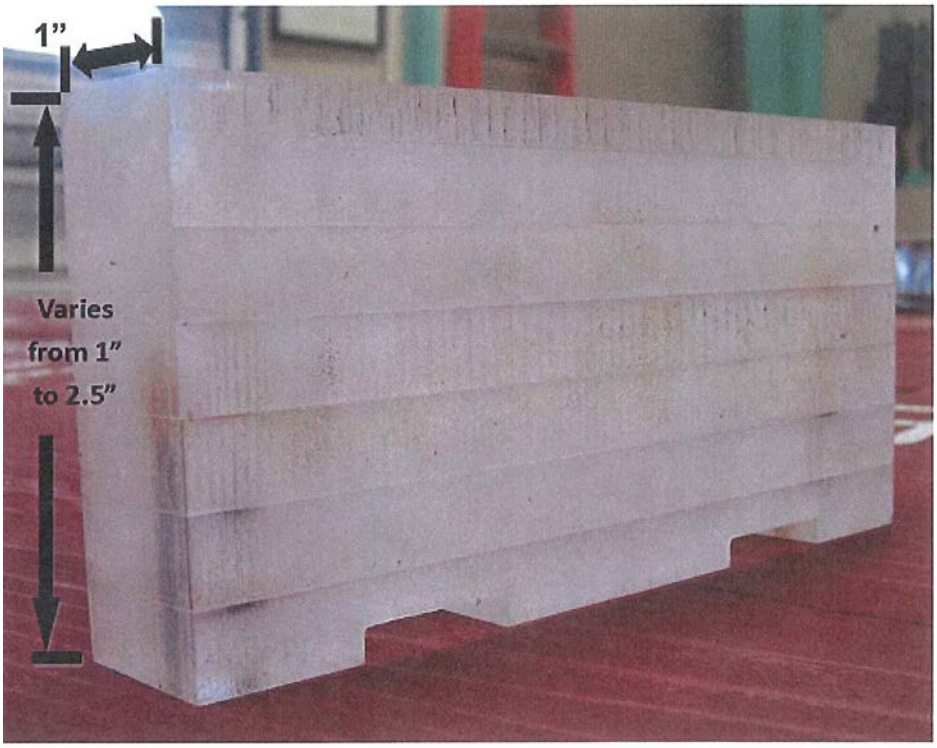

Figure 10. Typical sill dimensions

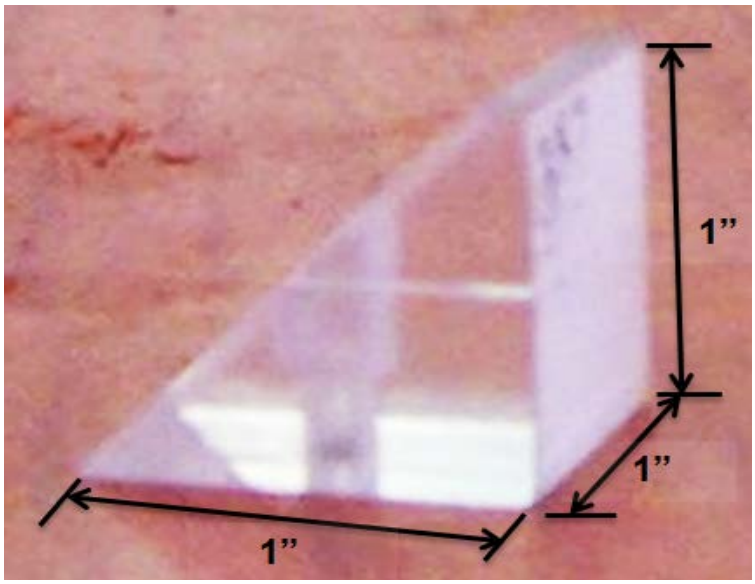

Figure 11. Example of flat faced friction block.

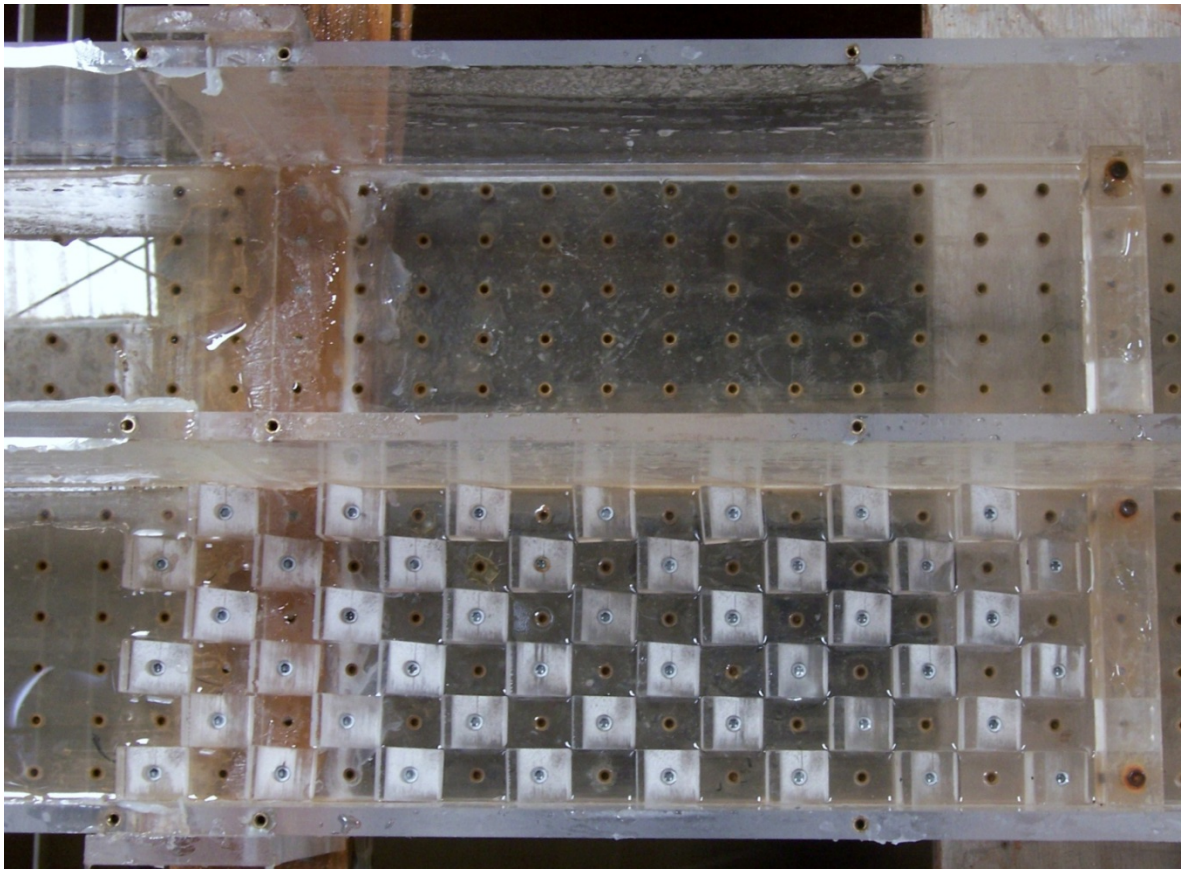

Figure 12. Example of flat faced friction blocks arranged on model bottom.

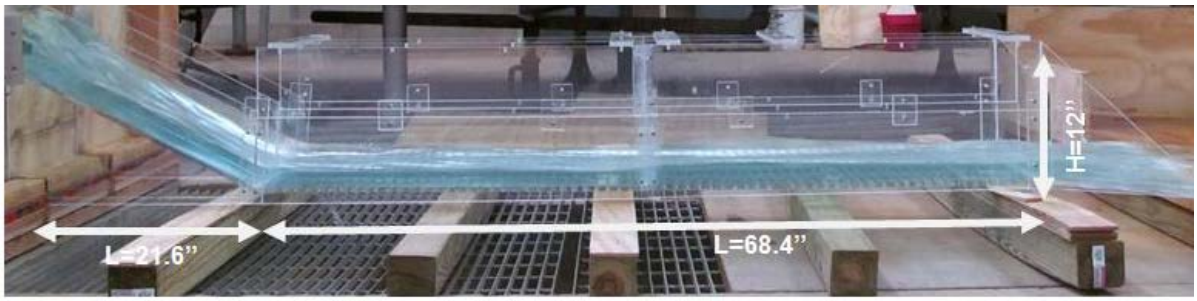

Figure 13. Example of extended channel height to apply open channel condition.

Figure 14. Downstream plywood channel after wingwall.

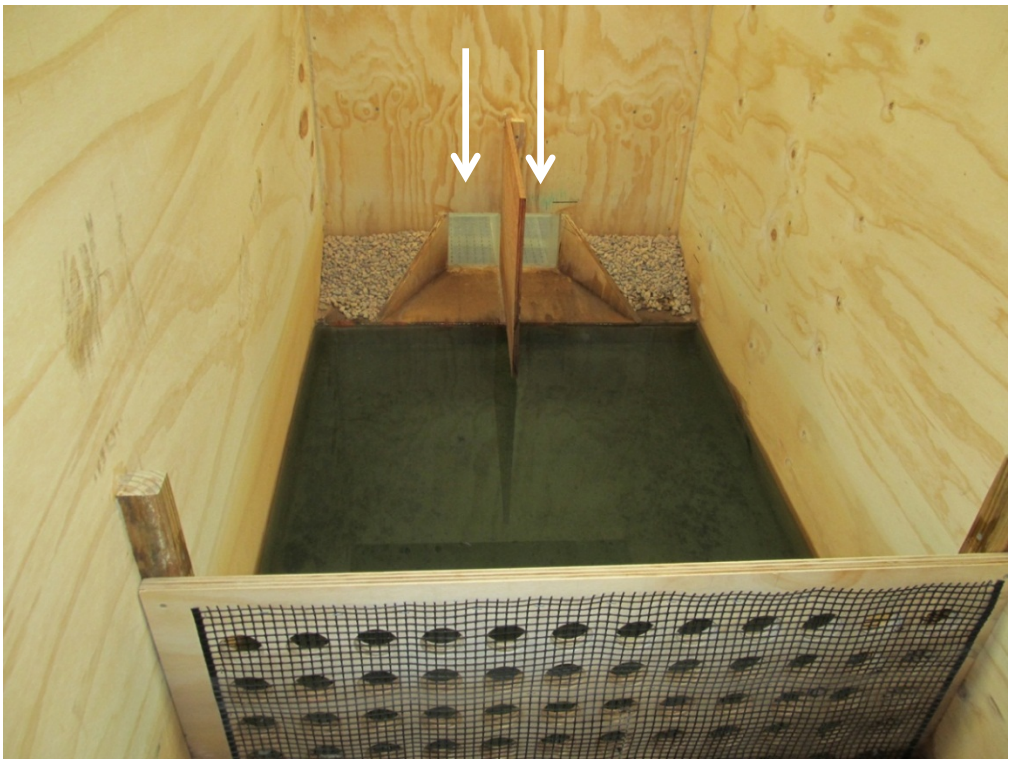

Figure 15. Reservoir and channel inlet for culvert model.

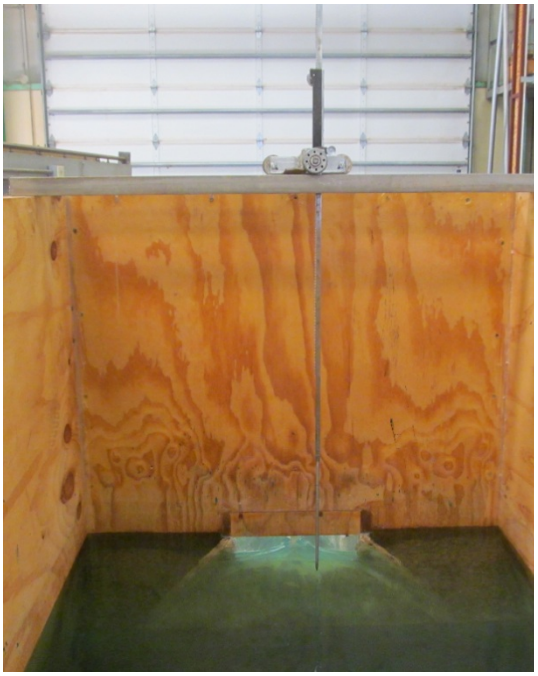

Figure 16-1. Point gauge front view

Figure 16-2. Point gauge side view

Figure 17. ADV plugged in the culvert model connected with the computer

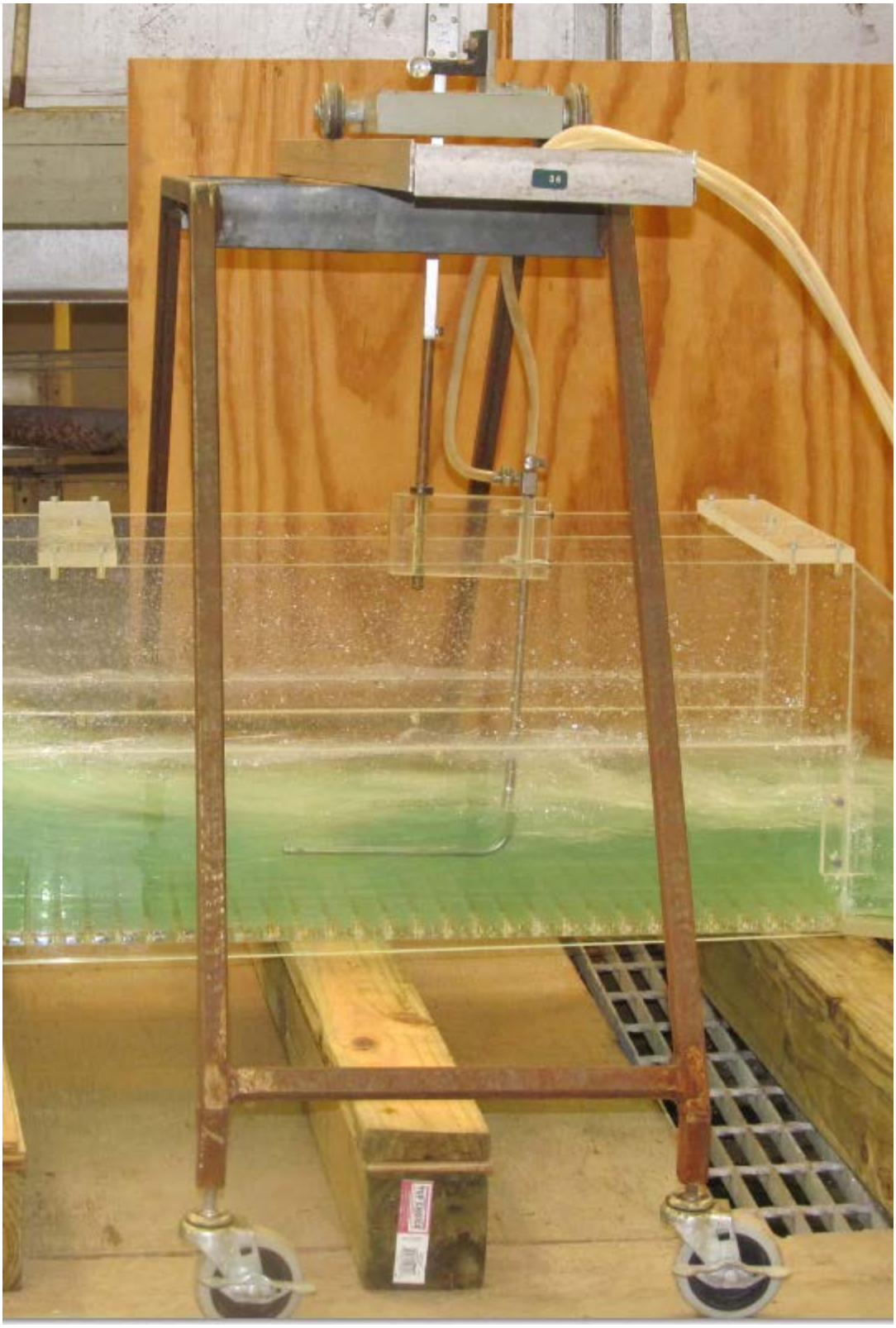

Figure 18. Pitot Tube with mount over the culvert model

5 DATA COLLECTION

Many experiments were conducted to create energy dissipation within a broken-back culvert. 37 experiments were done for this model with variations in length, height, width, and energy dissipators used. Each experiment tested three scenarios. They were run with upstream heads of 0.8d, 1.0d, and 1.2d with each depth denoted by A, B, or C, respectively. In this research, three slopes of Broken-back Culvert were evaluated: 1%, 0.6% and, 0.3%. Experiments were named according to this slope. For example, 8A represents the 8^{th} experiment run at 0.8d with a 1% slope, 13B represents the 13^{th} experiment run at 1.0d with a 0.6% slope, and 18C represents the 18^{th} experiment run at 1.2d with 0.3% slope. A SonTek 2D-side looking MicroADV sonar velocimeter was used to measure the velocity at the intake of the structure, after the hydraulic jump, and at the downstream end of the culvert. 2D-side looking denotes it has two receiver arms to give readings in the x and y planes. Also, a Pitot tube was used to measure velocity at the toe before the hydraulic jump. The flow rates for all experiments were measured for each of them and used to calculate the velocity at the intake of the structure which is at the inlet of the reservoir as shown in Figure 15.

For open channel flow conditions, experiments 1, 9, and 14 were performed to investigate the possibility of a hydraulic jump occurring without friction blocks or sills. For experiments 1 through 8 for 1% slope; and 9 through 13 for 0.6% slope, and 14 through 18 for 0.3% slope, the height of the culvert was 12 inches with the original length of 68.40 inches and width of 6 inches which represented the open channel condition. Different sill heights were used in the experiments. Experiments 2 and 3 were performed with 2-inch, 3-inch sill heights located at the end and middle of the culvert.

The reason for increasing the sill heights was to produce a hydraulic jump located at the toe of the sloped channel in order to maintain subcritical flow throughout the flat section of the Broken-Back culvert. In order to get the optimal location of the hydraulic jump with a lower possible sill height, the sill was moved toward the center of the culvert. Therefore, experiments 5, 10, and 15 were performed with a 3-inch sill height at 26 inches from the end of the culvert. Once these experiments were chosen as a possible solution, further investigation of energy dissipation was necessary. Different configurations and numbers of friction blocks were utilized in the same sill arrangement. Experiments 6, 11, and 16 were performed with fifteen regular flat faced friction blocks.

For pressure flow conditions, experiments 19 through 27 for 1% slope, 28 to 32 for 0.6% slope, and 33 to 37 for 0.3% slope, were run on a model with 2 barrels measuring 6 inches by 6 inches in area and a length of 68.40 inches which represented pressure flow condition. Different configurations of friction blocks and sills were used in the experiments. The selected experiments will be presented in data analysis, and all experiment photos and results can be seen in Appendix A.

In these experiments, the length of the hydraulic jump (L), the depth before the jump (Y_1), the depth after the jump (Y_2), the distance from the beginning of the hydraulic jump to the beginning of the sill (X), the depth of the water in the inclined channel (Y_s), and the depth of the water downstream of the culvert ($Y_{d/S}$) were measured. All dimensions were measured by using a ruler and point gage. The flow rate was measured by a two-plate manometer which measures the pressure difference in a fixed pipe opening size. As mentioned above, the velocity before the jump (V_1) was measured by a Pitot tube and the velocity at the inlet of the structure as seen in Figure

16 ($V_{u/s}$), the velocity after the jump (V_2), and the velocity downstream of culvert ($V_{d/s}$) were all measured by ADV.

The procedure of the experiment is as follows:

1. Install energy dissipation tool (such as sills or friction blocks) in the model
1. Set point gauge to the correct height in the reservoir (for example, Experiment 1A means the head equal to 0.8d) as shown in Figure 16.
2. Turn on pump in station
3. Adjust valve and coordinate the opening to obtain the amount of head for the experiment
4. Record the reading for flow rate (using a two plate manometer)
5. Run the model for 10 minutes before taking measurements (to allow flow to establish)
6. Measure Y_s, Y_1, Y_2, L, X, and $Y_{d/S}$, as seen in Figure 19
7. Measure velocities along the channel $V_{u/s}$, V_1, V_2, and $V_{d/S}$
8. Post process the raw ADV data to determine final velocity values

Post-processing the raw ADV data was essential to maintain data validity. A software program from the Bureau of Reclamation called WinADV was obtained to process the ADV data. The MicroADV was calibrated according to water temperature, salt content, and total suspended solids. The unit was calibrated to the manufacturer's specification for total suspended solids based on desired trace solution water content. At the end of each day of experiments, the reserve was drained to prevent mold growth which could affect the suspended solid concentration of the water. If this change in sediment concentration were to occur, it could minimally affect velocity readings.

The following notations are used as variables key in this report:

H. J. = Hydraulic jump

H = Head upstream of culvert, inches

Q = Flow rate, cfs

Y_s = Water depth at inclined channel, inch

Y_{toe} = Water depth at toe of culvert, inch

Y_1 = Water depth before hydraulic jump in supercritical flow, inch

Y_2 = Water depth after hydraulic jump in subcritical flow, inch

$Y_{d/s}$ = Water depth at downstream of culvert, inch

F_{r1} = Froude Number in supercritical flow

$V_{u/s}$ = Velocity at upstream of culvert, fps

V_1 = Velocity before hydraulic jump in supercritical flow, fps

V_2 = Velocity after hydraulic jump in subcritical flow, fps

$V_{d/s}$ = Velocity downstream of culvert, fps

X = Location of toe of the hydraulic jump to the beginning of the sill, inches

L = Length of hydraulic jump, inch

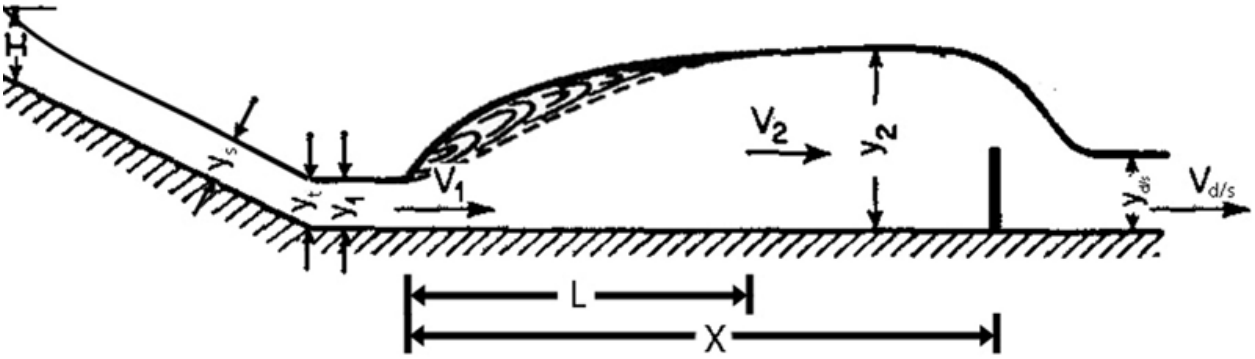

Figure 19. Hydraulic jump variables in a broken-back culvert.

6 DATA ANALYSIS

6.1 Open Channel Flow Conditions

Fifteen experiments were selected from eighteen experiments performed in the hydraulic laboratory. These experiments show the model runs without friction blocks, the effect of sill at the end of the model, with flat faced friction blocks, and the effect of slopes in Broken-Back culvert. After the effectiveness was evaluated, the numbers of blocks were varied by 15, 30, and 45 blocks.

Experiment 1 for 1% slope, 9 for 0.6% slope, and 14 for 0.3% slope were run without any energy dissipation devices or sill in order to allow evaluation the hydraulic characteristics of the model, including the Froude number and supercritical flow conditions. Experiments were run on three different slopes: experiment 1, for 1% slope; experiment 9, for 0.6% slope; and experiment 14, for 0.3% slope. These experiments did not produce a hydraulic jump. The results can be found in Table 1, below.

Table 1. Hydraulic parameters for Experiment 1, 9, and 14

SLOPE	**1%**			**0.6%**			**0.3%**		
CASE	1A	1B	1C	9A	9B	9C	14A	14B	14C
Q (cfs)	0.9481	1.2038	1.5352	0.9852	1.2364	1.6622	0.9852	1.2202	1.5787
$V_{u/s}$ (fps)	2.3703	2.4076	2.5587	2.4630	2.4728	2.7703	2.463	2.4404	2.6312
Y_s (in)	2.12	2.63	3.38	2.13	2.62	3.35	2.00	2.65	3.50
Y_t (in)	1.75	2.25	2.28	1.85	2.38	3.00	1.85	2.25	2.75
Y_1 (in)	1.87	1.75	2.32	1.50	2.00	2.35	1.65	1.85	2.50
$Y_{d/s}$ (in)	1.87	1.75	2.32	1.65	2.00	2.35	1.75	2.00	2.35
F_{r1}	3.4	3.7	3.3	4.1	3.9	3.7	4.1	4.0	3.5
V_1 (fps)	7.7412	8.0328	8.2241	8.2719	8.9722	9.1937	8.7081	8.8669	9.1645

The total head loss between upstream of structure and downstream of structure was calculated by applying the Bernoulli equation:

$$THL = \left(H + \frac{V_{u/s}^2}{2_g} + Z \right) - \left(Y_{d/s} + \frac{V_{d/s}^2}{2_g} \right) \quad (1)$$

Where; THL = Total head loss, inches

H = Water depth upstream of the culvert, inches

Z = Drop between upstream and downstream the model was 0.9 feet, representing a 18-foot drop in the prototype.

The loss of energy or energy dissipation in the jump was calculated by taking the difference between the specific energy before the jump and after the jump

$$\mathrm{AE} = \mathrm{E}_1 - \mathrm{E}_2 = \frac{\left(Y_2 - Y_1\right)^3}{4Y_1Y_2} \quad (2)$$

The efficiency of the jump was calculated by taking the ratio of the specific energy before and after the jump:

$$\frac{\mathrm{E}_2}{\mathrm{E}_1} = \frac{\left(8Fr_1^2 + 1\right)^{3/2} - 4Fr_1^2 + 1}{8Fr_1^2\left(2 + Fr_1^2\right)} \quad (3)$$

Where the downstream depth was known, the following equation was used to calculate the upstream supercritical flow Froude number (Fr) of the hydraulic jump:

$$F_{r1} = \sqrt{\frac{\left(\frac{2Y_2}{Y_1} + 1\right)^2 - 1}{8}} \quad (4)$$

The following equation was used to calculate the Froude number (F_{r1}) of the hydraulic jump:

$$F_{r1} = \frac{V_1}{\sqrt{gY_1}} \quad (5)$$

Experiments 5 (for 1% slope), 10 (for 0.6% slope) and 15 (for 0.3% slope) were run with a 3-inch sill at 26 inches from the end of the culvert, utilizing the increased culvert height of 12 inches. A hydraulic jump was observed in all three flow conditions in all three experiments. The results show that the Froude number values ranged from 3.2 to 3.9. This range of Froude number values is indicative of an Oscillating type of hydraulic jump. In an Oscillating jump, a cyclic jet of water enters the bottom of the jump and then rises to the water surface and back again with no periodicity in cycles. The energy loss due to hydraulic jump ranges between 3.38 inches to 5.28 inches and the total head loss for the whole culvert ranges between 8.47 inches to 9.76 inches. Additional results can be seen in Table 2.

Table 2. Hydraulic parameters for Experiments 5, 10, and 15.

SLOPE	**1%**			**0.6%**			**0.3%**		
CASE	5A	5B	5C	10A	10B	10C	15A	15B	15C
Q (cfs)	0.9354	1.2838	1.5404	0.9973	1.2460	1.6086	0.9354	1.2202	1.5609
$V_{u/s}$ (fps)	2.3385	2.5676	2.5673	2.4933	2.4920	2.6810	2.3385	2.4404	2.6015
Y_s (in)	2.25	2.50	3.50	2.13	2.75	3.13	2.25	2.65	3.25
Y_t (in)	1.65	1.85	2.50	1.75	2.13	2.85	2.00	2.13	2.65
Y_1 (in)	1.65	2.00	2.35	1.65	2.13	2.50	2.00	2.13	2.50
Y_2 (in)	7.50	8.25	9.50	8.25	8.75	9.50	8.00	8.50	9.50
$Y_{d/s}$ (in)	2.25	2.75	3.75	2.35	3.13	3.75	2.75	3.00	3.25
F_{r1}	3.8	3.7	3.6	3.9	3.5	3.2	3.5	3.4	3.3
V_{S1} (fps)	4.4019	5.1118	5.4646	4.5301	5.0943	5.5248	4.5518	4.0730	5.3762
V_{S2} (fps)	5.5310	7.2333	7.5330	5.4618	7.2309	4.8709	6.7574	5.5456	4.5983
V_1 (fps)	7.9409	8.5118	8.9722	8.1940	8.2719	8.3526	8.0250	8.1904	8.4326
V_2 (fps)	2.3166	3.0646	4.0125	2.5900	3.1509	4.1763	2.9757	3.0646	3.4749
$V_{d/s}$ (fps)	5.2572	5.6031	6.1292	5.2470	5.6031	6.0187	5.0913	5.6031	5.7915
L (in)	17.00	20.50	21.00	19.00	21.00	23.00	15.00	20.50	24.00
X (in)	40.00	32.00	37.00	40.00	34.00	35.00	40.00	40.00	41.00
ΔE (in)	4.0445	3.6991	4.0932	5.2800	3.8916	3.6105	3.3750	3.5691	3.6105
THL (in)	9.2190	9.4284	8.4782	9.2783	8.9772	8.8393	9.0390	9.0597	9.7611
E_2/E_1	0.6356	0.6481	0.6613	0.6202	0.6749	0.7076	0.6744	0.6795	0.7032

Experiments 6 (for 1% slope), 11 (for 0.6% slope), and 16 (for 0.3% slope) were run with a 3-inch sill at 26 inches from the end of the culvert with 15 flat faced friction blocks (FFB); utilizing the increased culvert height of 12 inches. A hydraulic jump was observed in all three flow conditions and in the three experiments. The results show that the Froude number values ranged from 3.2 to 3.7. These ranges of Froude number values are indicative of an Oscillating type of hydraulic jump. The energy loss due to hydraulic jump ranges between 1.53 inches to 3.46 inches and the total head loss for the whole culvert ranges between 8.04 inches to 9.45 inches. Additional results can be seen in Table 3.

Table 3. Hydraulic parameters for Experiments 6, 11, and 16.

SLOPE	**1%**			**0.6%**			**0.3%**		
CASE	6A	6B	6C	11A	11B	11C	16A	16B	16C
Q (cfs)	0.9648	1.2396	1.5430	0.9648	1.2776	1.5887	0.9648	1.2396	1.5762
$V_{u/s}$ (fps)	2.4120	2.4792	2.5717	2.4120	2.5552	2.6478	2.4120	2.4792	2.6270
Y_s (in)	2.00	2.75	3.35	2.00	2.85	3.25	2.00	2.75	3.50
Y_t (in)	1.75	2.13	2.50	1.85	2.35	2.85	2.00	2.50	2.75
Y_1 (in)	1.75	2.13	2.35	1.85	2.25	2.65	2.00	2.30	2.65
Y_2 (in)	6.75	7.50	7.00	7.50	8.25	9.25	7.50	8.25	9.75
$Y_{d/s}$ (in)	2.35	2.75	3.25	2.50	3.25	3.50	2.50	3.00	3.75
F_{r1}	3.7	3.6	3.4	3.5	3.3	3.2	3.3	3.5	3.2
V_{S1} (fps)	4.5508	4.9115	5.4721	4.4705	4.6158	5.4689	4.6353	4.7776	5.4448
V_{S2} (fps)	7.0179	7.2080	5.0467	6.9336	6.6699	7.6889	6.7294	7.1900	5.0615
V_1 (fps)	8.0250	8.5902	8.5118	7.7286	8.1412	8.5118	7.5955	8.2719	8.4643
V_2 (fps)	2.5900	3.8417	3.6629	2.5900	3.6629	3.8417	2.3166	3.1509	3.9109
$V_{d/s}$ (fps)	5.2470	5.7356	6.1858	5.2470	5.5550	6.3443	5.3080	5.4329	6.3443
L (in)	18.00	17.00	19.00	18.50	19.50	21.50	18.00	20.00	22.50
X (in)	42.00	33.00	36.00	42.00	39.00	37.00	42.00	38.00	36.00
ΔE (in)	2.6455	2.4234	1.528	3.4298	2.9091	2.9321	2.7729	3.2611	3.4631
THL (in)	9.2041	9.0653	8.8523	9.0541	9.0166	8.3064	8.9341	9.4453	8.0359
E_2/E_1	0.6445	0.6568	0.6861	0.6737	0.6951	0.7124	0.6999	0.6749	0.7149

Experiments 7 (for 1% slope), 12 (for 0.6% slope), and 17 (for 0.3%slope) were run with a 3 inch sill located 26 inches from the end of the culvert. In addition, 30 flat faced friction blocks were placed in the horizontal portion of the channel in the pattern shown in Figure 12. A hydraulic jump was observed in all three flow conditions and in all three experiments. The results show that the Froude number values ranged from 3.2 to 3.8. These ranges of Froude number values are indicative of an Oscillating type of hydraulic jump. The energy loss due to hydraulic jump ranges between 1.46 inches to 4.23 inches and the total head loss for the whole culvert ranges between 7.95 inches to 9.1212 inches. The efficiency of the hydraulic jump in these experiments ranges from 0.63 to 0.71. Additional results can be seen in Table 4.

Table 4. Hydraulic parameters for Experiments 7, 12, and 17.

SLOPE	**1%**			**0.6%**			**0.3%**		
CASE	7A	7B	7C	12A	12B	12C	17A	17B	17C
Q (cfs)	0.9648	1.2364	1.5837	0.9771	1.2619	1.6550	0.9812	1.2460	1.6037
$V_{u/s}$ (fps)	2.4120	2.4728	2.6395	2.4428	2.5238	2.7583	2.4530	2.4920	2.6728
Y_s (in)	2.00	2.63	3.25	2.00	2.63	3.50	2.00	2.75	3.50
Y_t (in)	1.75	2.13	2.75	1.85	2.50	3.00	1.75	2.25	2.75
Y_1 (in)	1.75	2.13	2.63	1.85	2.13	2.55	1.75	2.25	2.50
Y_2 (in)	6.50	9.00	7.50	7.50	7.50	9.75	7.75	8.00	10.00
$Y_{d/s}$ (in)	2.35	3.50	3.50	2.50	3.25	3.75	2.35	3.5	3.63
F_{r1}	3.8	3.5	3.3	3.6	3.5	3.2	3.7	3.4	3.3
V_{S1} (fps)	4.6562	5.2405	5.6250	4.7294	5.1103	5.5453	4.5637	5.0754	5.4838
V_{S2} (fps)	6.7764	6.6885	7.6331	6.9819	7.3877	7.3454	6.9719	7.3877	7.5698
V_1 (fps)	8.1904	8.4580	8.7081	7.9409	8.2881	8.3943	7.9746	8.3526	8.4326
V_2 (fps)	2.4626	4.0985	4.3340	2.3166	3.6629	4.0125	2.3166	3.4749	4.1763
$V_{d/s}$ (fps)	5.3080	5.7915	6.4906	5.2470	5.5550	6.2377	5.3080	5.4329	6.0631
L (in)	17.00	19.00	19.00	18.00	16.00	22.50	17.00	15.00	22.0
X (in)	42.00	36.00	40.00	39.00	40.00	40.00	42.00	34.00	42.00
ΔE (in)	2.3554	4.2285	1.4639	3.2498	2.4234	3.7531	3.9816	2.6404	4.2188
THL (in)	9.0841	8.1894	7.9482	9.0819	8.9869	8.4177	9.1212	8.9572	8.8512
E_2/E_1	0.6338	0.6645	0.7000	0.6611	0.6740	0.7099	0.6462	0.6831	0.7032

Experiments 8 (for 1% slope), 13 (for 0.6% slope), 18 (for 0.3% slope) were run with a 3-inch sill located 26 inches from the end of the culvert. In addition, 45 flat faced friction blocks were placed in the horizontal portion of the channel in the pattern shown in Figure 5. A hydraulic jump was observed in all three flow conditions. The results show that the Froude number values ranged from 3.2 to 3.7. These ranges of Froude number values are indicative of an Oscillating type of hydraulic jump. The energy loss due to hydraulic jump ranges between 2.49 inches to 3.61 inches; the total head loss for the whole culvert ranges between 8.30 inches to 9.29 inches. The energy dissipation ranges from 0.64 to 0.71. Additional results can be seen in Table 5.

Table 5. Hydraulic parameters for Experiments 8, 13, and 18.

SLOPE	1%			0.6%			0.3%		
CASE	8A	8B	8C	13A	13B	13C	18A	18B	18C
Q (cfs)	0.9606	1.2619	1.5987	0.9268	1.2588	1.5862	0.9565	1.2651	1.5762
$V_{u/s}$ (fps)	2.4015	2.5238	2.6645	2.3170	2.5176	2.6437	2.3913	2.5302	2.6270
Y_s (in)	1.85	2.85	3.13	1.87	2.75	3.35	2.25	2.85	3.25
Y_t (in)	1.75	2.13	2.75	2.00	2.13	2.75	2.13	2.25	2.75
Y_1 (in)	1.75	2.13	2.65	2.00	2.00	2.50	2.00	2.13	2.50
Y_2 (in)	7.00	7.85	9.50	7.50	8.00	9.00	7.25	8.50	9.50
$Y_{d/s}$ (in)	2.25	3.00	3.50	2.62	3.25	3.50	2.63	3.00	3.50
F_{r1}	3.7	3.5	3.3	3.4	3.5	3.2	3.3	3.5	3.3
V_{S1} (fps)	4.5499	5.0552	5.3756	4.6030	4.9160	5.4886	4.6030	5.0519	5.4694
V_{S2} (fps)	6.7574	5.1002	7.5539	6.8203	5.2614	7.5129	6.9602	7.2495	7.4927
V_1 (fps)	8.1081	8.2719	8.8214	7.8149	8.1904	8.3526	7.6833	8.3526	8.4326
V_2 (fps)	2.8373	4.1763	3.0646	2.3166	3.2762	4.0125	2.0062	3.8417	4.0125
$V_{d/s}$ (fps)	5.2470	5.7915	6.2805	5.1801	5.7915	6.3443	5.3080	5.5550	6.2377
L (in)	18.00	17.00	22.00	14.00	19.00	21.00	17.00	20.00	22.00
X (in)	39.00	34.00	33.00	42.00	40.00	39.00	42.00	39.00	37.00
ΔE (in)	2.9531	2.7982	3.1918	2.7729	3.3750	3.0514	2.4949	3.5619	3.6105
THL (in)	9.2946	8.7369	8.4729	8.9803	8.4811	8.3023	8.7855	9.2429	8.5359
E_2/E_1	0.6385	0.6749	0.6958	0.6867	0.6649	0.7076	0.6946	0.6704	0.7032

6.2 Pressure Flow Conditions

Nine experiments were selected from nineteen experiments performed in the hydraulic laboratory. These experiments show model runs without friction blocks, the effect of a sill at the end of the model, the effect of slopes in a Broken-Back culvert, and with friction blocks of different shapes as well as the sill. The flat faced friction blocks are used (see Figure 11). After the effectiveness was evaluated, the numbers of blocks were varied by 15, 30, and 45.

In these experiments, the optimum sill height was determined first, the optimum sill location was found next, and finally the effectiveness of friction blocks in combination with the optimum sill parameters was determined.

To solve the momentum equation for pressure flow conditions in the culvert hydraulic jump and then to simplify the solution graphically, numerous studies have been done for open channel flow conditions derived from the Belanger equation which expresses the ratio between sequent depths as functions of the upstream Froude number (Chow 1959, Lowe et al. 2011). Chow stated the hydraulic jump will form in the channel if the F_{r1} of the flow, the flow depth Y_1, and the depth after hydraulic jump Y_2 satisfy the following equation:

$$\frac{Y_2}{Y_1} = \left[\frac{1}{2} \left(\sqrt{1 + 8F_{r1}^2} - 1 \right) \right] \quad (6)$$

So, from the above equation, Y_2 can be calculated as following:

$$Y_2 = Y_1 \left[\frac{1}{2} \left(\sqrt{1 = 8 f_{r1}^2} - 1 \right) \right] \quad (7)$$

Experiments 19 (for 1% slope), 28 (for 0.6% slope), and 33 (for 0.3% slope) were run without any energy dissipation devices or sill in order to evaluate the hydraulic characteristics of the model, including the Froude number and supercritical flow conditions. This experiment is also an example of the current field practice to allow the kinetic energy of fluid to be transferred downstream without energy reduction. This experiment did not produce a hydraulic jump. The results can be found in Table 6, below.

Table 6. Hydraulic parameters for Experiments 19, 28, and 33.

SLOPE	**1%**			**0.6%**			**0.3%**		
CASE	19A	19B	19C	28A	28B	28C	33A	33B	33C
Q (cfs)	0.9771	1.2656	1.5736	0.9648	1.2524	1.5862	0.9648	1.2524	1.5962
$V_{u/s}$ (fps)	2.4428	2.5312	2.6227	2.412	2.5048	2.6437	2.4120	2.5048	2.6603
Y_s (in)	2.13	2.75	2.83	2.00	2.75	2.85	1.85	2.85	3.25
Y_t (in)	1.85	2.25	2.75	1.85	2.25	2.75	1.75	2.13	2.75
Y_1 (in)	1.75	2.00	2.50	1.35	1.85	2.35	1.50	1.85	2.50
$Y_{d/s}$ (in)	1.75	2.00	2.50	1.50	2.00	3.50	1.65	2.13	2.35
F_{r1}	3.9	3.7	3.5	4.6	4.0	3.6	4.3	4.0	3.5
V_1 (fps)	8.4326	8.6679	8.9722	8.7081	8.8214	9.0466	8.5902	8.8214	9.0466
THL (in)	2.9619	2.2438	1.8817	3.9341	2.4691	1.8023	4.0341	3.8391	3.7188

Experiments 24 (for 1% slope) , 29 (for 0.6% slope), and 34 (for 0.3% slope) were run with two sills: a 1.5-inch sill located at 37 inches from the end of the culvert and a 2-inch sill located at 27 inches from the end of the culvert. These experiments demonstrate the use of one sill to control the hydraulic jump under pressure flow conditions. Pressure flow is defined by the fluid excreting pressure against the top of the model. A hydraulic jump was observed in all experiments and three flow conditions. The results show that the Froude number values ranged from 3.3 to 4.3. These ranges of Froude number values are indicative of an Oscillating hydraulic jump. The total head loss for the whole culvert ranges between 7.71 inches to 9.59 inches. Additional results can be seen in Table 7.

Table 7. Hydraulic parameters for Experiments 24, 29, and 34.

SLOPE	**1%**			**0.6%**			**0.3%**		
CASE	24A	24B	24C	29A	29B	29C	34A	34B	34C
Q (cfs)	0.9523	1.2524	1.5987	0.9648	1.2524	1.6086	0.9565	1.2460	1.6012
$V_{u/s}$ (fps)	2.3808	2.5048	2.6645	2.4120	2.5048	2.6810	2.3913	2.4920	2.6687
Y_s (in)	1.85	2.85	3.25	2.00	2.75	2.50	1.85	2.65	3.25
Y_t (in)	1.75	2.50	2.85	1.75	1.13	2.75	1.75	3.25	2.85
Y_1 (in)	1.35	2.00	2.65	1.50	1.75	2.50	1.50	2.00	2.50
Y_2 (in)	7.65	9.63	11.29	8.03	8.97	10.65	8.28	9.76	10.44
$Y_{d/s}$ (in)	2.85	3.35	4.25	3.00	3.25	3.75	2.75	3.25	4.25
F_{r1}	4.3	3.7	3.3	4.1	4.0	3.3	4.2	3.9	3.3
V_{S1} (fps)	4.4978	4.9681	5.4829	4.4797	4.9952	5.4262	4.5755	4.9698	5.3987
V_{S2} (fps)	6.4887	7.2337	7.5416	6.4730	7.1493	7.5762	6.5590	7.3700	7.5933
V_1 (fps)	8.2719	8.6679	8.9272	8.2719	8.5902	8.6679	8.5118	8.7756	8.5118
V_2 (fps)	4.1763	5.9062	6.7540	3.0646	4.9143	4.9143	5.7915	6.7510	4.3340
$V_{d/s}$ (fps)	4.9143	5.5550	6.0187	5.1018	5.6745	5.6745	5.1801	6.1292	6.0187
L (in)	11.00	12.00	13.50	9.00	9.00	14.00	8.00	9.00	15.00
X (in)	49.00	53.00	60.00	49.00	49.00	62.00	51.00	50.00	66.00
ΔE (in)	6.0529	5.7660	5.3909	5.7764	6.0025	5.0803	6.2759	5.9865	4.7893
E_2/E_1	0.5707	0.6396	0.6919	0.5946	0.6127	0.6921	0.5816	0.6339	0.7007
THL (in)	9.3061	8.8691	8.3229	8.8341	8.7191	9.5893	8.9155	7.7072	8.3270

Experiments 25 (for 1% slope), 30 (for 0.6% slope), and 35 (for 0.3% slope) were run with two sills: a 1.5-inch sill located at 37 inches from the end of the culvert and a 2-inch sill located at 27 inches from the end of the culvert and 15 flat faced friction blocks. These experiments demonstrate the use of two sills to control the hydraulic jump under open channel and pressure flow conditions. Pressure flow is defined by the fluid-excreting pressure against the top of the model. A hydraulic jump was observed in all experiments and three flow conditions. The results show that the Froude number values ranged from 2.9 to 3.9. These ranges of Froude number values are indicative of an oscillating hydraulic jump. The total head loss for the whole culvert ranges between 8.05 inches to 9.79 inches. Additional results can be seen in Table 8.

Table 8. Hydraulic parameters for Experiments 25, 30, and 35.

SLOPE	1%			0.6%			0.3%		
CASE	25A	25B	25C	30A	30B	30C	35A	35B	35C
Q (cfs)	0.9606	1.2524	1.5812	0.9648	1.2534	1.5812	0.9565	1.2524	1.5837
$V_{u/s}$ (fps)	2.4015	2.5048	2.6353	2.4120	2.5068	2.6353	2.3913	2.5048	2.6395
Y_s (in)1.85	1.85	2.85	3.25	1.85	2.85	3.50	1.85	2.75	3.25
Y_t (in)	1.75	2.13	3.00	1.75	2.25	3.25	1.75	2.25	3.00
Y_1 (in)	1.75	2.25	3.00	1.75	2.13	3.00	1.75	2.13	3.00
Y_2 (in)	7.54	9.22	10.72	8.75	9.91	10.72	8.89	9.96	10.84
$Y_{d/s}$ (in)	2.75	3.25	4.00	2.75	3.50	4.25	2.75	3.75	4.25
F_{r1}	3.4	3.2	2.9	3.9	3.6	2.9	3.9	3.6	2.9
V_{S1} (fps)	4.4772	4.9507	5.3514	4.4683	4.4061	5.4642	4.4098	4.9567	5.3757
V_{S2} (fps)	7.0530	7.1713	7.1927	6.7016	7.1991	7.4309	6.8428	7.2124	7.5118
V_1 (fps)	7.3258	7.9409	8.1081	8.3943	8.6679	8.1081	8.5118	8.7081	8.1904
V_2 (fps)	3.6629	5.0489	5.1801	3.2762	4.7079	4.7079	3.2762	5.3080	7.0457
$V_{d/s}$ (fps)	4.9143	5.1801	5.7915	4.7079	5.5065	6.0187	4.7079	5.3080	6.1292
L (in)	7.50	8.00	12.00	8.00	9.00	11.00	7.00	9.00	12.00
X (in)	62.50	60.00	68.00	60.00	61.00	68.40	61.00	61.00	68.40
ΔE (in)	3.6737	4.0804	3.5733	5.6032	5.5747	3.5733	5.8409	5.6549	3.7035
E_2/E_1	0.6873	0.7085	0.7657	0.6234	0.6544	0.7657	0.6170	0.6522	0.7611
THL (in)	9.4246	9.7191	9.0441	9.8041	8.8209	8.2941	9.7855	8.9691	8.0482

Experiments 26 (for 1% slope), 31 (for 0.6% slope), and 36 (for 0.3% slope) were run with two sills: a 1.5-inch sill located at 37 inches from the end of the culvert and a 2-inch sill located at 27 inches from the end of the culvert and 30 flat faced friction blocks. These experiments demonstrate the use of two sills to control the hydraulic jump under open channel and pressure flow conditions. A hydraulic jump was observed in all experiments and three flow conditions. The results show that the Froude number values ranged from 2.8 to 3.9. These ranges of Froude number values are indicative of an oscillating hydraulic jump. The total head loss for the whole culvert ranges between 7.82 inches to 11.68 inches. Additional results can be seen in Table 9.

Table 9. Hydraulic parameters for Experiments 26, 31, and 36.

SLOPE	1%			0.6%			0.3%		
CASE	26A	26B	26C	31A	31B	31C	36A	36B	36C
Q (cfs)	0.9771	1.2524	1.6012	0.9648	1.2425	1.5635	0.9648	1.2460	1.5987
$V_{u/s}$ (fps)	2.4428	2.5048	2.6687	2.4120	2.4850	2.6058	2.4120	2.4920	2.6645
Y_s (in)	2.00	2.85	3.50	1.85	2.75	3.50	1.85	2.75	3.35
Y_t (in)	1.75	2.13	3.00	1.75	2.25	2.75	1.75	1.25	3.00
Y_1 (in)	1.75	2.00	3.00	1.75	2.13	2.75	1.75	2.00	3.00
Y_2 (in)	8.61	8.95	10.96	8.89	9.96	10.26	7.74	9.57	10.59
$Y_{d/s}$ (in)	2.75	3.25	4.25	2.75	3.50	4.25	3.25	3.50	4.25
F_{r1}	3.8	3.5	2.9	3.9	3.6	2.8	3.5	3.7	2.8
V_{S1} (fps)	4.6042	4.9249	5.2757	4.4289	4.8886	5.4364	4.1903	5.0529	5.5069
V_{S2} (fps)	6.9389	7.2291	7.4947	6.7692	7.1114	6.9282	6.1663	6.9197	6.5599
V_1 (fps)	8.2719	8.1081	8.2719	8.5118	8.7081	8.0683	7.5067	8.6214	8.0250
V_2 (fps)	2.4626	4.0125	5.5065	4.1763	5.2470	5.3080	3.2762	4.3340	5.4329
$V_{d/s}$ (fps)	4.7758	5.5065	6.1858	3.4749	5.3583	6.1292	4.7758	5.4329	6.2377
L (in)	8.00	8.00	12.00	8.00	9.00	12.00	8.00	9.00	12.00
X (in)	60.00	60.00	68.00	61.00	61.00	68.40	60.00	61.00	68.40
ΔE (in)	5.3609	4.6884	3.8348	5.8409	5.6549	3.7504	3.9709	5.6720	3.442
E_2/E_1	0.6303	0.6710	0.7565	0.6170	0.6522	0.7480	0.6758	0.6421	0.7704
THL (in)	9.7119	9.0691	7.9470	11.6841	9.1007	8.0153	9.1841	8.9572	7.8229

Experiments 27 (for 1% slope), 32 (for 0.6 slope), and 37(for 0.3 slope) were run with two sills: a 1.5-inch sill located 37 inches from the end of the culvert and a 2-inch sill located at 27 inches from the end of the culvert and 45 flat faced friction blocks. These experiments demonstrate the use of two sills to control the hydraulic jump under pressure flow conditions. Experiment 27, 32, and 37 were chosen for two reasons: (1) a hydraulic jump formed inside the horizontal section of the model for all three flow conditions, and (2) it is an example of the field being under pressure due to the confines of the model. This experiment produced a hydraulic jump for all three conditions. Pressure flow is defined by the fluid excreting pressure against the top of the model. A hydraulic jump was observed in all experiments and three flow conditions. The results

show that the Froude number values ranged from 3.1 to 3.9. These ranges of Froude number values are indicative of an oscillating hydraulic jump. The total head loss for the whole culvert ranges between 7.81 inches to 9.68 inches. Additional results can be seen in Table 10.

Table 10. Hydraulic parameters for Experiments 27, 32, and 37.

SLOPE	**1%**			**0.6%**			**0.3%**		
CASE	27A	27B	27C	32A	32B	32C	37A	37B	37C
Q (cfs)	0.9648	1.2524	1.5762	0.9648	1.2524	1.5937	0.9656	1.2556	1.5635
$V_{u/s}$ (fps)	2.4120	2.5048	2.6270	2.4120	2.5048	2.6562	2.3913	2.5112	2.6058
Y_s (in)	1.85	2.85	3.13	1.85	2.75	3.35	1.85	2.75	3.50
Y_t (in)	1.75	2.13	2.75	1.85	2.13	2.65	1.65	2.25	2.65
Y_1 (in)	1.75	2.00	2.50	1.75	2.00	2.50	1.50	2.13	2.50
Y_2 (in)	8.89	9.44	10.00	8.83	9.44	10.00	6.9352	9.2479	9.7755
$Y_{d/s}$ (in)	2.75	3.25	3.75	2.75	3.25	4.00	2.75	3.25	3.75
F_{r1}	3.9	3.7	3.1	3.9	3.7	3.1	3.6	3.4	3.1
V_{S1} (fps)	4.5233	5.0140	4.8963	4.5059	5.0772	5.3528	4.4332	4.2472	5.4555
V_{S2} (fps)	6.9423	7.1733	7.4953	6.9625	7.3695	7.6226	6.6984	7.1428	7.6597
V_1 (fps)	8.5118	8.5118	8.1904	8.4643	8.5118	8.1904	7.2336	8.1412	8.0250
V_2 (fps)	4.0125	2.3166	3.2762	3.7712	4.3340	6.4492	5.3583	4.3340	6.3443
$V_{d/s}$ (fps)	4.9143	5.6745	6.3443	4.7758	5.5550	6.3443	4.8317	5.5550	6.2377
L (in)	7.50	9.00	10.00	8.00	9.00	11.00	8.00	9.00	12.00
X (in)	61.00	60.00	61.00	60.00	60.00	61.00	61.00	61.00	62.00
ΔE (in)	5.8409	5.4538	4.2188	5.7443	5.4538	4.2188	3.8587	4.5769	3.9396
E_2/E_1	0.6170	0.6481	0.7188	0.6196	0.6481	0.7188	0.6570	0.6839	0.7283
THL (in)	9.4341	8.7191	8.0359	9.6841	8.9691	7.8146	9.5655	8.9751	8.2653

7 RESULTS

7.1 Open Channel Flow Condition

After careful evaluation, Experiments 5 (for 1% slope), 10 (for 0.6% slope), and 15 (for 0.3% slope) were selected from the data analysis portion for open channel flow conditions. These experiments were selected by examining many factors, including their relatively low downstream velocities, high total hydraulic head losses, acceptable hydraulic jump efficiency, and possible reduction in channel length. These experiments have similar sill arrangements, which consist of a 3-inch sill at 26 inches from the end of the culvert; and three different slopes: 1%, 0.6%, and 0.3%. It was found that these experiments yielded results most applicable to the new construction of culverts due to the increased ceiling height of the culvert. The culvert barrel could be reduced by reducing a section at the end of the channel where the water surface profile is more uniform. Figure 17 shows characteristics of the hydraulic jump for Experiment 5, Figure 18 shows characteristics of Experiment 10, and Figure 19 shows Experiment 15 characteristics; all are included in Table 11.

Table 11. Selected factors for Experiments 5, 10, and 15.

SLOPE	**1%**			**0.6%**			**0.3%**		
CASE	5A	5B	5C	10A	10B	10C	15A	15B	15C
Q (cfs)	0.9354	1.2838	1.5404	0.9973	1.2460	1.6086	0.9354	1.2202	1.5609
$V_{u/s}$ (fps)	2.3385	2.5676	2.5673	2.4933	2.4920	2.6810	2.3385	2.4404	2.6015
Y_1 (in)	1.65	2.00	2.35	1.65	2.13	2.50	2.00	2.13	2.50
Y_2 (in)	7.50	8.25	9.50	8.25	8.75	9.50	8.00	8.50	9.50
V_1 (fps)	7.9409	8.5118	8.9722	8.1940	8.2719	8.3526	8.0250	8.1904	8.4326
V_2 (fps)	2.3166	3.0646	4.0125	2.5900	3.1509	4.1763	2.9757	3.0646	3.4749
ΔE (in)	4.0445	3.6991	4.0932	5.2800	3.8916	3.6105	3.3750	3.5691	3.6105
E_2/E_1	0.6356	0.6481	0.6613	0.6202	0.6749	0.7076	0.6744	0.6795	0.7032
THL (in)	9.2190	9.4284	8.4782	9.2783	8.9772	8.8393	9.0390	9.0597	9.7611
Culvert Reduction (ft)	43	41	40	43	43	40	43	41	40

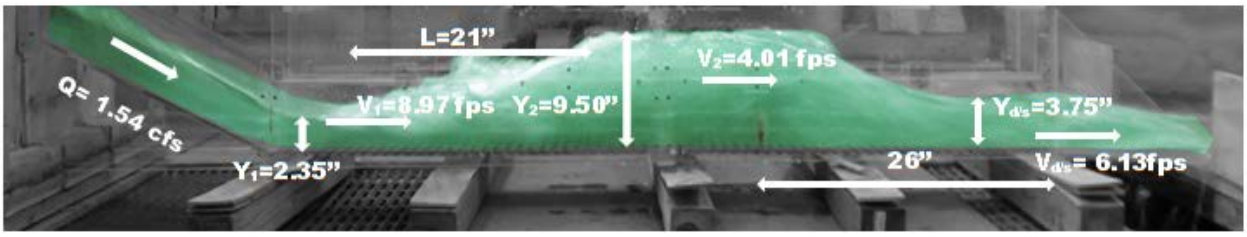

Figure 20. Hydraulic jump characteristics for Experiment 5C. 1% slope. 1.2d.

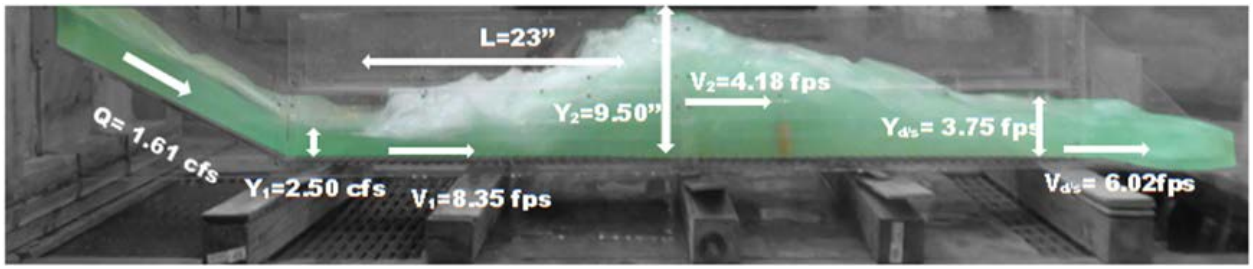

Figure 21. Hydraulic jump characteristics for Experiment 10C. 0.6% slope, 1.2d.

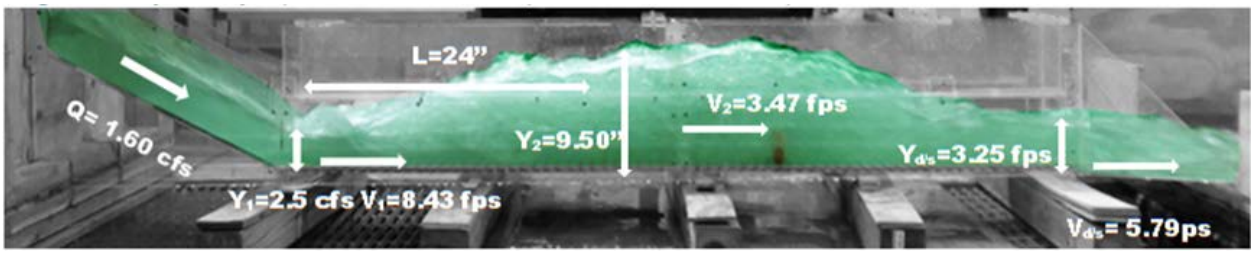

Figure 22. Hydraulic jump characteristics for Experiment 15C. 0.3% slope, 1.2d.

Experiments 6 (for 1% slope), 11 (for 0.6% slope), and 16 (for 0.3% slope) were selected from the data analysis portion for an open channel flow conditions. These experiments were selected by examining many factors, including their relatively low downstream velocities, high total hydraulic head losses, acceptable hydraulic jump efficiency, and possible reduction in channel length. These experiments have similar sill arrangements, which consist of a 3-inch sill at 26 inches from the end of the culvert with 15 flat faced friction blocks; and three different slopes: 1%, 0.6%, and 0.3%. With these experiments, it was found that the friction blocks represented only a 2% increase in the energy dissipation; therefore, they are not economically or practically adequate to the culvert. The culvert barrel could be reduced by reducing a section at the end of the channel where the water surface profile is more uniform. Selected factors for the experiments are included in Table 12.

Table 12. Selected factors for Experiments 6, 11, and 16.

SLOPE	**1%**			**0.6%**			**0.3%**		
CASE	6A	6B	6C	11A	11B	11C	16A	16B	16C
Q (cfs)	0.9648	1.2396	1.5430	0.9648	1.2776	1.5887	0.9648	1.2396	1.5762
$V_{u/s}$ (fps)	2.4120	2.4792	2.5717	2.4120	2.5552	2.6478	2.4120	2.4792	2.6270
Y_1 (in)	1.75	2.13	2.35	1.85	2.25	2.65	2.00	2.13	2.65
Y_2 (in)	6.75	7.50	7.00	7.50	8.25	9.25	7.50	8.25	9.75
V_1 (fps)	8.0250	8.5902	8.5118	7.7286	8.1412	8.5118	7.5955	8.2719	8.4643
V_2 (fps)	2.5900	3.8417	3.6629	2.5900	3.6629	3.8417	2.3166	3.1509	3.9109
ΔE (in)	2.6455	2.4234	1.528	3.4298	2.9091	2.9321	2.7729	3.2611	3.4631
THL (in)	9.2041	9.0653	8.8523	9.0541	9.0166	8.3064	8.9341	9.4453	8.0359
E_2/E_1	0.6445	0.6568	0.6861	0.6737	0.6951	0.7124	0.6999	0.6749	0.7149
Culvert Reduction (ft)	43	41	40	43	43	40	43	41	40

7.2 PRESSURE FLOW CONDITIONS

After careful evaluation, Experiments 24 (for 1% slope), 29 (for 0.6% slope), and 34 (for 0.3% slope) were selected from the data analysis portion for pressure flow conditions. These experiments were selected by examining many factors; including their relatively low downstream velocities, high total hydraulic head losses, and possible reduction in channel length. These experiments have similar sill arrangements, which consist of a 2-inch sill at 27 inches from the end of the culvert and a 1.5-inch sill at 37 inches from the end of the culvert; and three different slopes: 1%, 0.6%, and 0.3%. It was found that these experiments yielded results most applicable to modifying existing culverts with the addition of sills and/or friction blocks. The culvert barrel could be reduced by reducing a section at the end of the channel where the water surface profile is more uniform. Figure 20 shows characteristics of the hydraulic jump for Experiment 24C, Figure 21 shows characteristics for Experiment 29C, and Figure 22 shows Experiment 34C characteristics; all are included in Table 13.

Table 13. Selected factors for Experiments 24, 29, and 34.

SLOPE	**1%**			**0.6%**			**0.3%**		
CASE	24A	24B	24C	29A	29B	29C	34A	34B	34C
Y_1 (in)	1.35	2.00	2.65	1.50	1.75	2.50	1.50	2.00	2.50
Y_2 (in)	7.65	9.63	11.29	8.03	8.97	10.65	8.28	9.76	10.44
$Y_{d/s}$ (in)	2.85	3.35	4.25	3.00	3.25	3.75	2.75	3.25	4.25
V_1 (fps)	8.2719	8.6679	8.9272	8.2719	8.5902	8.6679	8.5118	8.7756	8.5118
V_2 (fps)	4.1763	5.9062	6.7540	3.0646	4.9143	4.9143	5.7915	6.7510	4.3340
$V_{d/s}$ (fps)	4.9143	5.5550	6.0187	5.1018	5.6745	5.6745	5.1801	6.1292	6.0187
ΔE (in)	6.0529	5.7660	5.3909	5.7764	6.0025	5.0803	6.2759	5.9865	4.7893
E_2/E_1	0.5707	0.6396	0.6919	0.5946	0.6127	0.6921	0.5816	0.6339	0.7007
THL (in)	9.3061	8.8691	8.3229	8.8341	8.7191	9.5893	8.9155	7.7072	8.3270
Culvert Reduction (ft)	40	38	30	40	35	25	36	32	25

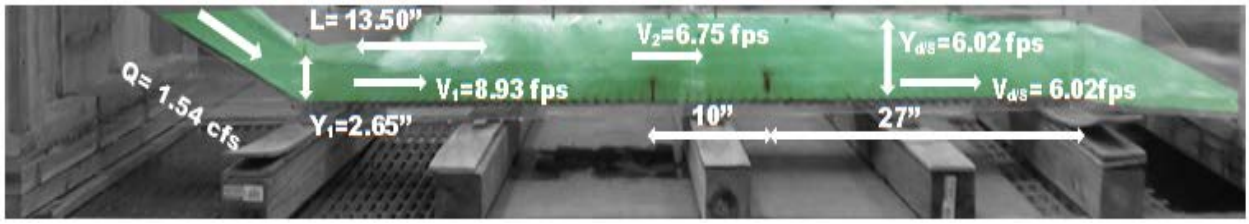

Figure 23. Hydraulic jump characteristics for Experiment 24C for 1% slope. 1.2d.

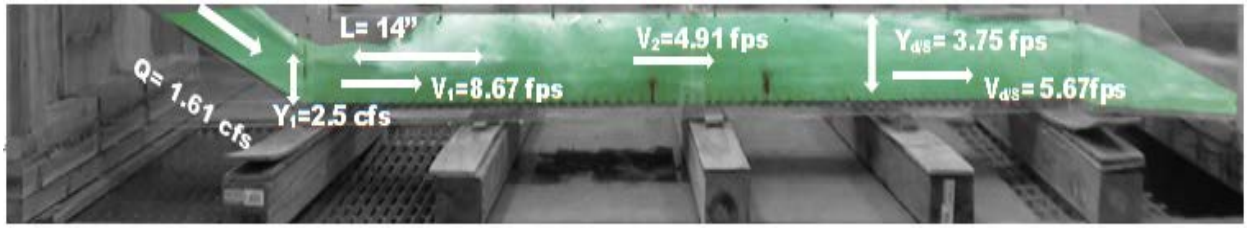

Figure 24. Hydraulic jump characteristics for Experiment 29C for 0.6% slope, 1.2d.

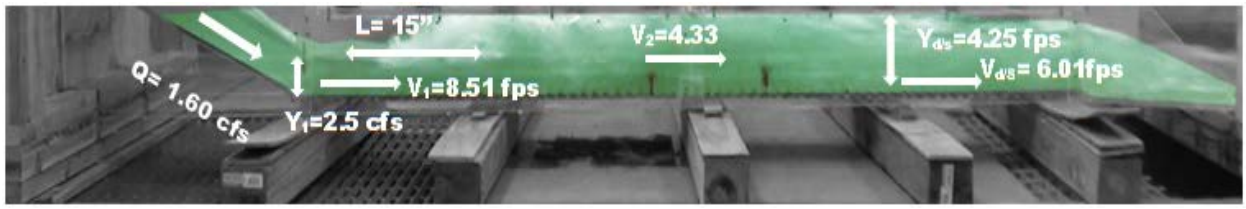

Figure 25. Hydraulic jump characteristics for Experiment 34C for 3% slope, 1.2d

Experiments 25 (for 1% slope), 30 (for 0.6% slope), and 35 (for 0.3% slope) were selected from the data analysis portion for pressure flow conditions. These experiments

were selected by examining many factors; including their relatively low downstream velocities, high total hydraulic head losses, and possible reductions in channel length. These experiments have a similar sill arrangement, which consists of a 2-inch sill at 27 inches from the end of the culvert and a 1.5-inch sill at 37 inches from the end of the culvert with 15 flat faced friction blocks; and three different slopes: 1%, 0.6%, and 0.3%. It was found that these experiments yielded results most applicable to modifying existing culverts with the addition of sills and/or friction blocks. The culvert barrel could be reduced by reducing a section at the end of the channel where the water surface profile is more uniform. The characteristics of the hydraulic jumps for Experiments 25, 30, and 35 are in Table 14.

Table 14. Selected factors for Experiments 25, 30, and 35.

SLOPE	**1%**			**0.6%**			**0.3%**		
CASE	25A	25B	25C	30A	30B	30C	35A	35B	35C
Y_1 (in)	1.75	2.25	3.00	1.75	2.13	3.00	1.75	2.13	3.00
Y_2 (in)	7.54	9.22	10.72	8.75	9.91	10.72	8.89	9.96	10.84
$Y_{d/s}$ (in)	2.75	3.25	4.00	2.75	3.50	4.25	2.75	3.75	4.25
V_1 (fps)	7.3258	7.9409	8.1081	8.3943	8.6679	8.1081	8.5118	8.7081	8.1904
V_2 (fps)	3.6629	5.0489	5.1801	3.2762	4.7079	4.7079	3.2762	5.3080	7.0457
$V_{d/s}$ (fps)	4.9143	5.1801	5.7915	4.7079	5.5065	6.0187	4.7079	5.3080	6.1292
ΔE (in)	3.6737	4.0804	3.5733	5.6032	5.5747	3.5733	5.8409	5.6549	3.7035
E_2/E_1	0.6873	0.7085	0.7657	0.6234	0.6544	0.7657	0.6170	0.6522	0.7611
THL (in)	9.4246	8.7191	8.0441	9.8041	8.8209	8.2941	9.7855	8.9691	8.0482
Culvert Reduction (ft)	40	38	30	40	35	20	36	32	25

8 CONCLUSIONS

A laboratory model was constructed to represent a broken-back culvert. The idealized prototype contains a 1 (vertical) to 2 (horizontal) slope, a 36-foot horizontal length of a slanted part of the culvert continuing down to a 114-foot flat culvert. The model was built with the ability to change the channel slope to 1, 0.6, and 0.3 percent. The model was made to 1:20 scale. The following dimensions are in terms of the prototype culvert. It was noted that the current practice of not using any energy dissipaters (as in Experiment 1) allowed all the energy to flow through the culvert instead of reducing or dissipating it. The following conclusions can be drawn based on the laboratory experiments for open channel flow conditions and pressure flow conditions:

8.1 Open Channel Flow Conditions

1. For new culvert construction, Experiments 5 for 1% slope, 10 for 0.6% slope, and 15 for 0.3% slope are the best options for an open channel flow conditions. These options include one 5-foot sill with two small orifices at the bottom, so that water can be completely drained from the culvert. The sill is located 43 feet from the end of the culvert. The height of the culvert should be 16 feet to allow an open channel condition in the culvert.
2. If one 5.0-foot high sill is placed in the flat part of the culvert, it results in 66% of energy dissipation as seen in Experiment 5C for 1% slope; and 71% of energy dissipation as seen in Experiment 10C for 0.6% slope, and results in 70% of energy dissipation as seen in Experiment 15C for 0.3% slope.

3. If one 5.0-foot high sill with 15 flat faced friction blocks is placed in the flat part of the culvert starting at initiation of hydraulic jump, energy dissipation of 68% occurs as seen in Experiment 6C for 1% slope, 71% of energy dissipation occurs as seen in Experiment 11C for 0.6% slope, and 71% occurs as seen in Experiment 16C for 0.3% slope.
4. The reduction of energy due to 15 friction blocks is marginal. The optimal 5.0-foot sill is the most economical option.
5. Experiments 5, 10, and 15 show an opportunity to reduce the culvert length at the end in the range of 35 to 43 feet. The 35-foot reduction was determined by eliminating the downstream segment of the culvert where the water surface is no longer uniform after the jump. The 43-foot reduction results from removing a portion of the downstream culvert from the sill to the beginning of the downstream wingwall section. This option is important if there are problems with the right-of-way.

8.2 Pressure Flow Conditions

6. For retrofitting an existing culvert, Experiments 24 for slope 1%, 29 for slope 0.6%, and 34 for slope 0.3% are the best option for pressure flow conditions. Each experiment consists of three flow conditions: 0.8, 1.0 and 1.2 times the upstream culvert depth of 10 feet. This scenario uses two sills, a 3.33-foot sill at 45 feet from the end of the culvert, and a 2.5-foot sill located 62 feet from the end of the culvert.

7. Optimal placement of two sills, 2.5 feet and 3.33 feet high, resulted in 14 feet THL in Experiment 24C for 1% slope, 16 feet THL in Experiment 29C for 0.6% slope, and 14 feet THL in experiment 34C for 0.3% slope.
8. For Experiments 24, 30, and 34, reductions in culvert length can be made between 25 feet to 40 feet, as seen in Table 13.
9. If two sills, one 3.33-foot sill at 45 feet from the end of the culvert and one 2.5-foot sill located 62 feet from the end of the culvert, and 15 flat faced friction blocks are placed in the flat part of the culvert starting at the formation of the hydraulic jump, the THL is 13 feet in Experiment 25C for slope 1%, 14 feet in Experiment 30C for 0.6% slope, and 13 feet in Experiment 35C for 0.3% slope.
10. If two sills, 3.33 feet and 2.5 feet, and 45 flat faced friction blocks are placed in the flat part of the culvert starting at the formation of the hydraulic jump, the total head loss is 13 feet in Experiment 27C for 1% slope, 13 feet in Experiment 32C for 0.6% slope, and 14 feet in Experiment 37C for 0.3% slope.
11. The reduction of energy due to the region of friction blocks is marginal.
12. Experiments 24 for 1% slope, 29 for 0.6% slope, and 34 for 0.3% slope offer similar performance to friction block experiments without the additional cost.

REFERENCES

Alikhani, A., Behroz-Rad, R., and Fathi-Moghadam, M. (2010). Hydraulic Jump in Stilling Basin with Vertical End Sill. International Journal of Physical Sciences. 5(1), 25-29.

Bhutto, H., Mirani, S. and Chandio, S. (1989). Characteristics of Free Hydraulic Jump in Rectangular Channel. *Mehran University Research Journal of Engineering and Technology, 8(2)*, 34 – 44.

Baylar, A., Unsal, M., and O
zkan, F. (2011). "The Effect of Flow Patterns and Energy Dissipation over Stepped Chutes on Aeration Efficiency." *KSCE Journal of Civil Engineering.* 15(8), PP. 1329-1334

Bessaih, N., and Rezak, A. (2002). "Effect of Baffle Blocks with Sloping Front Face on the Length of the Jump*." Journal of Civil Engineering*., 30(2), PP. 101-108.

Chanson, H. (2008). Acoustic Doppler velocimetery (ADV) in the field and in laboratory: practical experiences. *International Meeting on Measurements and Hydraulics of Sewers*, 49-66.

Chanson, H. (2009). Current knowledge in hydraulic jumps and related phenomena. European Journal of Mechanics B/Fluid. 29(2009), 191-210.

Chow, V.T. (1959). Open-channel Hydraulics. McGraw-Hill, New York, NY, 680 pages.

Debabeche, M., and Achour, B. (2007). "Effect of sill in the hydraulic jump in a triangular channel." *Journal of Hydraulic Research.* 45(1), PP. 135-139

Eloubaidy, A., Al-baidbani, J., and Ghazali, A. (1999). Dissipation of Hydraulic Energy by Curved Baffle Blocks. *Pertanika Journal Science Technology*. 7 (1), 69-77 (1999).

Federal Highway Administration (2006). The Hydraulic Design of Energy Dissipaters for Culverts and Channels.

Finnemore, J. E., and Franzini, B. J., (2002) Fluid Mechanics with Engineering Applications. McGraw-Hill, New York, NY, 790.

Gharanglk, A. and Chaudhry, M. (1991). Numerical simulation of hydraulic jump. *Journal of Hydraulic Engineering. 117(9),* 1195 – 1211.

Goring, D., Nikora, V. (2002). Despiking Ascoustic doppler Velocimeter Data. *Journal of Hydraulic Engineering, 128(1),* 117-128.

Hotchkiss, R. and Donahoo, K. (2001). Hydraulic design of broken-back culvert. *Urban Drainage Modeling, American Society of Civil Engineers*, 51 – 60.

Hotchkiss, R., Flanagan, P. and Donahoo, K. (2003). Hydraulic Jumps in Broken-Back Culvert. *Transportation Research Record* (1851), 35 – 44.

Hotchkiss, R. and Larson, E. (2005). Simple Methods for Energy Dissipation at Culvert Outlets. *Impact of Global Climate Change*. World Water and Environmental Resources Congress.

Hotchkiss, R., Thiele, E., Nelson, J., and Thompson, P. (2008). Culvert Hydraulics: Comparison of Current Computer Models and Recommended Improvements*. Journal of the Transportation Research Board*, No. 2060, Transportation Research Board of the National Academies, Washington, D.C, 2008, pp. 141-149.

Habibzadeh, A., and Loewen, M. R., Rajaratnam, N. (2011). "Performance of Baffle Blocks in Submerged Hydraulic Jumps." *Journal of Hydraulic Engineering.,*

Habibzadeh, A., Wu, S., Ade, F., Rajaratnam, N., and Loewen, M. R. (2011). "Exploratory study of submerged hydraulic jumps with blocks." *Journal of Hydraulic Engineering.,* PP.706-710

Larson, E. (2004). *Energy dissipation in culverts by forcing a hydraulic jump at the outlet.* Master's Thesis, Washington State University.

Jamshidnia, J., Takeda, Y., and Firoozabadi, B. (2010). "Effect of standing baffle on the flow structure in a rectangular open channel." *Journal of Hydraulic Research*. 48(3) PP. 400-404

Mignot, E. and Cienfuegos, R. (2010). Energy dissipation and turbulent production in weak hydraulic jumps. Journal of Hydraulic Engineering, ASCE, 136 (2), 116-121.

Mori, N. Suzuki, T., and Kakuno, S. (2007). Noise of acoustic doppler velocimeter data in bubbly flows. *Journal of Engineering Mechanics*, *133(1),* 122-125.

Meselhe, E. and Hebert, K., (2007). "Laboratory Measurements of Flow through Culverts." *Journal of Hydraulic Engineering.,* 133(8), PP. 973-976

Noshi, H., (1999). *Energy dissipation near the bed downstream end-sill.* 28th IAHR Congress, Hydraulic Research Institute, National Water Research Center.

Ohtsu I., Yasuda, Y., and Hashiba, H. (1996). Incipient jump conditions for flows over a vertical sill. *Journal of Hydraulic Engineering*, *ASCE*. 122(8) 465-469. doi: 10.1061/(ASCE)0733-29(1996)122:8(465).

Ohtsu, I et al. (2001). Hydraulic condition for undular jump formation. *Journal of Hydraulic Research*. 39(2), 203-209.
Oosterholt, G.A. (1947). "An Investigation of the Energy Dissipated in a Surface Roller." *Applying Science Resource*. A1, 107-130

Pagliara, S., Lotti, I., and Palermo, M. (2008). Hydraulic jump on rough bed of stream rehabilitation structures. *Journal of Hydro-environment Research* 2(1), 29-38.

Rusch, R. (2008) Personal communication, Oklahoma Department of Transportation.

SonTek/YSI, Inc. *ADVField/Hydra System Manual* (2001).

Tyagi, A. K. and Schwarz, B. (2002). A Prioritizing Methodology for Scour-critical Culverts in Oklahoma. Oklahoma Transportation Center. Oklahoma, 13 pp.

Tyagi, A.K. and Albert, J. (2008). "Review of Laboratory Experiments and Computer Models for Broken-box Culverts" Oklahoma Department of Transportation, ODOT Item Number: 2193, Oklahoma, 43 pp.

Tyagi, A.K., et al., (2009). "Laboratory Modeling of Energy Dissipation in Broken-back Culverts – Phase I," Oklahoma Transportation Center, Oklahoma, 82 pp.

Tyagi, A.K. et al., (2010a). Energy Dissipation in Broken-back Culverts under Open Channel Flow Conditions. Am. Soc. Civil Engineers International Perspective on Current and Future State of Water Resources, 10 pp.

Tyagi, A.K., Al-Madhhachi, A., and Brown, J. (2010b). Energy Dissipation in Broken-back Culverts under Pressure Flow Conditions. ASCE, *Journal Hydraulic Engineering*. (submitted for peer review).

Tyagi, A.K., Johnson, N. and Ali, A. (2011). Energy Dissipation in 24-foot Drop Broken Back Culverts under Open Channel Conditions. ASCE, *Journal Hydraulic Engineering.* (Submitted or peer review)

Tyagi, A.K., et al., (2011). "Laboratory Modeling of Energy Dissipation in Broken-back Culverts – Phase II," Oklahoma Transportation Center, Oklahoma, 80 pp.

Tyagi, A.K., Johnson, N. Ali, A. and Brown, J. (2012). Energy Dissipation in Six-Foot Drop Broken Back Culverts under Open Channel Conditions. *5th International Perspective on Water Resources and the Environment Conference, Marrakech, Morocco.*

Tyagi, A.K., Johnson, N. and Ali, A. (2012). Energy Dissipation in Six-Foot Drop Broken Back Culverts under Open Channel Conditions. *Journal Hydraulic Engineering.* ASCE. (Submitted or peer review)

Utah Department of Transportation (2004.) *Manual of Instruction – Roadway Drainage and Culverts*.

Varol, F., Cevik, E., and Yuksel, Y. (2009). The effect of water jet on the hydraulic jump. Thirteenth International Water Technology Conference, IWTC. 13 (2009), 895-910, Hurghada, Egypt.

Wahl, T. (2000). Analyzing ADV data using WinADV. *2000 joint water resources engineering and water resources planning and management,* July 30- August 2, 2000- Minneapolis, Minnesota.

Wahl, T. (2003). Discussion of “Despiking acoustic Doppler velocimeter data” by Goring, D. and Nikora, V. *Journal of Hydraulic Engineering,129(6),* 484-487.

APPENDIX A

LABORATORY EXPERIMENTS FOR HYDRAULIC JUMP

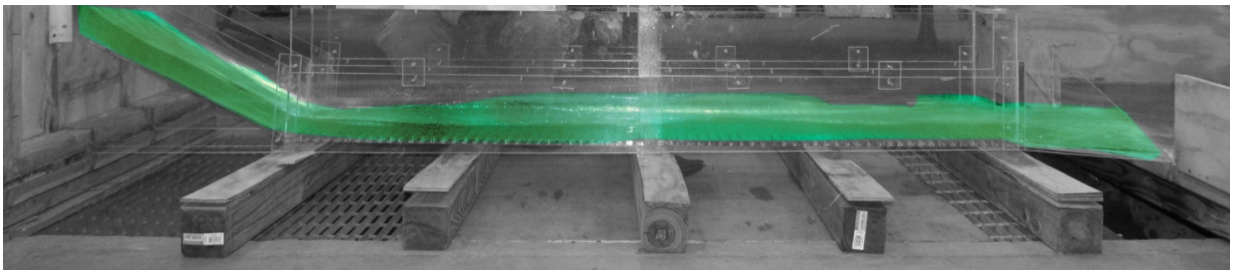

Figure A1. Experiment 1A for 1% slope.

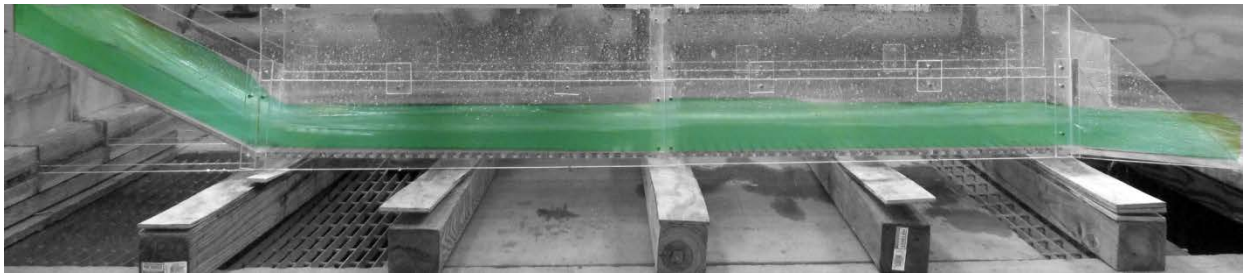

Figure A2. Experiment 1B for 1% slope.

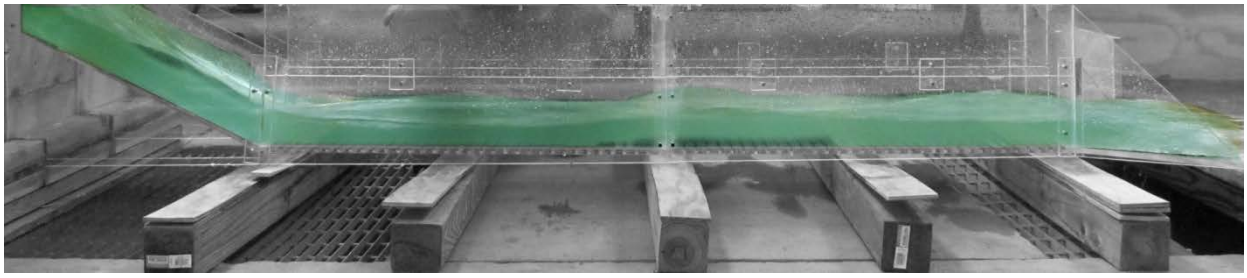

Figure A3. Experiment 1C for 1% slope.

Table A1. Experiment 1 for 1% slope using Open Channel Flow Condition with no sill in the culvert.

H.J.	Run	H	W_{temp}	Q	$V_{u/s}$	Y_s	Y_{toe}	Y_1	Y_2	$Y_{d/s}$	Fr1	V_1	V_2	$V_{d/s}$	L	X	ΔE	THL	E_2/E_1
N	1A	0.8d	-	0.9481	2.3703	2.12	1.75	-	-	1.87	3.5	7.7412 P-tube	-	8.3943 P-tube	-	-	-	1.6469	-
N	1B	1.0d	-	1.2038	2.4076	2.63	2.25	-	-	1.75	3.7	8.0328 P-tube	-	8.8292 P-tube	-	-	-	2.2551	-
N	1C	1.2d	-	1.5352	2.5587	3.38	2.28	-	-	2.32	3.3	8.2241 P-tube	-	8.9722 P-tube	-	-	-	1.8999	-

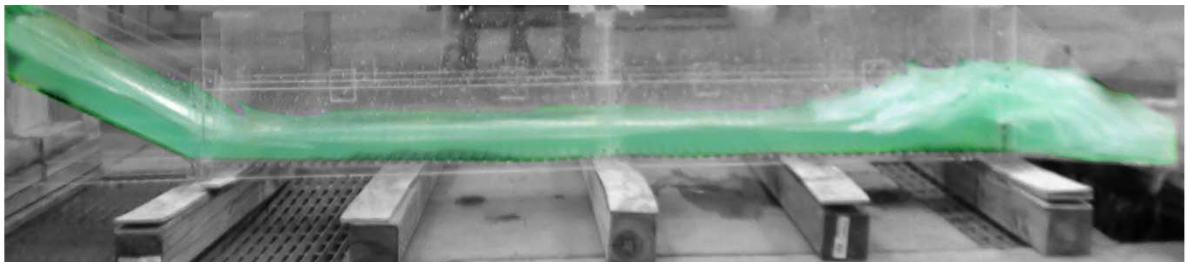

Figure A4. Experiment 2A for 1% slope

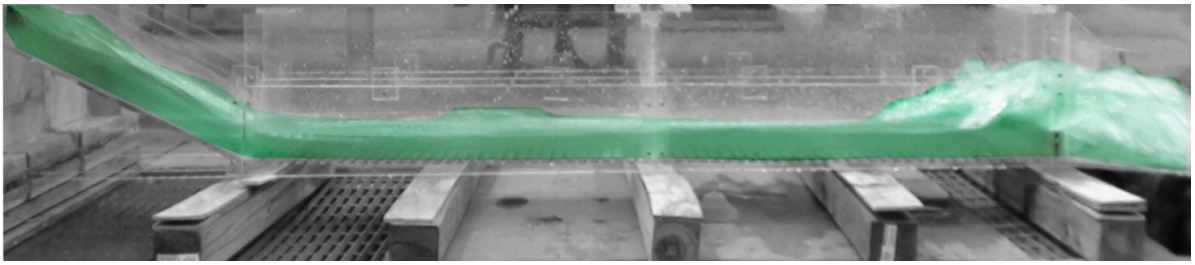

Figure A5. Experiment 2B for 1% slope

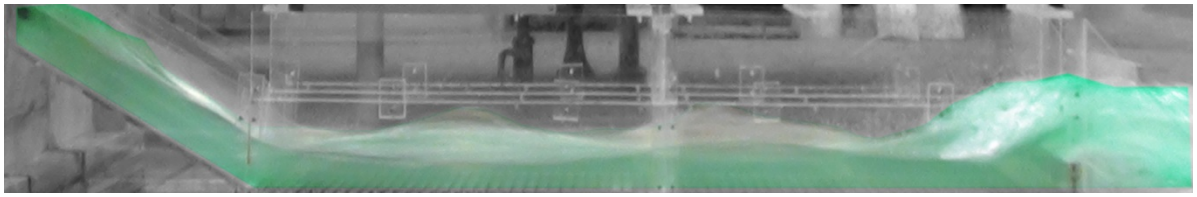

Figure A6. Experiment 2C for 1% slope

Table A2. Experiment 2 for 1% slope using Open Channel Flow Condition with a 2'' end sill.

H.J.	Run	H	W_{temp}	Q	$V_{u/s}$	Y_s	Y_{toe}	Y_1	Y_2	$Y_{d/s}$	Fr1	V_1	V_2	$V_{d/s}$	L	X	ΔE	THL	E_2/E_1
Y	2A	0.8d	-	0.9565	2.3913	2.00	1.65	1.70	5.50	5.50	3.9	8.3526 P-tube	-	- P-tube	9.00	15	1.4672	11.1655	0.6190
Y	2B	1.0d	-	1.2332	2.4664	3.00	2.13	2.00	6.00	6.00	3.7	8.5902 P-tube	-	- P-tube	8.50	12	1.3333	11.9335	0.6438
Y	2C	1.2d	-	1.5558	2.5930	3.35	3.37	3.37	8.00	8.00	2.9	8.8214 P-tube	-	- P-tube	6.00	13	0.9204	11.2529	0.7537

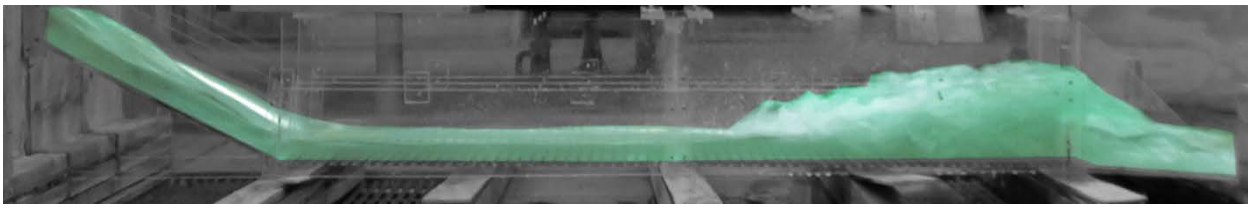

Figure A7. Experiment 3A for 1% slope

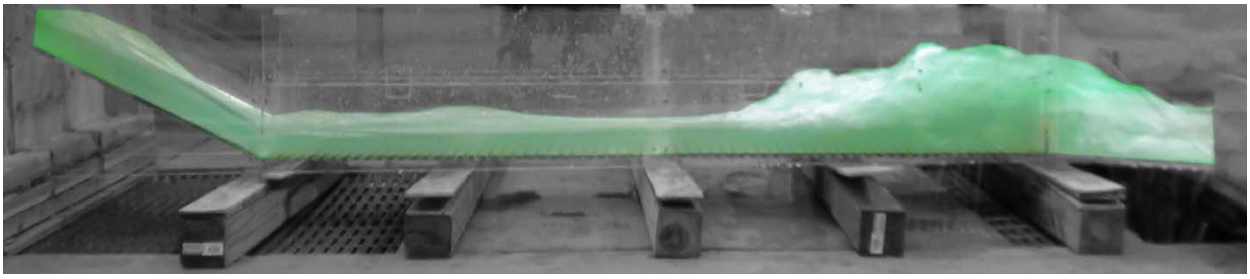

Figure A8. Experiment 3B for 1% slope

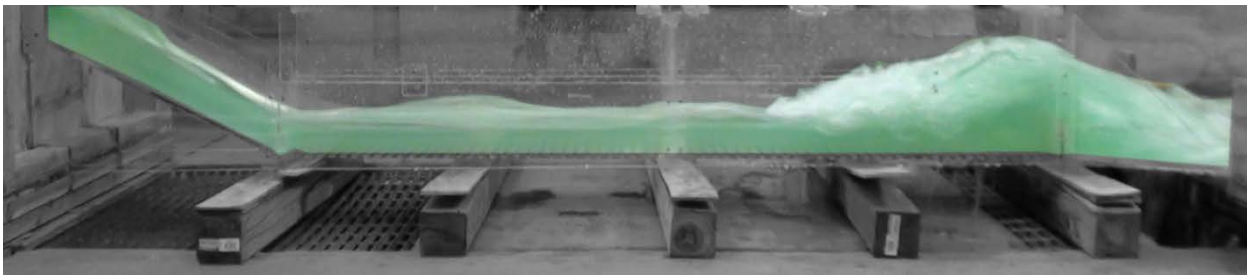

Figure A9. Experiment 3C for 1% slope

Table A3. Experiment 3 for 1% slope using Open Channel Flow Condition with a 3'' end sill.

H.J.	Run	H	W_{temp}	Q	$V_{u/s}$	Y_s	Y_{toe}	Y_1	Y_2	$Y_{d/s}$	Fr1	V_1	V_2	$V_{d/s}$	L	X	ΔE	THL	E_2/E_1
Y	3A	0.8d	-	0.9225	2.3063	2.35	1.65	2.00	6.75	6.75	3.7	8.4643 P-tube	5.3080	2.2573 P-tube	13.00	26	1.9847	8.8916	0.6508
Y	3B	1.0d	-	1.2588	2.5176	2.75	2.00	2.35	7.50	7.50	3.5	8.9122 P-tube	5.1801	2.9155 P-tube	20.00	25	1.9375	8.8972	0.6644
Y	3C	1.2d	-	1.5937	26562	3.50	3.35	3.00	8.00	8.00	3.2	9.1205 P-tube	5.8377	3.1413 P-tube	16.00	20	1.3021	9.4759	0.7111

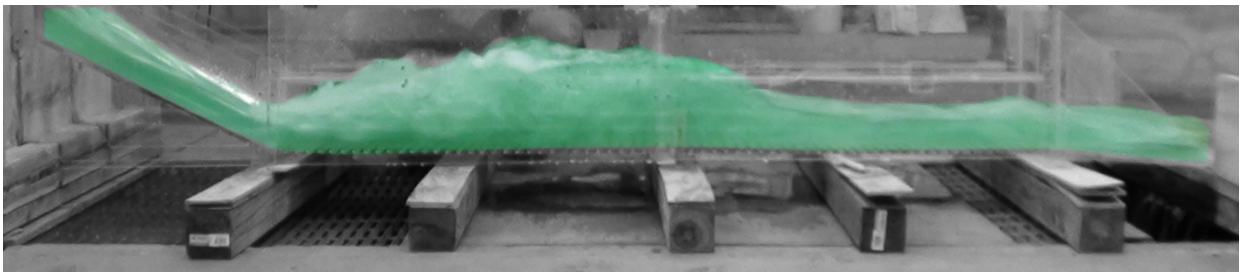

Figure A10. Experiment 4A for 1% slope

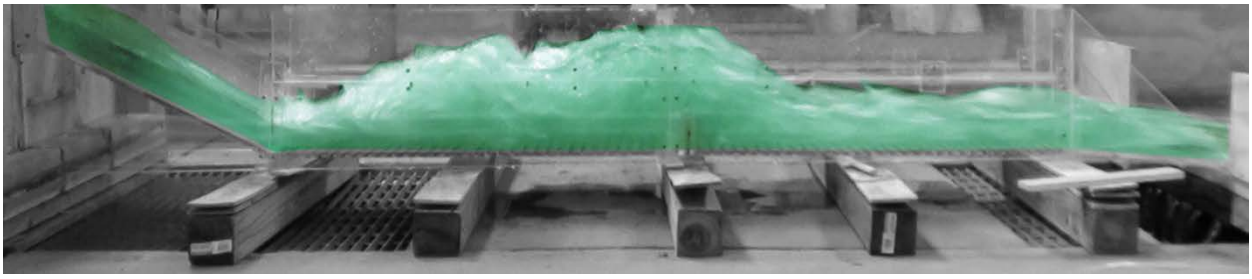

Figure A11. Experiment 4B for 1% slope

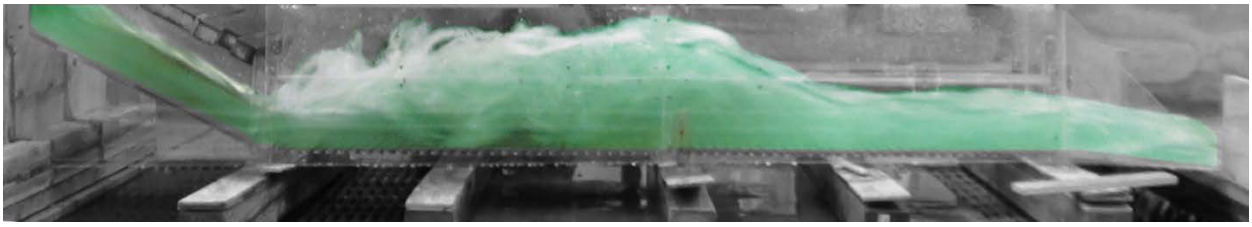

Figure A12. Experiment 4C for 1% slope

Table A4. Experiment 4 for 1% slope using Open Channel Flow Condition with a 3''sill 33'' from the end.

H.J.	Run	H	W_{temp}	Q	$V_{u/s}$	Y_s	Y_{toe}	Y_1	Y_2	$Y_{d/s}$	Fr1	V_1	V_2	$V_{d/s}$	L	X	ΔE	THL	E_2/E_1
Y	4A	0.8d	-	0.9730	2.4325	2.62	2.35	2.35	8.00	2.75	3.1	7.6833 P-tube	3.2762	5.1801 P-tube	14.00	36	2.3984	8.9525	0.7342
Y	4B	1.0d	-	1.2428	2.4856	2.50	2.50	2.75	8.75	3.00	3.0	8.1904 P-tube	4.8317	5.5791 P-tube	16.00	35	2.2442	9.1512	0.7410
Y	4C	1.2d	-	1.5584	1.5584	3.62	3.25	3.25	9.00	3.87	2.9	8.5432 P-tube	4.7758	6.0187 P-tube	16.50	34	1.6249	8.6371	0.7601

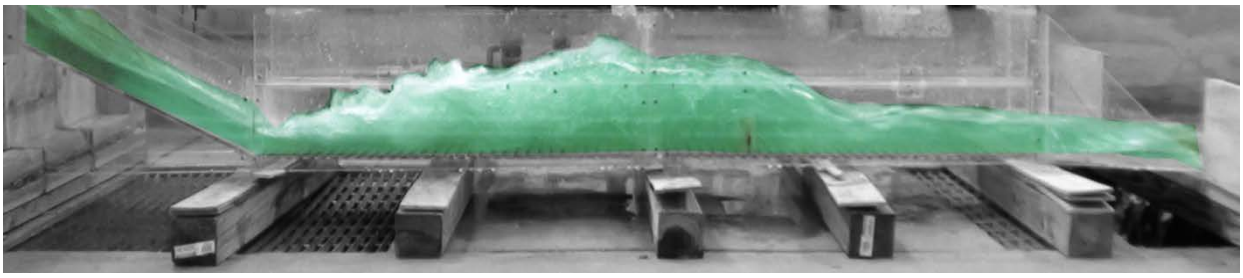

Figure A13. Experiment 5A for 1% slope

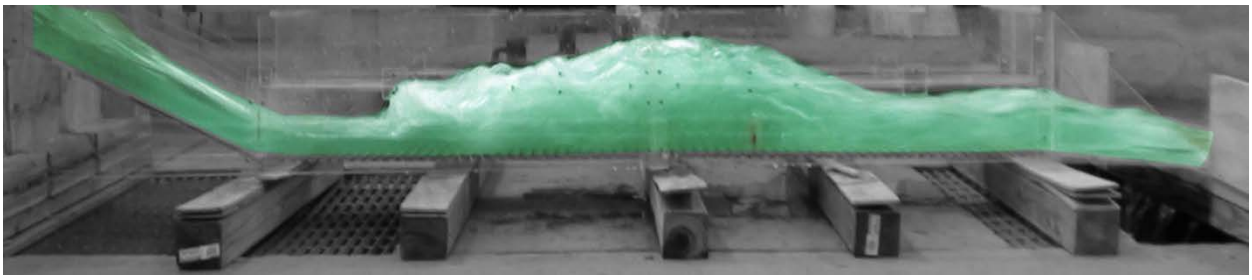

Figure A14. Experiment 5B for 1% slope

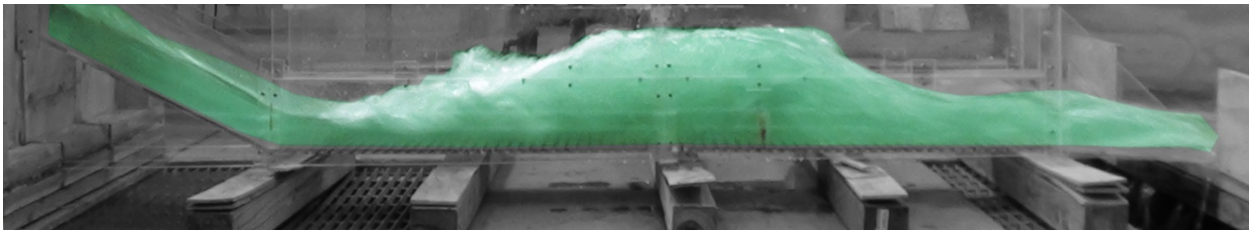

Figure A15. Experiment 5C for 1% slope

Table A5. Experiment 5 for 1% slope using Open Channel Flow Condition with a 3''sill 26'' from the end.

H.J.	Run	H	W_{temp}	Q	$V_{u/s}$	Y_s	Y_{toe}	Y_1	Y_2	$Y_{d/s}$	Fr1	V_1	V_2	$V_{d/s}$	L	X	ΔE	THL	E_2/E_1
Y	5A	0.8d	-	0.9354	2.3385	2.25	1.65	1.65	7.50	2.25	3.8	7.9409 P-tube	2.3166	5.2572 P-tube	17.00	40	4.0445	9.2190	0.6356
Y	5B	1.0d	-	1.2838	2.5676	2.50	1.85	2.00	8.25	2.75	3.7	8.5118 P-tube	3.0646	5.6031 P-tube	20.50	32	3.6991	9.4284	0.6481
Y	5C	1.2d	-	1.5404	1.5673	3.50	2.50	2.35	9.50	3.75	3.6	8.9722 P-tube	4.0125	6.1292 P-tube	21.00	37	4.0932	8.4782	0.6613

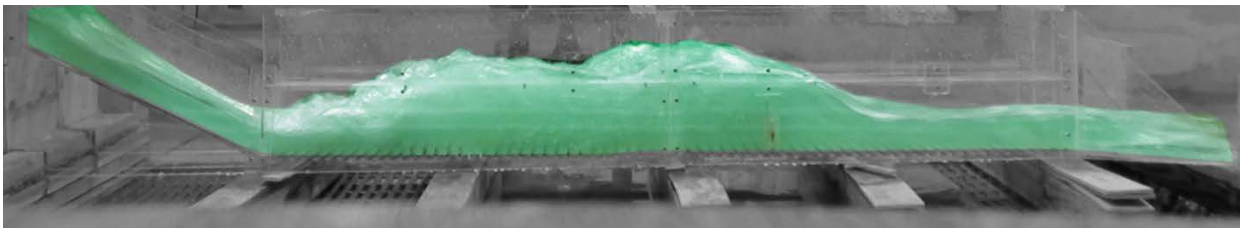

Figure A16. Experiment 6A for 1% slope

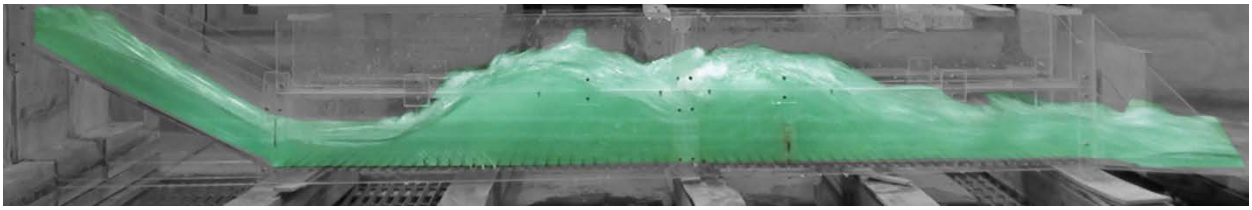

Figure A17. Experiment 6B for 1% slope

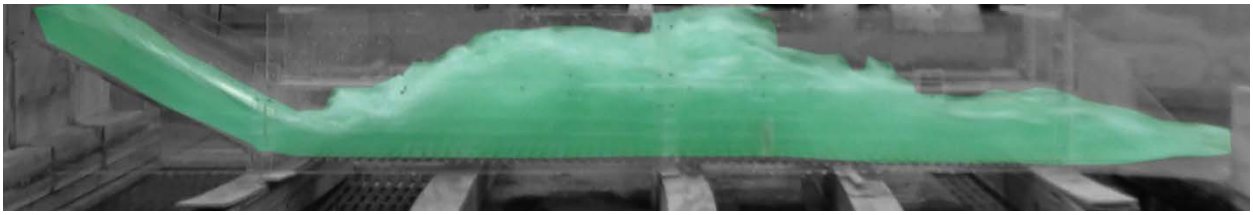

Figure A18. Experiment 6C for 1% slope

Table A6. Experiment 6 for 1.0% slope using Open Channel Flow Condition with a 3''sill at 26'' from the end and15 flat faced friction blocks at 12'' from the toe

H.J.	Run	H	W_{temp}	Q	$V_{u/s}$	Y_s	Y_{toe}	Y_1	Y_2	$Y_{d/s}$	Fr1	V_1	V_2	$V_{d/s}$	L	X	ΔE	THL	E_2/E_1
Y	6A	0.8d	-	0.9648	2.4120	2.00	1.75	1.75	6.75	2.35	3.7	8.0250 P-tube	2.5900	5.2470 P-tube	18.00	42	2.6455	9.2041	0.6445
Y	6B	1.0d	-	1.2396	2.4792	2.75	2.13	2.13	7.50	2.75	3.6	8.5902 P-tube	3.8417	5.7356 P-tube	17.00	33	2.4234	9.0653	0.6586
Y	6C	1.2d	-	1.5430	2.5717	3.35	2.50	2.35	7.00	3.25	3.4	8.5118 P-tube	3.6629	6.1858 P-tube	19.00	36	1.5280	8.8523	0.6861

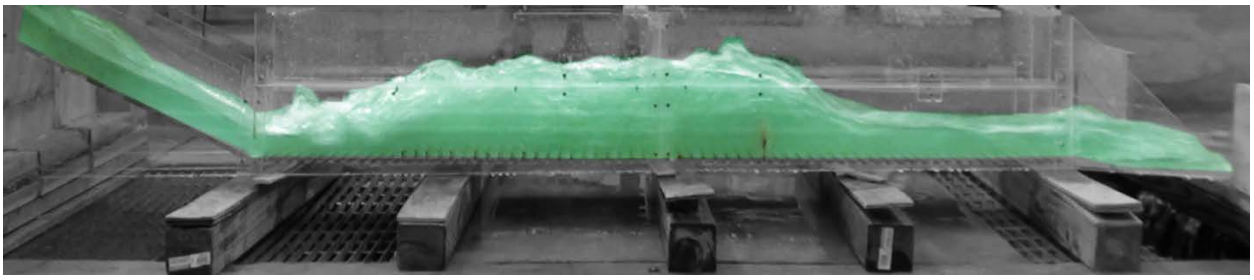

Figure A19. Experiment 7A for 1% slope

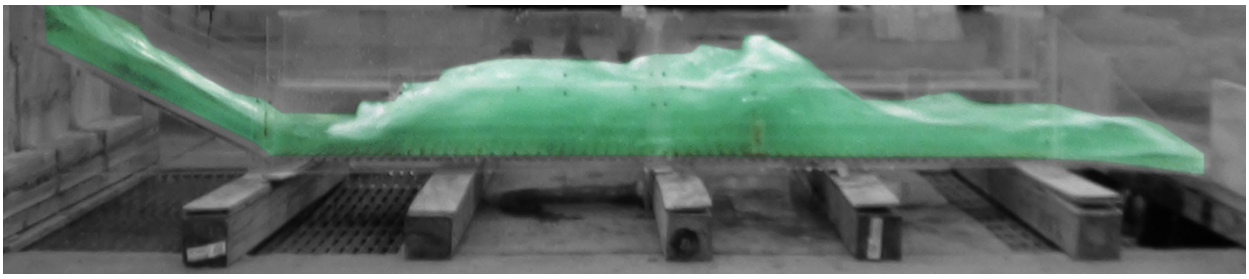

Figure A20. Experiment 7B for 1% slope

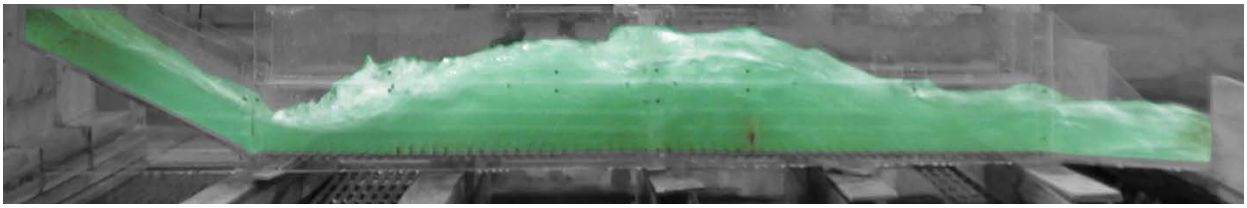

Figure A21. Experiment 7C for 1% slope

Table A7. Experiment 7 for 1.0% slope using Open Channel Flow Condition with a 3''sill at 26'' from the end with 30 flat faced friction blocks at 12'' from the toe.

H.J.	Run	H	W_{temp}	Q	$V_{u/s}$	Y_s	Y_{toe}	Y_1	Y_2	$Y_{d/s}$	Fr1	V_1	V_2	$V_{d/s}$	L	X	ΔE	THL	E_2/E_1
Y	7A	0.8d	-	0.9648	2.4120	2.00	1.75	1.75	6.50	2.35	3.8	8.1904 P-tube	2.4626	5.3080 P-tube	17.00	42	2.3554	9.0841	0.6338
Y	7B	1.0d	-	1.2364	2.4728	2.63	2.13	2.13	9.00	3.50	3.5	8.4580 P-tube	4.0985	5.7915 P-tube	19.00	36	4.2285	8.1894	0.6645
Y	7C	1.2d	-	1.5837	2.6395	3.25	2.75	2.63	7.50	3.50	3.3	8.7081 P-tube	4.3340	6.4906 P-tube	19.00	40	1.4639	7.9482	0.7000

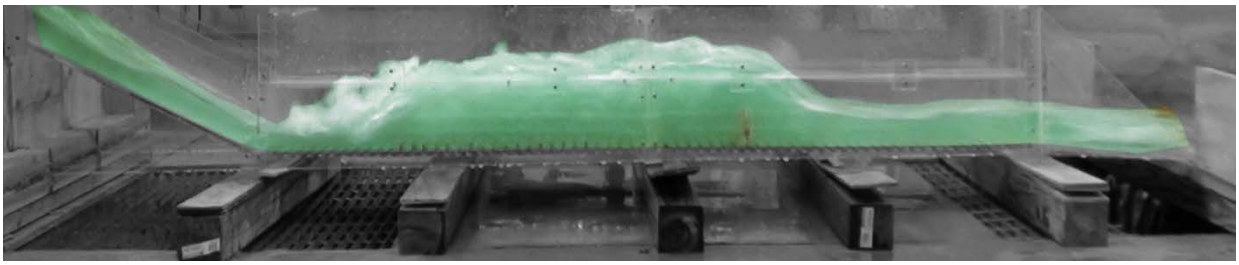

Figure A22. Experiment 8A for 1% slope

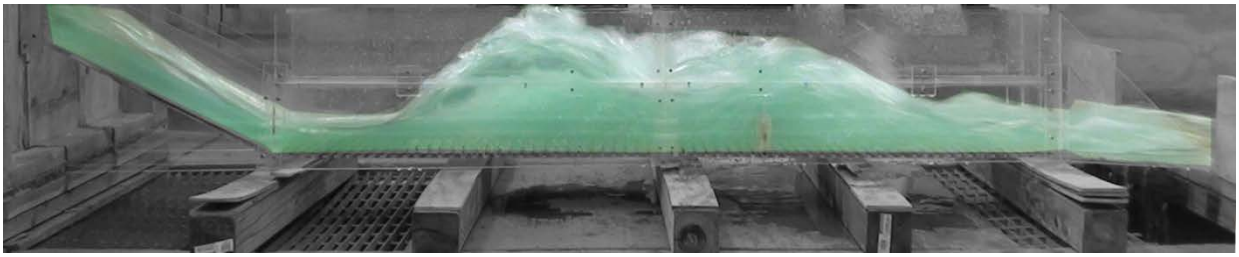

Figure A23. Experiment 8B for 1% slope

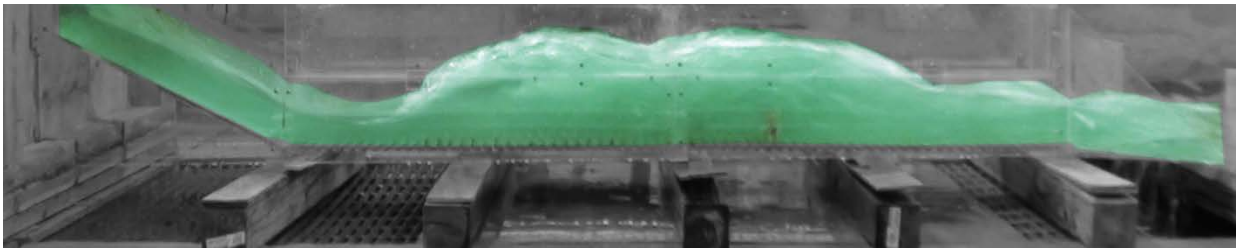

Figure A24. Experiment 8C for 1% slope

Table A8. Experiment 8 for 1.0% slope using Open Channel Flow Condition with a 3''sill at 26'' from the end with 45 flat faced friction blocks at 12'' from the toe.

H.J.	Run	H	W_{temp}	Q	$V_{u/s}$	Y_s	Y_{toe}	Y_1	Y_2	$Y_{d/s}$	Fr1	V_1	V_2	$V_{d/s}$	L	X	ΔE	THL	E_2/E_1
Y	8A	0.8d	-	0.9606	2.4015	1.85	1.75	1.75	7.00	2.25	3.7	8.1081 P-tube	2.8373	5.2470 P-tube	18.00	39	2.9531	9.2646	0.6385
Y	8B	1.0d	-	1.2619	2.5238	2.85	2.13	2.13	7.85	3.00	3.5	8.2719 P-tube	4.1763	5.7915 P-tube	17.00	34	2.7982	8.7369	0.6749
Y	8C	1.2d	-	1.5987	2.6645	3.13	2.75	2.65	9.50	3.50	3.3	8.8214 P-tube	3.0646	6.2805 P-tube	22.00	33	3.1918	8.4729	0.6958

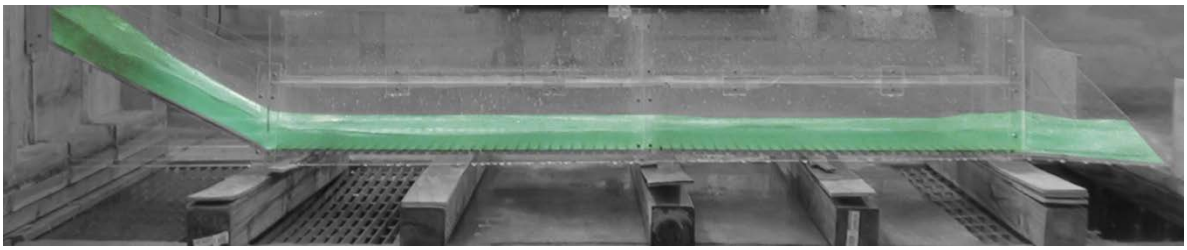

Figure A25. Experiment 9A for 0.6% slope

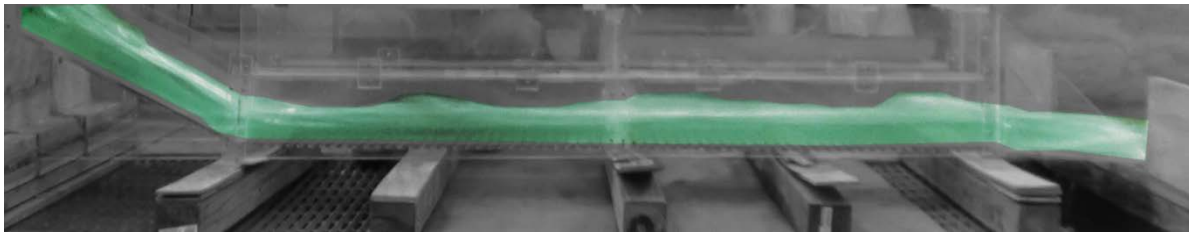

Figure A26. Experiment 9B for 0.6% slope

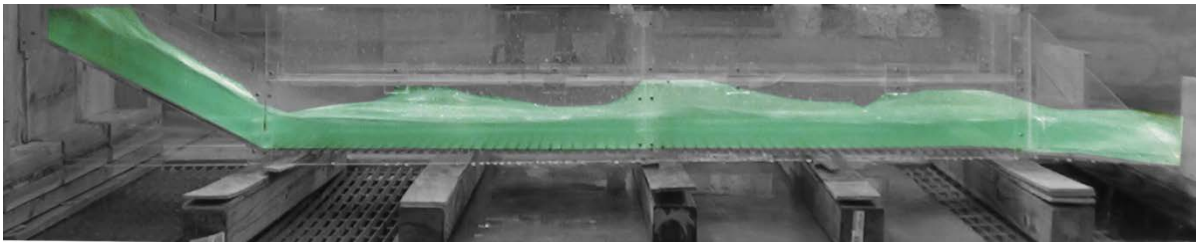

Figure A27. Experiment 9C for 0.6% slope

Table A9. Experiment 9 for 0.6% slope using Open Channel Flow Condition with no sill in the culvert.

H.J.	Run	H	W_{temp}	Q	$V_{u/s}$	Y_s	Y_{toe}	Y_1	Y_2	$Y_{d/s}$	Fr1	V_1	V_2	$V_{d/s}$	L	X	ΔE	THL	E_2/E_1
N	9A	0.8d	-	0.9852	2.4630	2.13	1.85	-	-	1.65	4.1	8.2719 P-tube	-	8.1412 P-tube	-	-	-	2.7304	-
N	9B	1.0d	-	1.2364	2.4728	2.62	2.38	-	-	2.00	3.9	8.9722 P-tube	-	8.5118 P-tube	-	-	-	2.4393	-
N	9C	1.2d	-	1.6622	2.7703	3.35	3.00	-	-	2.35	3.7	9.1937 P-tube	-	8.9722 P-tube	-	-	-	2.0801	-

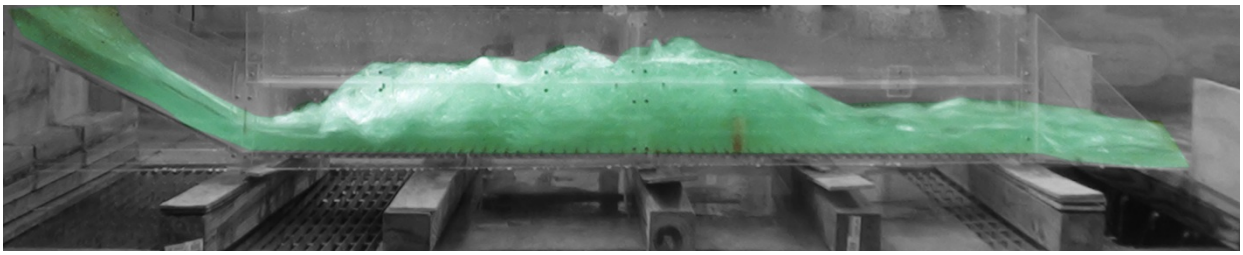

Figure A28. Experiment 10A for 0.6% slope

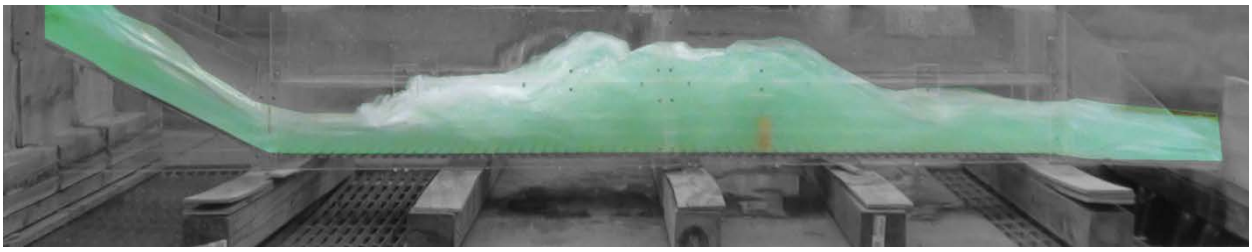

Figure A29. Experiment 10B for 0.6% slope

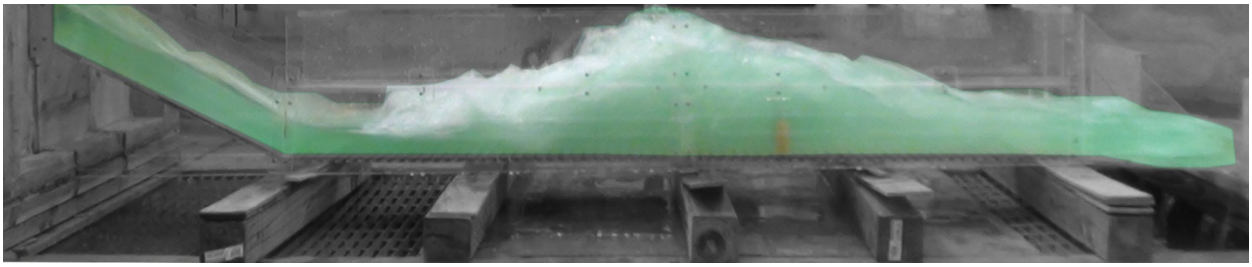

Figure A30. Experiment 10C for 0.6% slope

Table A10. Experiment 10 for 0.6% slope using Open Channel Flow Condition with a 3''sill at 26'' from the end.

H.J.	Run	H	W_{temp}	Q	$V_{u/s}$	Y_s	Y_{toe}	Y_1	Y_2	$Y_{d/s}$	Fr1	V_1	V_2	$V_{d/s}$	L	X	ΔE	THL	E_2/E_1
Y	10A	0.8d	-	0.9973	2.4933	2.13	1.75	1.65	8.25	2.35	3.9	8.1904 P-tube	2.5900	5.2470 P-tube	19.00	40	5.2800	9.2783	0.6202
Y	10B	1.0d	-	1.2460	2.4920	2.75	2.13	2.13	8.75	3.13	3.5	8.2719 P-tube	3.1509	5.6031 P-tube	21.00	34	3.8916	8.9772	0.6749
Y	10C	1.2d	-	1.6086	2.6810	3.13	2.85	2.50	9.50	3.75	3.2	8.3526 P-tube	4.1763	6.0187 P-tube	23.00	35	3.6105	8.8393	0.7076

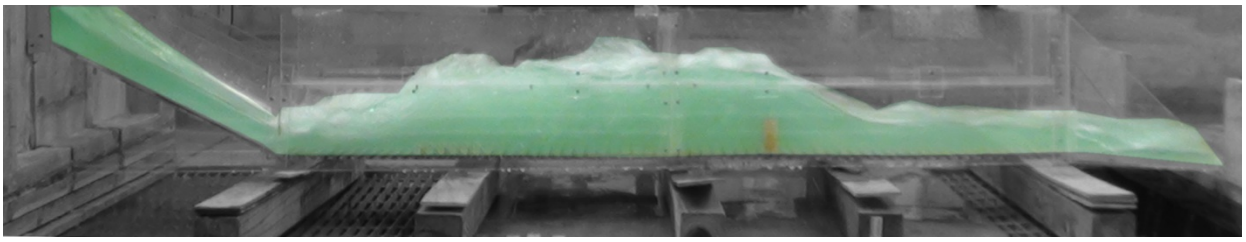

Figure A31. Experiment 11A for 0.6% slope.

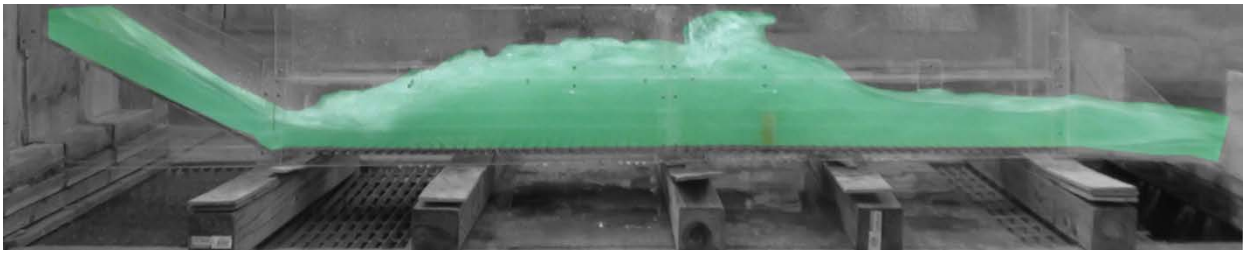

Figure A32. Experiment 11B for 0.6% slope.

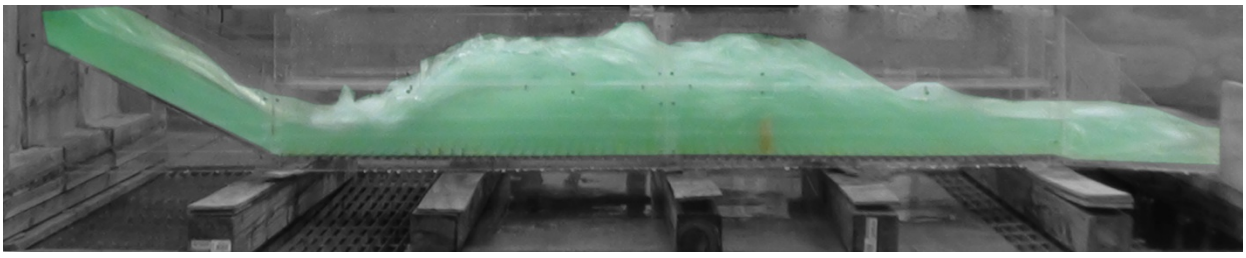

Figure A33. Experiment 11C for 0.6% slope.

Table A11. Experiment 11 for 0.6% slope using Open Channel Flow Condition with a 3''sill at 26'' from the end and 15 flat faced friction blocks at 12'' from the toe.

H.J.	Run	H	W_{temp}	Q	$V_{u/s}$	Y_s	Y_{toe}	Y_1	Y_2	$Y_{d/s}$	Fr1	V_1	V_2	$V_{d/s}$	L	X	ΔE	THL	E_2/E_1
Y	11A	0.8d	-	0.9648	2.4120	2.00	1.85	1.85	7.50	2.50	3.5	7.7286 P-tube	2.5900	5.2470 P-tube	18.50	42	3.2498	9.0541	0.6737
Y	11B	1.0d	-	1.2776	2.5552	2.85	2.35	2.25	8.25	3.25	3.3	8.1412 P-tube	3.6629	5.5550 P-tube	19.50	39	2.9091	9.0166	0.6951
Y	11C	1.2d	-	1.5887	2.6478	3.25	2.85	2.65	9.25	3.50	3.2	8.5118 P-tube	3.8417	6.3443 P-tube	21.50	37	2.9321	8.3064	0.7124

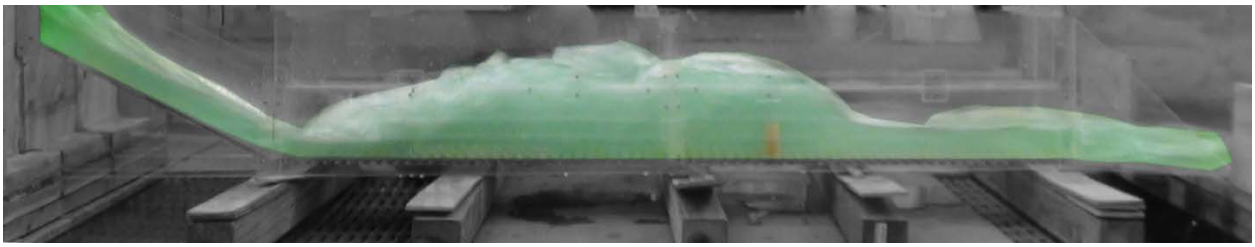

Figure A34. Experiment 12A for 0.6% slope

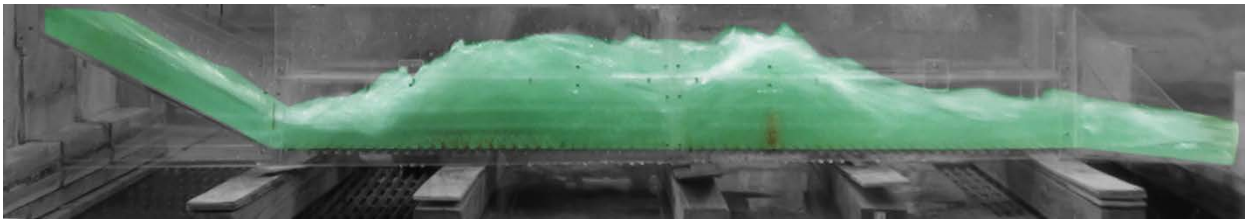

Figure A35. Experiment 12B for 0.6% slope

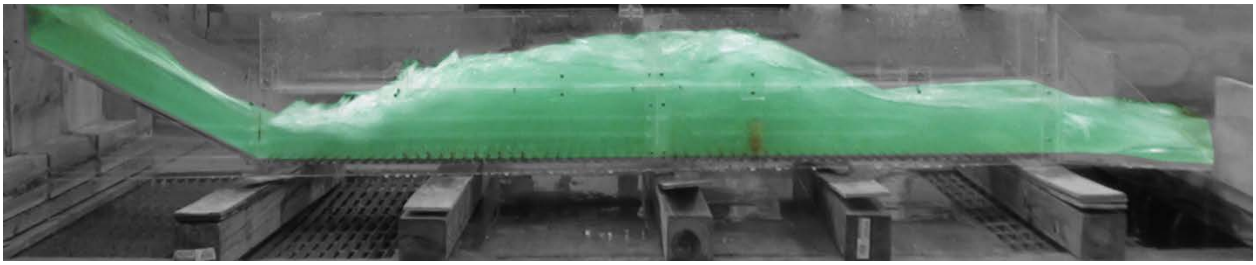

Figure A36. Experiment 12C for 0.6% slope

Table A12. Experiment 12 for 0.6% slope using Open Channel Flow Condition with a 3''sill at 26'' from the end with 30 flat faced friction blocks at 12'' from the toe.

H.J.	Run	H	W_{temp}	Q	$V_{u/s}$	Y_s	Y_{toe}	Y_1	Y_2	$Y_{d/s}$	Fr1	V_1	V_2	$V_{d/s}$	L	X	ΔE	THL	E_2/E_1
Y	12A	0.8d	-	0.9771	2.4428	2.00	1.85	1.85	7.50	2.50	3.6	7.9409 P-tube	2.3166	5.2470 P-tube	18.00	39	3.2498	9.0819	0.6611
Y	12B	1.0d	-	1.2619	2.5238	2.63	2.50	2.13	7.50	3.25	3.5	8.2881 P-tube	3.6629	5.5550 P-tube	16.00	40	2.4234	8.9826	0.6740
Y	12C	1.2d	-	1.6550	2.7583	3.50	3.00	2.55	9.75	3.75	3.2	8.3943 P-tube	4.0125	6.2377 P-tube	22.50	40	3.7531	8.4177	0.7099

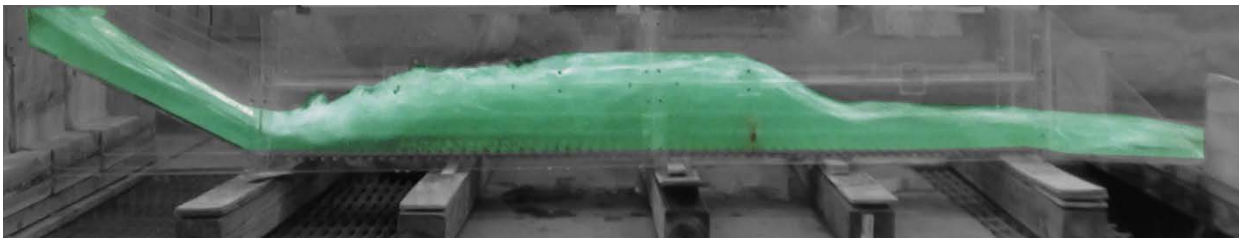

Figure A37. Experiment 13A for 0.6% slope

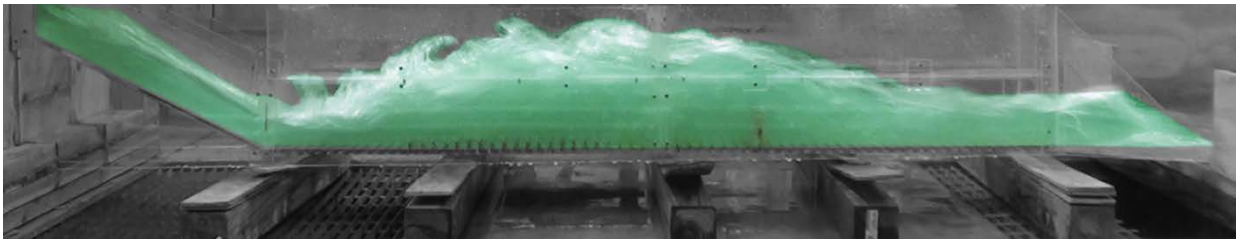

Figure A38. Experiment 13B for 0.6% slope

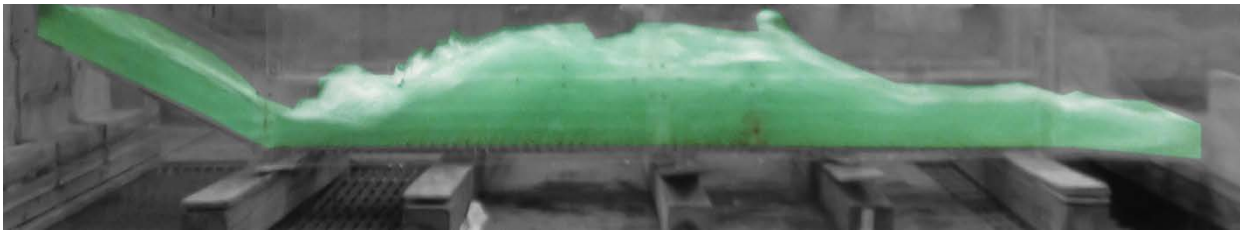

Figure A39. Experiment 13C for 0.6% slope

Table A13. Experiment 13 for 0.6% slope using Open Channel Flow Condition with a 3''sill at 26'' from the end with 45 flat faced friction blocks at 12'' from the toe.

H.J.	Run	H	W_{temp}	Q	$V_{u/s}$	Y_s	Y_{toe}	Y_1	Y_2	$Y_{d/s}$	Fr1	V_1	V_2	$V_{d/s}$	L	X	ΔE	THL	E_2/E_1
Y	13A	0.8d	-	0.9268	2.3170	1.87	2.00	2.00	7.50	2.62	3.4	7.8149 P-tube	2.3166	5.1801 P-tube	14.00	42	2.7729	8.9803	0.6867
Y	13B	1.0d	-	1.2588	2.5176	2.75	2.13	2.00	8.00	3.25	3.6	8.3526 P-tube	3.2762	5.7915 P-tube	19.00	40	3.3750	8.4811	0.6557
Y	13C	1.2d	-	1.5862	2.6437	3.35	2.75	2.50	9.00	3.50	3.2	8.3526 P-tube	4.0125	6.3443 P-tube	21.00	39	3.0514	8.3023	0.7076

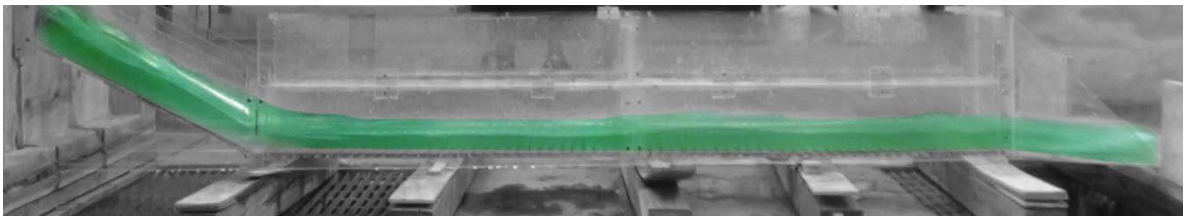

Figure A40. Experiment 14A for 0.3% slope

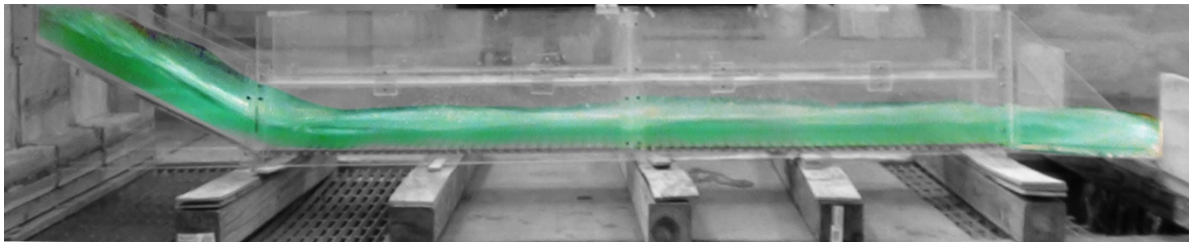

Figure A41. Experiment 14B for 0.3% slope.

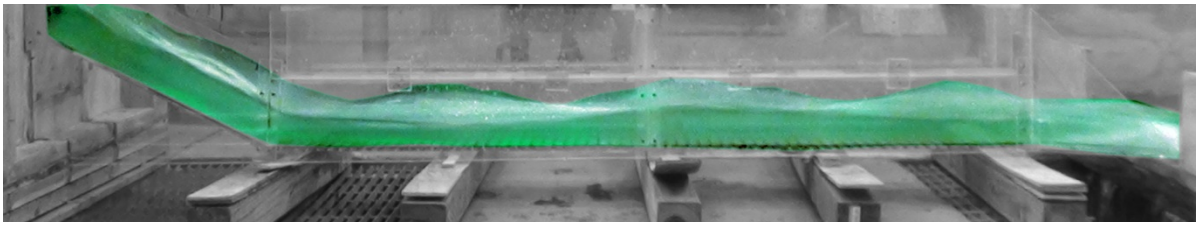

Figure A42. Experiment 14C for 0.3% slope.

Table A14. Experiment 14 for 0.3% slope using Open Channel Flow Condition with no sill in the culvert.

H.J.	Run	H	W_{temp}	Q	$V_{u/s}$	Y_s	Y_{toe}	Y_1	Y_2	$Y_{d/s}$	Fr1	V_1	V_2	$V_{d/s}$	L	X	ΔE	THL	E_2/E_1
N	14A	0.8d	-	0.9852	2.4630	2.00	1.85	-	-	1.75	4.1	8.7081 P-tube	-	8.0250 P-tube	-	-	-	2.9804	-
N	14B	1.0d	-	1.2202	2.4404	2.65	2.25	-	-	2.00	4.0	8.8669 P-tube	-	8.1904 P-tube	-	-	-	3.4097	-
N	14C	1.2d	-	1.5787	2.6312	3.50	2.75	-	-	2.35	3.5	9.1645 P-tube	-	8.8669 P-tube	-	-	-	2.2900	-

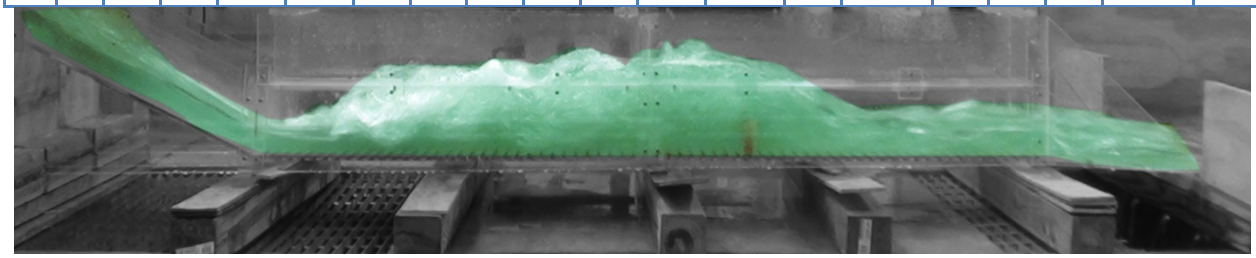

Figure A43. Experiment 15A for 0.3% slope.

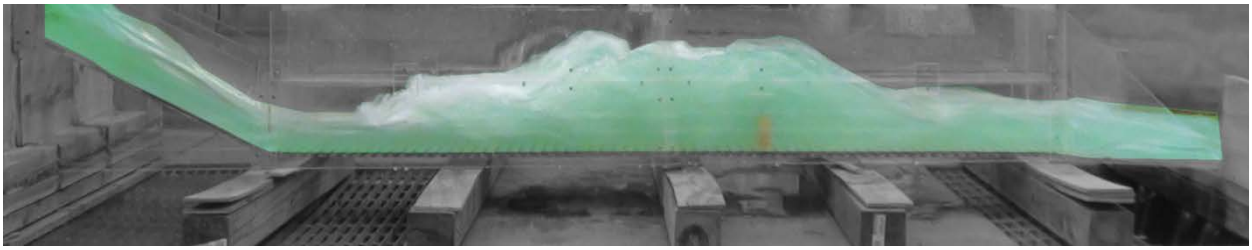

Figure A44. Experiment 15B for 0.3% slope.

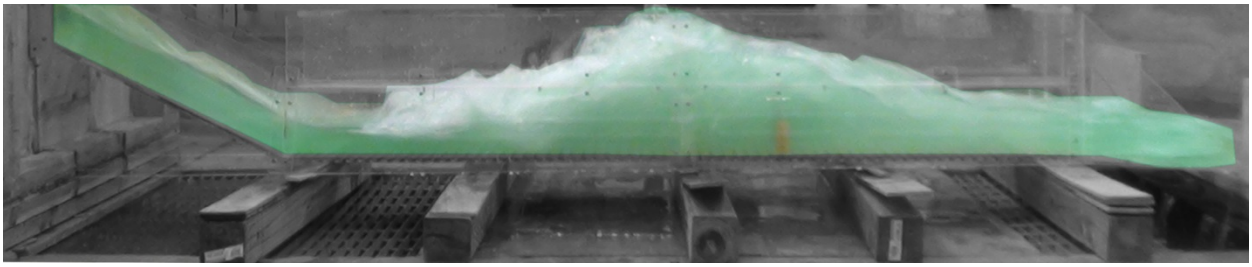

Figure A45. Experiment 15C for 0.3% slope.

Table A15. Experiment 15 for 0.3% slope using Open Channel Flow Condition with a 3''sill at 26'' from the end.

H.J.	Run	H	W_{temp}	Q	$V_{u/s}$	Y_s	Y_{toe}	Y_1	Y_2	$Y_{d/s}$	Fr1	V_1	V_2	$V_{d/s}$	L	X	ΔE	THL	E_2/E_1
Y	15A	0.8d	-	0.9354	2.3385	2.25	2.00	2.00	8.00	2.75	3.5	8.0250 P-tube	2.9757	5.0913 P-tube	15.00	40	3.3750	9.0390	0.6744
Y	15B	1.0d	-	1.2202	2.4404	2.65	2.13	2.13	8.50	3.00	3.4	8.1904 P-tube	3.0646	5.6031 P-tube	20.50	40	3.5691	9.0597	0.6795
Y	15C	1.2d	-	1.5606	2.6015	3.25	2.65	2.50	9.50	3.25	3.3	8.4326 P-tube	3.4749	5.7915 P-tube	24.00	41	3.6105	9.7611	0.7032

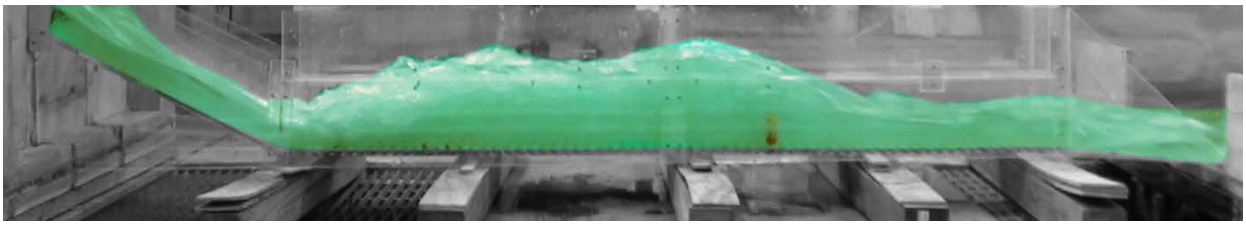

Figure A46. Experiment 16A for 0.3% slope.

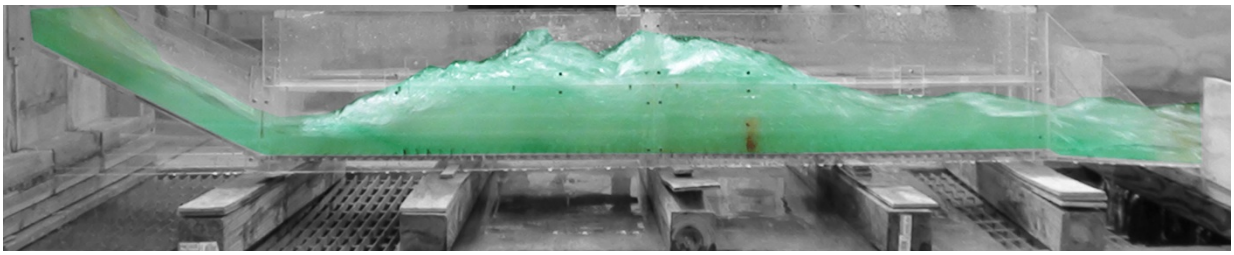

Figure A47. Experiment 16B for 0.3% slope.

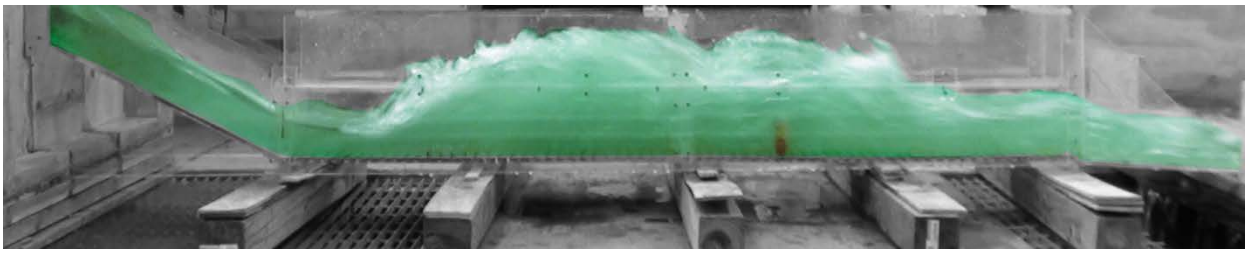

Figure A48. Experiment 16C for 0.3% slope.

Table A16. Experiment 16 for 0.3% slope using Open Channel Flow Condition with a 3''sill at 26'' from the end with 15 flat faced friction blocks at 12'' from the toe.

H.J.	Run	H	W_{temp}	Q	$V_{u/s}$	Y_s	Y_{toe}	Y_1	Y_2	$Y_{d/s}$	Fr1	V_1	V_2	$V_{d/s}$	L	X	ΔE	THL	E_2/E_1
Y	16A	0.8d	-	0.9648	2.4120	2.00	2.00	2.00	7.50	2.50	3.3	7.5955 P-tube	2.3166	5.3080 P-tube	18.00	42	2.7729	8.9341	0.6999
Y	16B	1.0d	-	1.2396	2.4792	2.75	2.50	2.13	8.25	3.00	3.5	8.2719 P-tube	3.1509	5.4329 P-tube	20.00	38	3.2611	9.4453	0.6749
Y	16C	1.2d	-	1.5762	2.6270	3.50	2.75	2.65	9.75	3.75	3.2	8.4643 P-tube	3.9109	6.3443 P-tube	22.50	36	3.4631	8.0359	0.7149

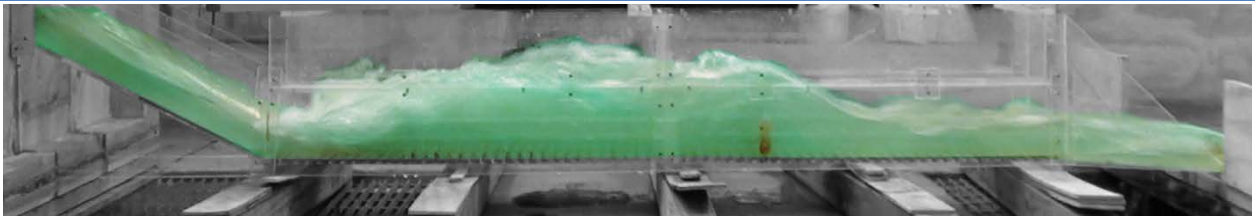

Figure A49. Experiment 17A for 0.3% slope.

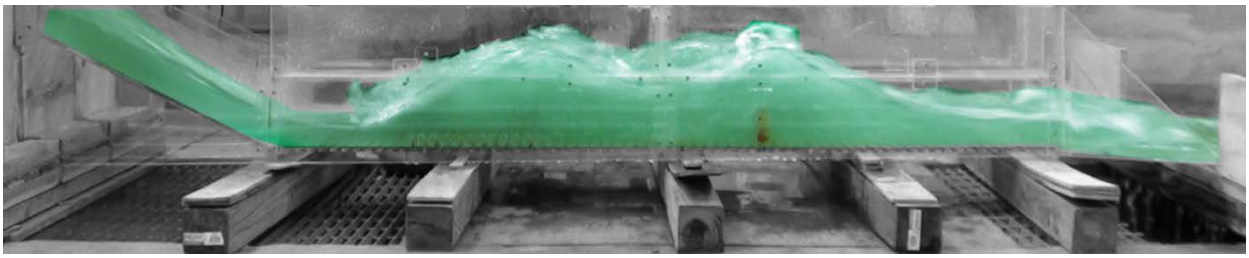

Figure A50. Experiment 17B for 0.3% slope.

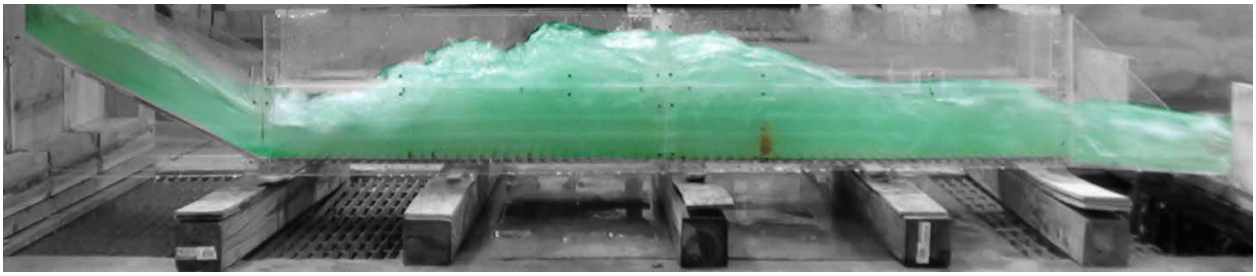

Figure A51. Experiment 17C for 0.3% slope.

Table A17. Experiment 17 for 0.3% slope using Open Channel Flow Condition with a 3''sill at 26'' from the end with 30 flat faced friction blocks at 12'' from the toe.

H.J.	Run	H	W_{temp}	Q	$V_{u/s}$	Y_s	Y_{toe}	Y_1	Y_2	$Y_{d/s}$	Fr1	V_1	V_2	$V_{d/s}$	L	X	ΔE	THL	E_2/E_1
Y	17A	0.8d	-	0.9812	2.4530	2.00	1.75	1.75	7.75	2.35	3.7	7.9746 P-tube	2.3166	5.3080 P-tube	17.00	42	3.9816	9.1212	0.6462
Y	17B	1.0d	-	1.2460	2.4920	2.75	2.25	2.25	8.00	3.50	3.4	8.3526 P-tube	3.4749	5.4329 P-tube	15.00	34	2.6404	8.9572	0.6831
Y	17C	1.2d	-	1.6037	2.6728	3.50	2.75	2.50	10.00	3.63	3.3	8.4326 P-tube	4.1763	6.0631 P-tube	22.00	42	4.2188	8.8512	0.7032

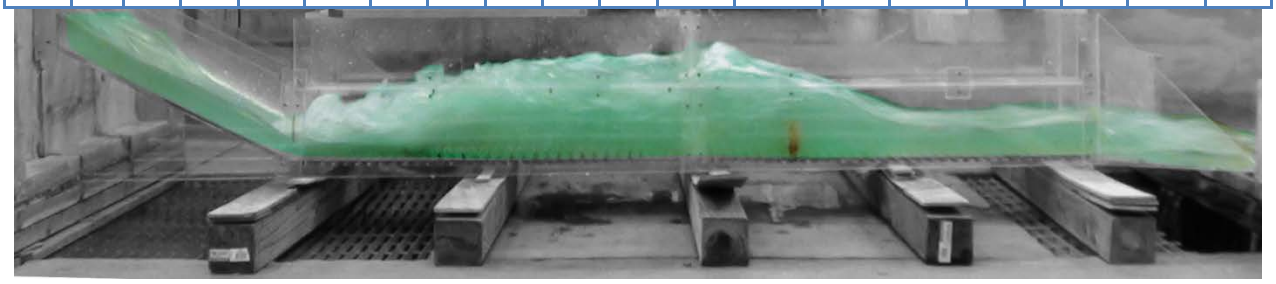

Figure A52. Experiment 18A for 0.3% slope.

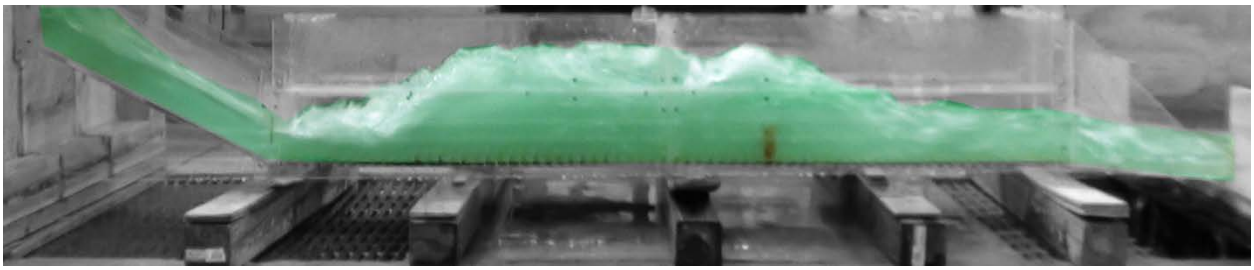

Figure A53. Experiment 18B for 0.3% slope.

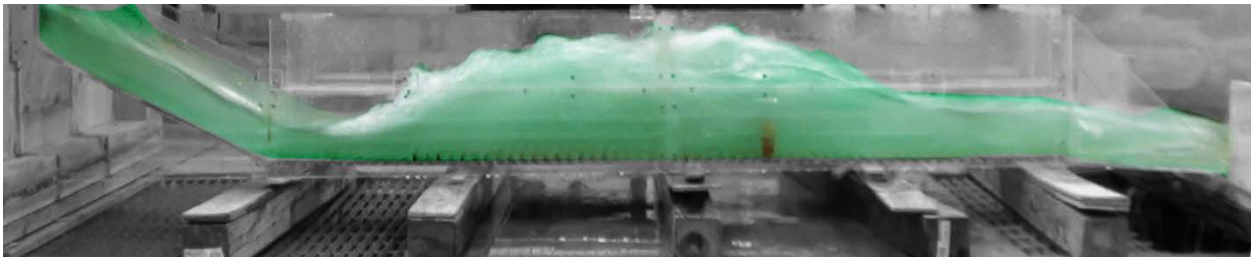

Figure A54. Experiment 18C for 0.3% slope.

Table A18. Experiment 18 for 0.3% slope using Open Channel Flow Condition with a 3''sill at 26'' from the end with 45 flat faced friction blocks at 12'' from the toe.

H.J.	Run	H	W_{temp}	Q	$V_{u/s}$	Y_s	Y_{toe}	Y_1	Y_2	$Y_{d/s}$	Fr1	V_1	V_2	$V_{d/s}$	L	X	ΔE	THL	E_2/E_1
Y	18A	0.8d	-	0.9565	2.3913	2.25	2.13	2.00	7.25	2.63	3.3	7.6833 P-tube	2.0062	5.3080 P-tube	17.00	42	2.4949	9.9855	0.6946
Y	18B	1.0d	-	1.2651	2.5302	2.85	2.25	2.13	8.50	3.00	3.5	8.3526 P-tube	3.8417	5.5550 P-tube	20.00	39	3.5691	9.2429	0.6704
Y	18C	1.2d	-	1.5762	2.6270	3.25	2.75	2.50	9.50	3.50	3.3	8.4326 P-tube	4.0125	6.2377 P-tube	22.00	37	3.6105	8.5359	0.7032

Figure A55. Experiment 19A for 1% slope.

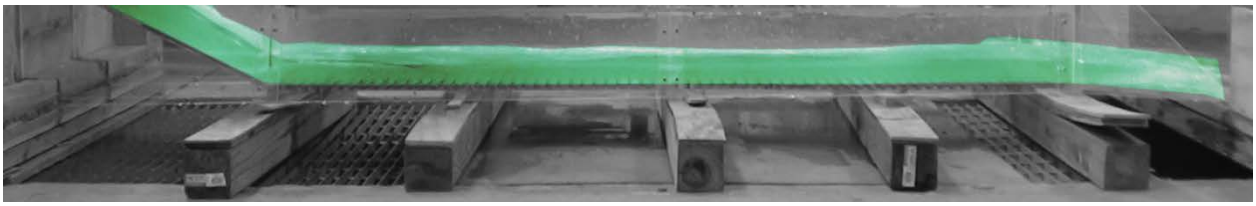

Figure A56. Experiment 19B for 1% slope.

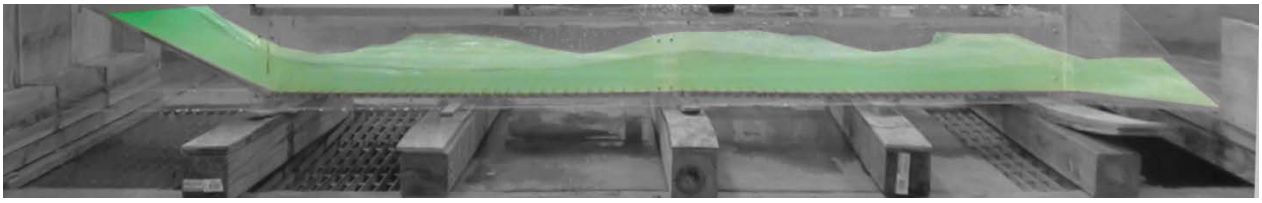

Figure A57. Experiment 19C for 1% slope.

Table A19. Experiment 19 for 1.0% slope horizontal channel using Pressure Flow Condition without any friction blocks.

H.J.	Run	H	W_{temp}	Q	$V_{u/s}$	Y_s	Y_{toe}	Y_1	Y_2	$Y_{d/s}$	Fr1	V_1	V_2	$V_{d/s}$	L	X	ΔE	THL	E_2/E_1
N	19A	0.8d	-	0.9771	2.4428	2.13	1.85	1.75	1.75	1.75	3.9	8.4326 P-tube	-	8.0250 P-tube	-	-	-	2.9619	-
N	19B	1.0d	-	1.2656	2.5312	2.75	2.25	2.00	2.13	2.00	3.7	8.6679 P-tube	-	8.5902 P-tube	-	-	-	2.2438	-
N	19C	1.2d	-	1.5736	2.6227	2.83	2.75	2.50	2.50	2.50	3.5	8.9722 P-tube	-	8.9422 P-tube	-	-	-	1.8817	-

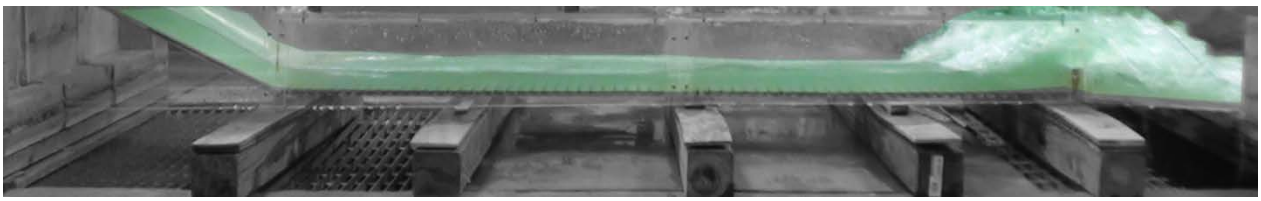

Figure A58. Experiment 20A for 1% slope.

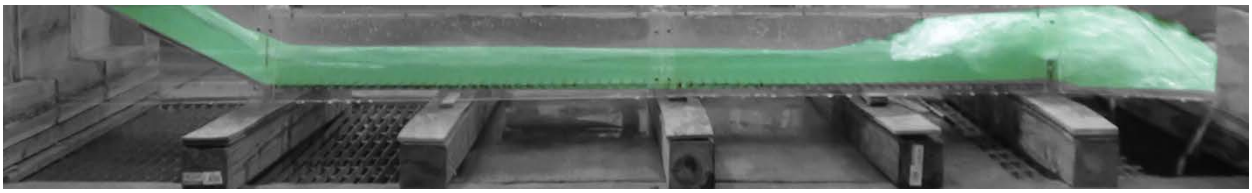

Figure A59. Experiment 20B for 1% slope.

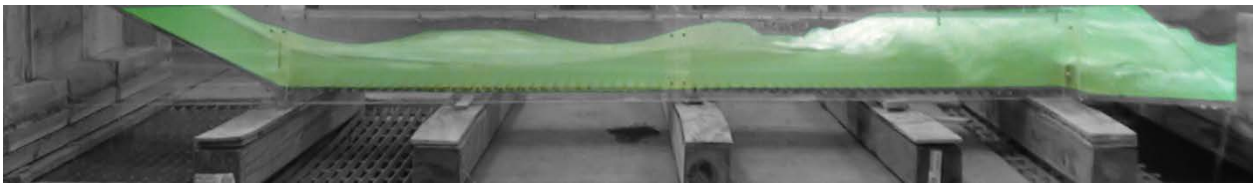

Figure A60. Experiment 20C for 1% slope.

Table A20. Experiment 20 for 1.0% slope using Pressure Flow Condition with a 2'' end sill.

H.J.	Run	H	W_{temp}	Q	$V_{u/s}$	Y_s	Y_{toe}	Y_1	Y_2	$Y_{d/s}$	Fr1	V_1	V_2	$V_{d/s}$	L	X	ΔE	THL	E_2/E_1
Y	20A	0.8d	-	0.9893	2.4733	2.00	1.75	1.75	8.61		3.8	8.2719 P-tube	6.6539	6.6539 P-tube	11.00	12.00	5.3609	8.4898	0.6303
Y	20B	1.0d	-	1.2524	2.5048	2.75	2.13	2.00	9.25		3.6	8.3526 P-tube	7.3258	7.3258 P-tube	11.00	14.00	5.1449	7.9691	0.6570
Y	20C	1.2d	-	1.5837	2.6395	3.50	2.85	3.13	12.39		3.1	9.0763 P-tube	7.6833	7.6833 P-tube	15.00	18.00	5.1137	8.2982	0.7233

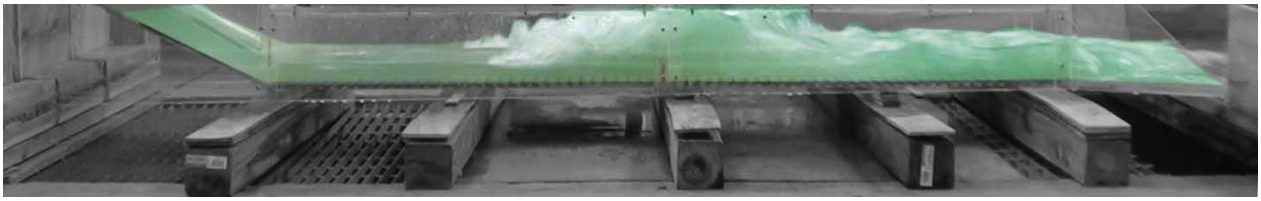

Figure A61. Experiment 21A for 1% slope.

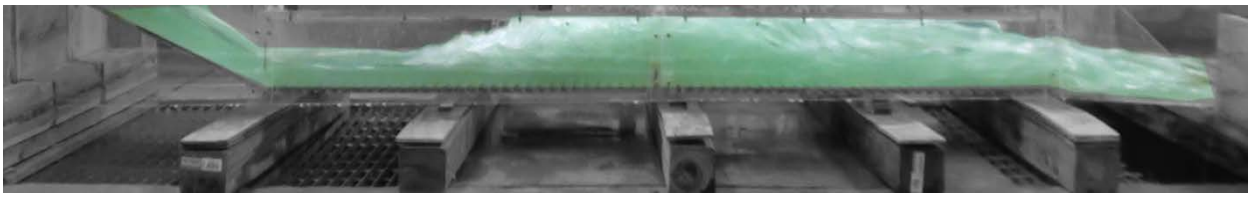

Figure A62. Experiment 21B for 1% slope.

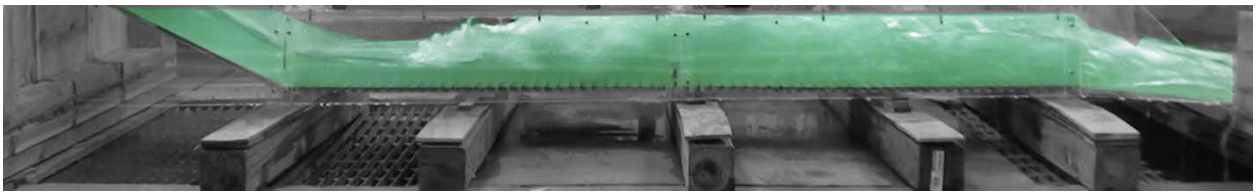

Figure A63. Experiment 21C for 1% slope.

Table A21. Experiment 21 for 1.0% slope using Pressure Flow Condition with a 2''sill at 34'' from the end.

H.J.	Run	H	W_{temp}	Q	$V_{u/s}$	Y_s	Y_{toe}	Y_1	Y_2	$Y_{d/s}$	Fr1	V_1	V_2	$V_{d/s}$	L	X	ΔE	THL	E_2/E_1
Y	21A	0.8d	-	0.9812	2.4530	2.00	1.85	1.50	7.22	3.00	3.7	7.5067 P-tube	5.6031	4.9847 P-tube	14.00	16.00	4.3245	9.0912	0.6396
Y	21B	1.0d	-	1.2460	2.4920	2.75	2.13	1.85	9.30	3.25	3.9	8.6679 P-tube	6.0631	5.4968 P-tube	14.50	22.00	6.0001	9.0772	0.6214
Y	21C	1.2d	-	1.5887	2.6478	3.50	2.65	2.13	8.67	3.50	3.2	7.6833 P-tube	7.3258	6.1292 P-tube	16.00	34.00	3.7924	8.8064	0.7112

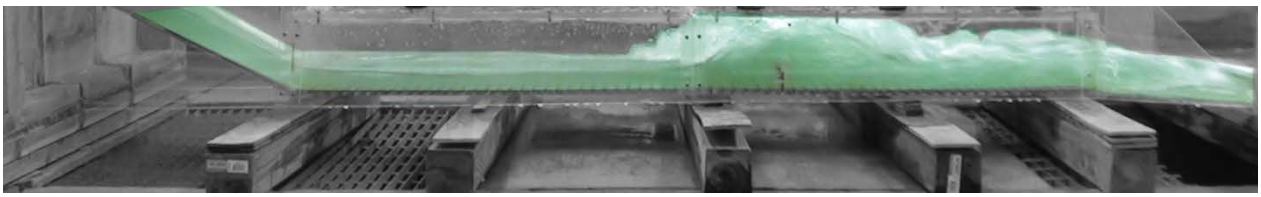

Figure A64. Experiment 22A for 1% slope.

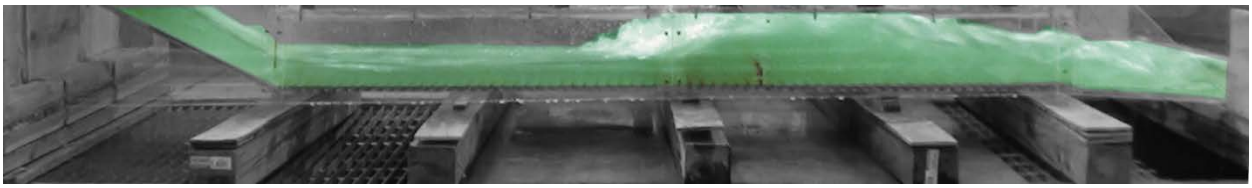

Figure A65. Experiment 22B for 1% slope.

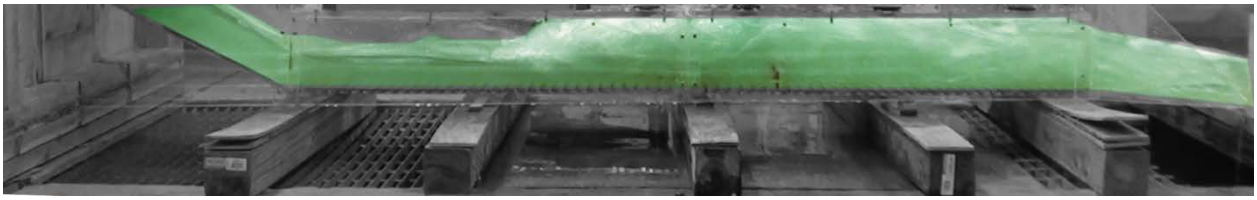

Figure A67. Experiment 22C for 1% slope.

Table A22. Experiment 22 for 1.0% slope using Pressure Flow Condition with a 2.5''sill at 26'' from the end.

H.J.	Run	H	W_{temp}	Q	$V_{u/s}$	Y_s	Y_{toe}	Y_1	Y_2	$Y_{d/s}$	Fr1	V_1	V_2	$V_{d/s}$	L	X	ΔE	THL	E_2/E_1
Y	22A	0.8d	-	0.9648	2.4120	1.85	1.75	1.50	7.81	2.75	4.0	8.0683 P-tube	5.3080	4.9143 P-tube	6.00	6.00	5.3690	9.4341	0.6061
Y	22B	1.0d	-	1.2524	2.5048	2.85	2.13	2.00	9.50	3.25	3.7	8.5589 P-tube	6.6539	5.3080 P-tube	9.50	14.00	5.5471	9.4691	0.6456
Y	22C	1.2d	-	1.6086	2.6810	3.25	2.75	2.50	10.69	4.00	3.4	8.6989 P-tube	5.9062	5.5065 P-tube	12.00	25.00	5.1389	9.6893	0.6904

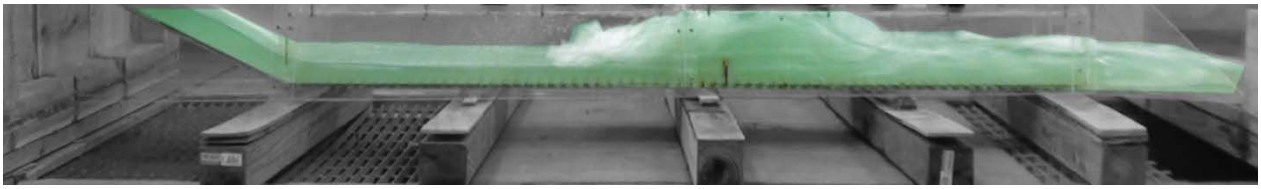

Figure A68. Experiment 23A for 1% slope.

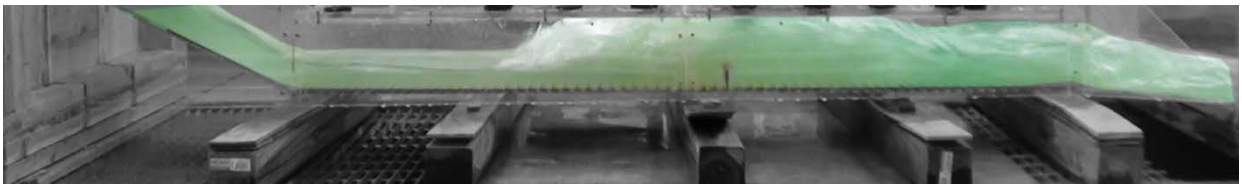

Figure A69. Experiment 23B for 1% slope.

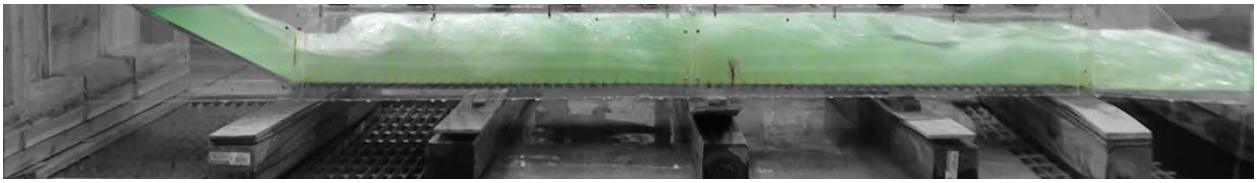

Figure A70. Experiment 23C for 1% slope.

Table A23. Experiment 23 for 1.0% slope using Pressure Flow Condition with a 2''sill at 30'' from the end.

H.J.	Run	H	W_{temp}	Q	$V_{u/s}$	Y_s	Y_{toe}	Y_1	Y_2	$Y_{d/s}$	Fr1	V_1	V_2	$V_{d/s}$	L	X	ΔE	THL	E_2/E_1
Y	23A	0.8d	-	0.9606	2.4015	2.00	1.75	1.50	7.77	2.75	4.0	8.0250 P-tube	2.3166	5.1018 P-tube	10.50	14.00	5.2842	9.0746	0.6086
Y	23B	1.0d	-	1.2524	2.5048	2.85	2.13	2.85	10.99	3.50	3.1	8.4643 P-tube	2.8373	5.5550 P-tube	13.50	21.00	4.3092	8.7191	0.7340
Y	23C	1.2d	-	1.6086	2.6810	3.35	2.75	2.50	10.65	4.00	3.3	8.6679 P-tube	4.6332	6.5524 P-tube	14.00	35.00	5.0803	7.3393	0.6921

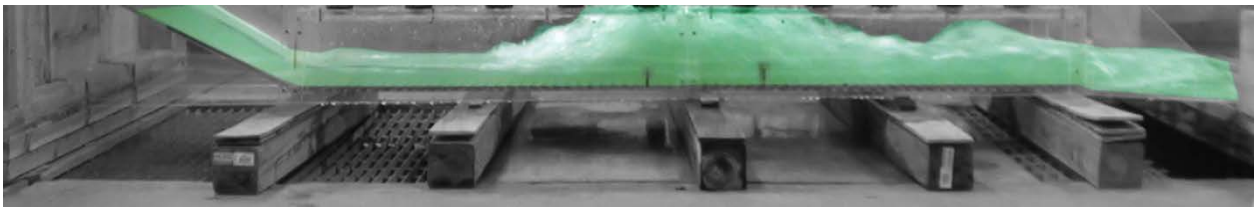

Figure A71. Experiment 24A for 1% slope.

Figure A72. Experiment 24B for 1% slope.

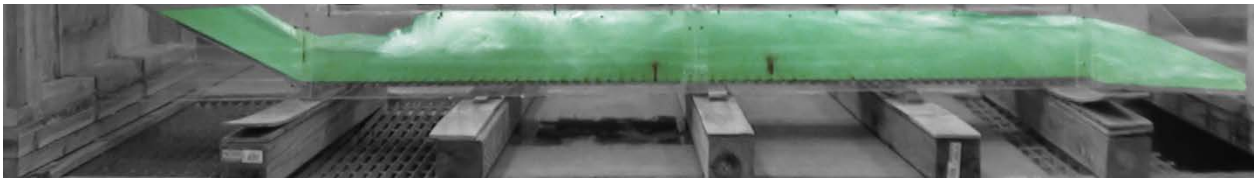

Figure A73. Experiment 24C for 1% slope.

Table A24. Experiment 24 for 1.0% slope using Pressure Flow Condition and a 1.5''sill at 37'' from the end and 2'' sill at 27'' from the end.

H.J.	Run	H	W_{temp}	Q	$V_{u/s}$	Y_s	Y_{toe}	Y_1	Y_2	$Y_{d/s}$	Fr1	V_1	V_2	$V_{d/s}$	L	X	ΔE	THL	E_2/E_1
Y	24A	0.8d	-	0.9523	2.3808	1.85	1.75	1.35	7.65	2.85	4.3	8.2719 P-tube	4.1763	4.9143 P-tube	11.00	22.00	6.0529	9.3061	0.5707
Y	24B	1.0d	-	1.2524	2.5048	2.85	2.50	2.00	9.63	3.35	3.7	8.6679 P-tube	5.9062	5.5550 P-tube	12.00	26.00	5.7660	8.8691	0.6396
Y	24C	1.2d	-	1.5987	2.6645	3.25	2.85	2.65	11.29	4.25	3.3	8.9272 P-tube	6.7540	6.0187 P-tube	13.50	33.00	5.3909	8.3229	0.6919

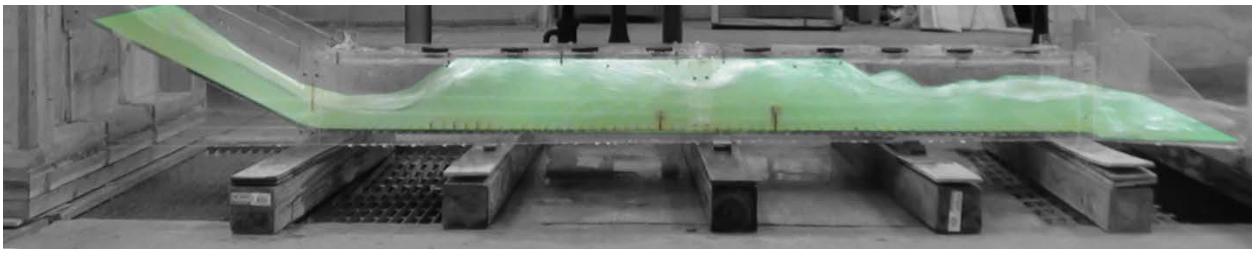

Figure A74. Experiment 25A for 1% slope.

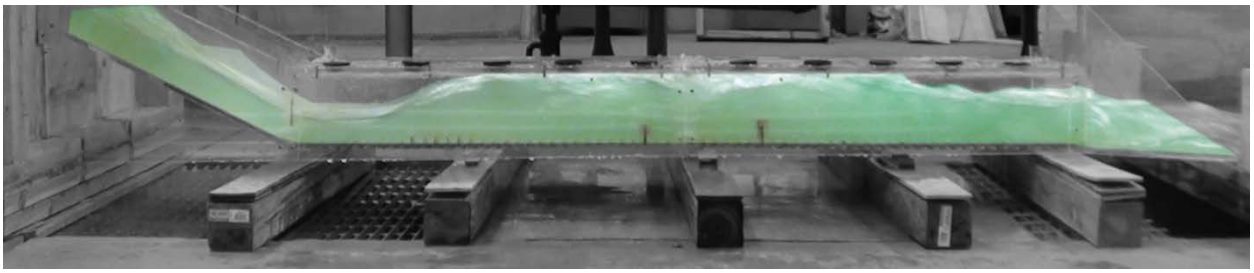

Figure A75. Experiment 25B for 1% slope.

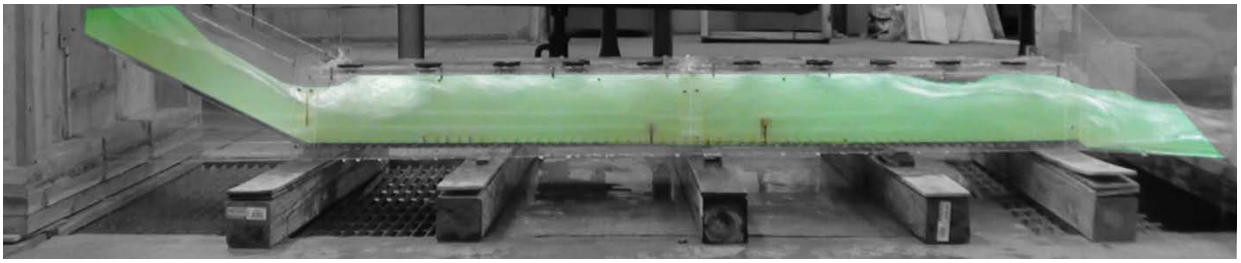

Figure A76. Experiment 25C for 1% slope.

Table A25. Experiment 25 for 1% slope using Pressure Flow Condition with 15 flat faced friction blocks and a 1.5''sill at 37'' from the end and a 2'' sill at 27'' from the end.

H.J.	Run	H	W_{temp}	Q	$V_{u/s}$	Y_s	Y_{toe}	Y_1	Y_2	$Y_{d/s}$	Fr1	V_1	V_2	$V_{d/s}$	L	X	ΔE	THL	E_2/E_1
Y	25A	0.8d	-	0.9606	2.4015	1.85	1.75	1.75	7.54	2.75	3.4	7.3258 P-tube	3.6629	4.9143 P-tube	7.50	35.50	3.6737	9.4246	0.6873
Y	25B	1.0d	-	1.2524	2.5048	2.85	2.13	2.25	9.22	3.25	3.2	7.9409 P-tube	5.0489	5.1801 P-tube	8.00	33.00	4.0804	9.7191	0.7085
Y	25C	1.2d	-	1.5812	2.6353	3.25	3.00	3.00	10.72	4.00	2.9	8.1081 P-tube	5.1801	5.7915 P-tube	12.00	41.00	3.5733	9.0441	0.7657

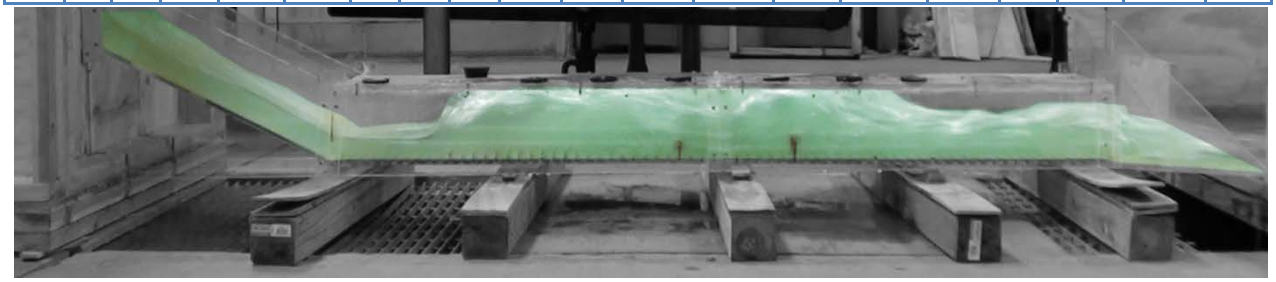

Figure A77. Experiment 26A for 1% slope.

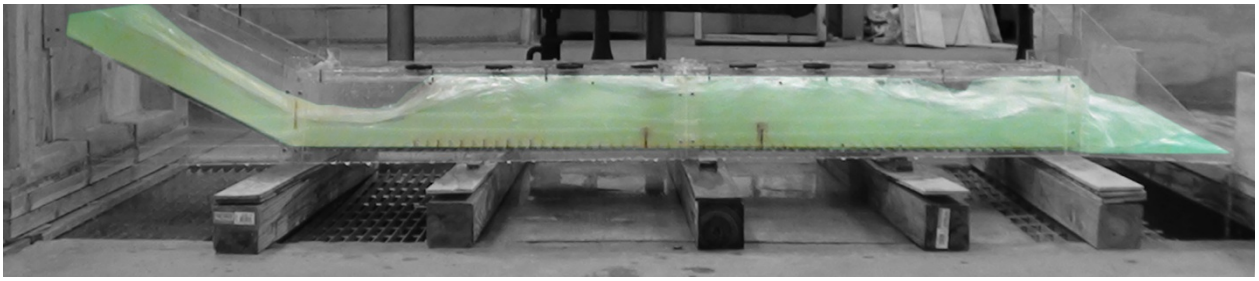

Figure A78. Experiment 26B for 1% slope.

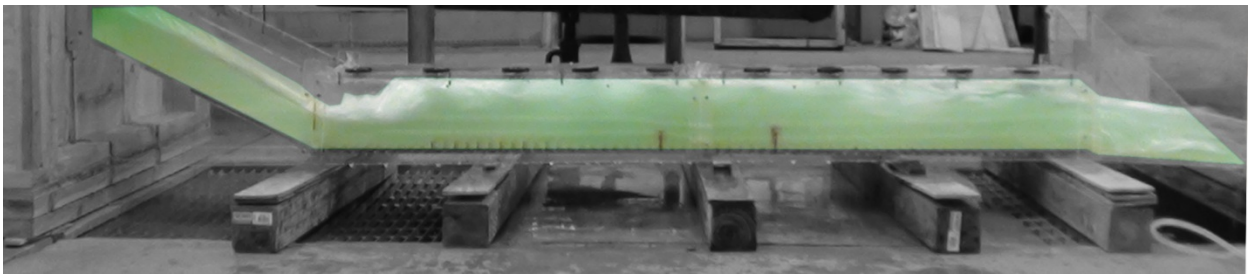

Figure A79. Experiment 26C for 1% slope.

Table A26. Experiment 26 for 1.0% slope using Pressure Flow Condition with 30 flat faced friction blocks and a 1.5''sill at 37'' from the end and a 2'' sill at 27'' from the end.

H.J.	Run	H	W_{temp}	Q	$V_{u/s}$	Y_s	Y_{toe}	Y_1	Y_2	$Y_{d/s}$	Fr1	V_1	V_2	$V_{d/s}$	L	X	ΔE	THL	E_2/E_1
Y	26A	0.8d	-	0.9771	2.4428	2.00	1.75	1.75	8.6127	2.75	3.8	8.2719 P-tube	2.4626	4.7758 P-tube	8.00	33.00	5.3609	9.7119	0.6303
Y	26B	1.0d	-	1.2524	2.5048	2.85	2.13	2.00	8.9499	3.25	3.5	8.1081 P-tube	4.0125	5.5065 P-tube	8.00	33.00	4.6884	9.0691	0.6710
Y	26C	1.2d	-	1.6012	2.6687	3.50	3.00	3.00	10.9599	4.25	2.9	8.2719 P-tube	5.5065	6.1858 P-tube	12.00	41.00	3.8348	7.9470	0.7565

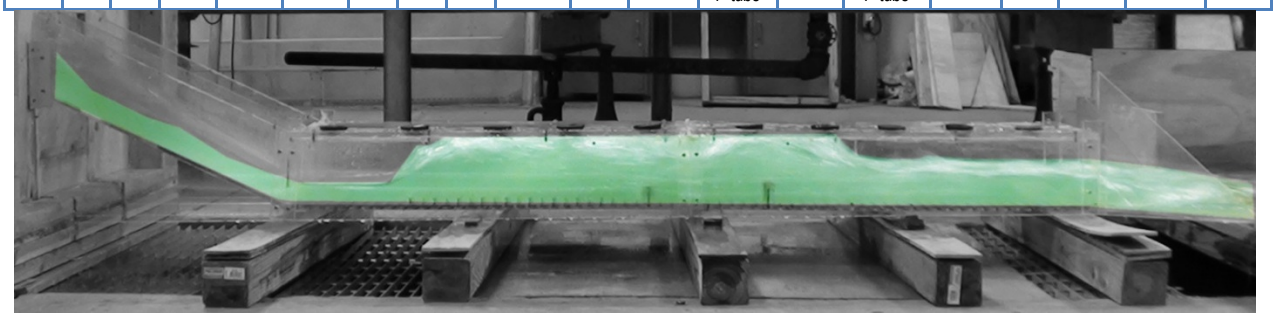

Figure A80. Experiment 27A for 1% slope.

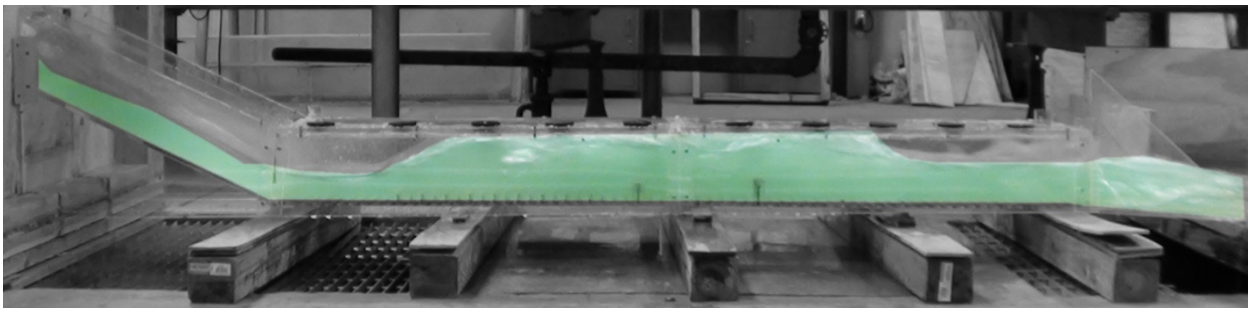

Figure A81. Experiment 27B for 1% slope.

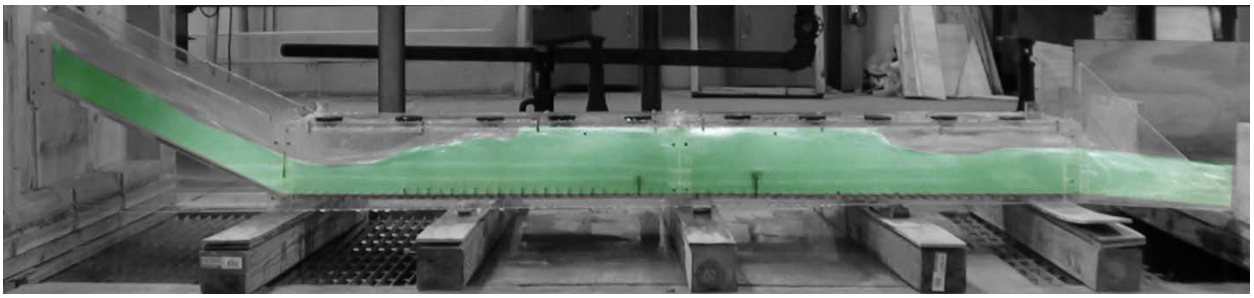

Figure A82. Experiment 27C for 1% slope.

Table A27. Experiment 27 for 1.0% slope using Pressure Flow Condition with 45 flat faced friction blocks and a 1.5''sill at 37'' from the end and a 2'' sill at 27'' from the end.

H.J.	Run	H	W_{temp}	Q	$V_{u/s}$	Y_s	Y_{toe}	Y_1	Y_2	$Y_{d/s}$	Fr1	V_1	V_2	$V_{d/s}$	L	X	ΔE	THL	E_2/E_1
Y	27A	0.8d	-	0.9648	2.4120	1.85	1.75	1.75	8.8854	2.75	3.9	8.5118 P-tube	4.0125	4.9143 P-tube	7.50	34.00	5.8409	9.4341	0.6170
Y	27B	1.0d	-	1.2524	2.5048	2.85	2.13	2.00	9.4403	3.25	3.72	8.5118 P-tube	2.3166	5.6745 P-tube	9.00	33.00	5.4538	8.7191	0.6481
Y	27C	1.2d	-	1.5762	2.6270	3.13	2.75	2.50	10.0000	3.75	3.2	8.1904 P-tube	3.2762	6.3443 P-tube	10.00	34.00	4.2188	8.0359	0.7188

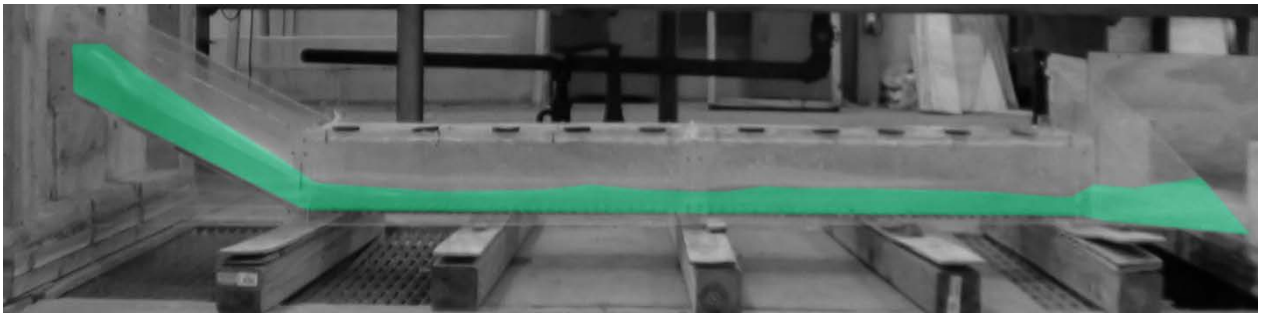

Figure A83. Experiment 28A for 0.6% slope.

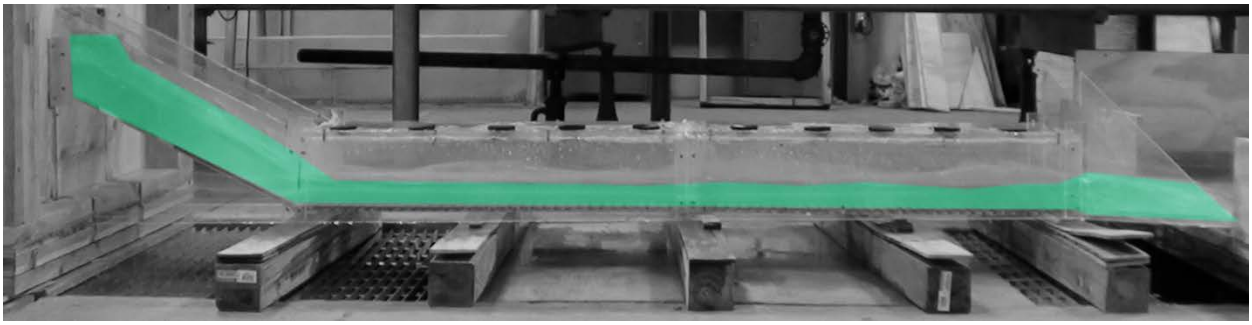

Figure A84. Experiment 28B for 0.6% slope.

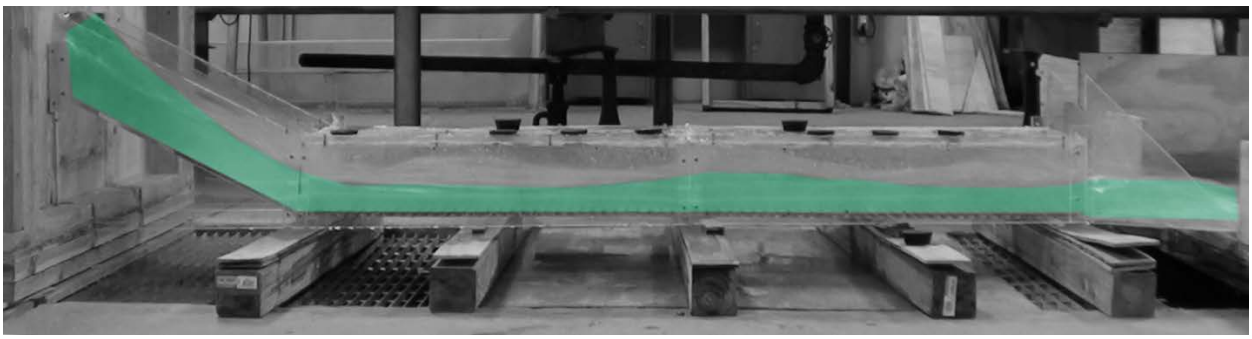

Figure A85. Experiment 28C for 0.6% slope.

Table A28. Experiment 28 for 0.6% slope horizontal channel using Pressure Flow Condition without any friction blocks.

H.J.	Run	H	W_{temp}	Q	$V_{u/s}$	Y_s	Y_{toe}	Y_1	Y_2	$Y_{d/s}$	Fr1	V_1	V_2	$V_{d/s}$	L	X	ΔE	THL	E_2/E_1
N	28A	0.8d	-	0.9648	2.4120	2.00	1.85	1.35	1.50	1.50	4.6	8.7081 P-tube	8.1904	7.7701 P-tube	-	-	-	3.9341	-
N	28B	1.0d	-	1.2524	2.5048	2.75	2.25	1.85	2.00	2.00	4.0	8.8214 P-tube	8.8669	8.5118 P-tube	-	-	-	2.4691	-
N	28C	1.2d	-	1.5862	2.6437	2.85	2.75	2.35	2.25	3.50	3.6	9.0466 P-tube	8.8971	8.6679 P-tube	-	-	-	1.8023	-

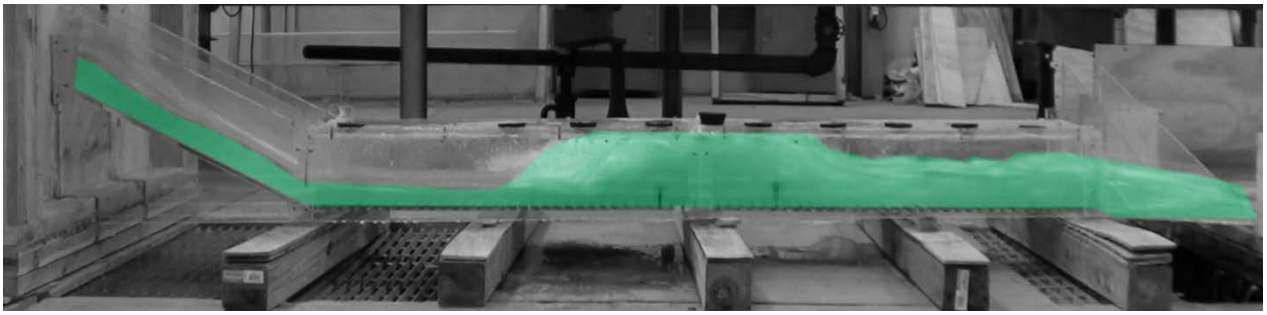

Figure A86. Experiment 29A for 0.6% slope.

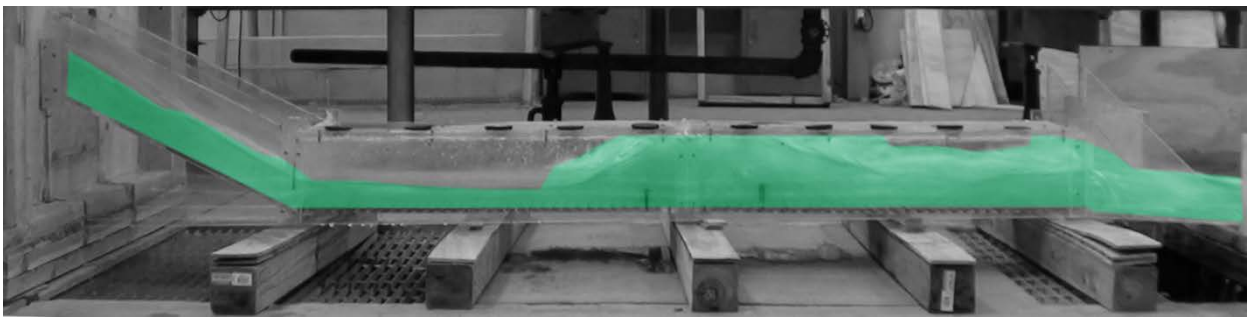

Figure A87. Experiment 29B for 0.6% slope.

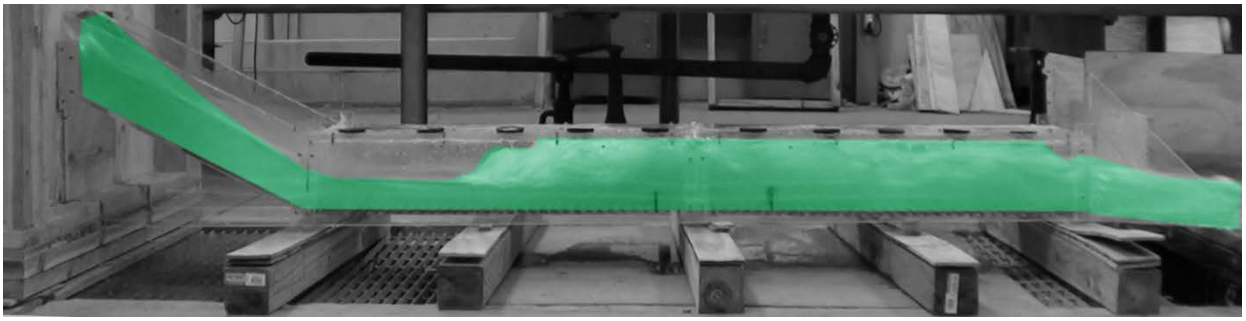

Figure A88. Experiment 29C for 0.6% slope.

Table A29. Experiment 29 for 0.6% slope using Pressure Flow Condition and a 1.5''sill at 37'' from the end and a 2'' sill at 27'' from the end.

H.J.	Run	H	W_{temp}	Q	$V_{u/s}$	Y_s	Y_{toe}	Y_1	Y_2	$Y_{d/s}$	Fr1	V_1	V_2	$V_{d/s}$	L	X	ΔE	THL	E_2/E_1
Y	29A	0.8d	-	0.9648	2.4120	2.00	1.75	1.50	8.03	3.00	4.1	8.2719 P-tube	3.0646	5.1018 P-tube	9.00	22.00	5.7764	8.8341	0.5946
Y	29B	1.0d	-	1.2524	2.5048	2.75	1.13	1.75	8.97	3.25	4.0	8.5902 P-tube	4.9143	5.6745 P-tube	9.00	22.00	6.0025	8.7191	0.6127
Y	29C	1.2d	-	1.6086	2.6810	2.50	2.75	2.50	10.65	3.75	3.3	8.6679 P-tube	4.9143	5.6745 P-tube	14.00	35.00	5.0803	9.5893	0.6921

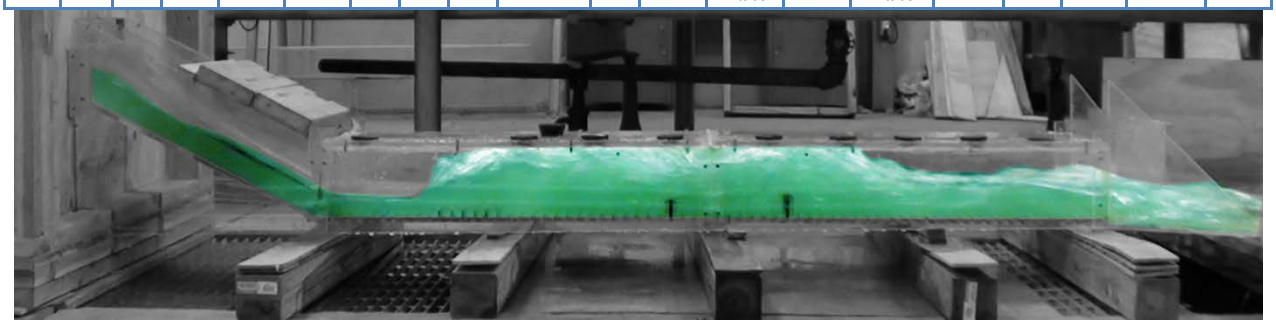

Figure A89. Experiment 30A for 0.6% slope.

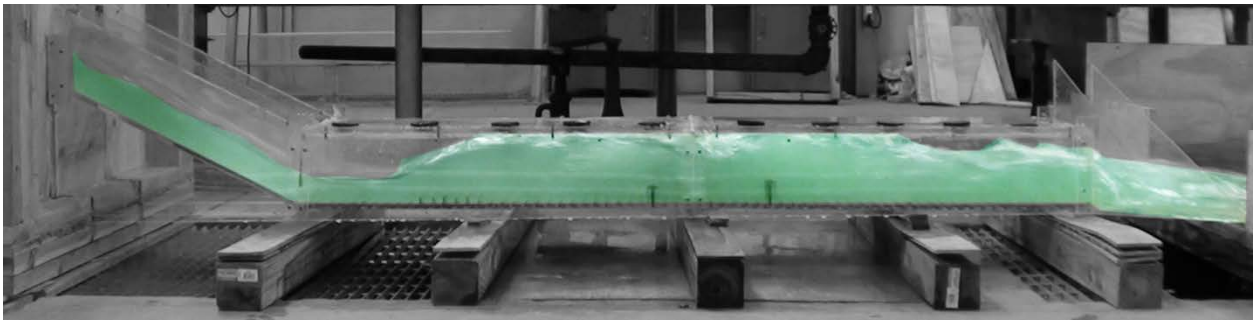

Figure A90. Experiment 30B for 0.6% slope.

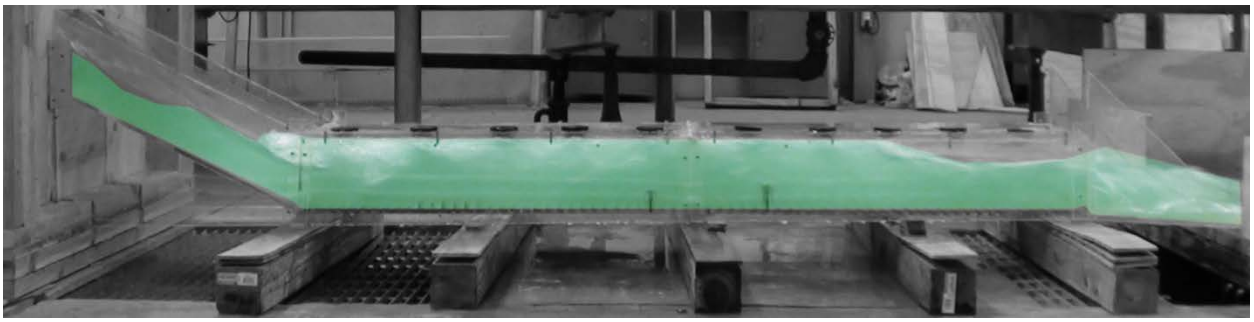

Figure A91. Experiment 30C for 0.6% slope.

Table A30. Experiment 30 for 0.6% slope using Pressure Flow Condition with 15 flat faced friction blocks and a 1.5''sill at 37'' from the end and a 2'' sill at 27'' from the end.

H.J.	Run	H	W_{temp}	Q	$V_{u/s}$	Y_s	Y_{toe}	Y_1	Y_2	$Y_{d/s}$	Fr1	V_1	V_2	$V_{d/s}$	L	X	ΔE	THL	E_2/E_1
Y	30A	0.8d	-	0.9648	2.4120	1.85	1.75	1.75	8.7518	2.75	3.9	8.3943 P-tube	3.2762	4.7079 P-tube	8.00	33.00	5.6032	9.8041	0.6234
Y	30B	1.0d	-	1.2534	2.5068	2.85	2.25	2.13	9.9083	3.50	3.6	8.6679 P-tube	4.7079	5.5065 P-tube	9.00	34.00	5.5747	8.8209	0.6544
Y	30C	1.2d	-	1.5812	2.6353	3.50	3.25	3.00	10.7168	4.25	2.97	8.1081 P-tube	4.7079	6.0187 P-tube	11.00	41.40	3.5733	8.2941	0.7657

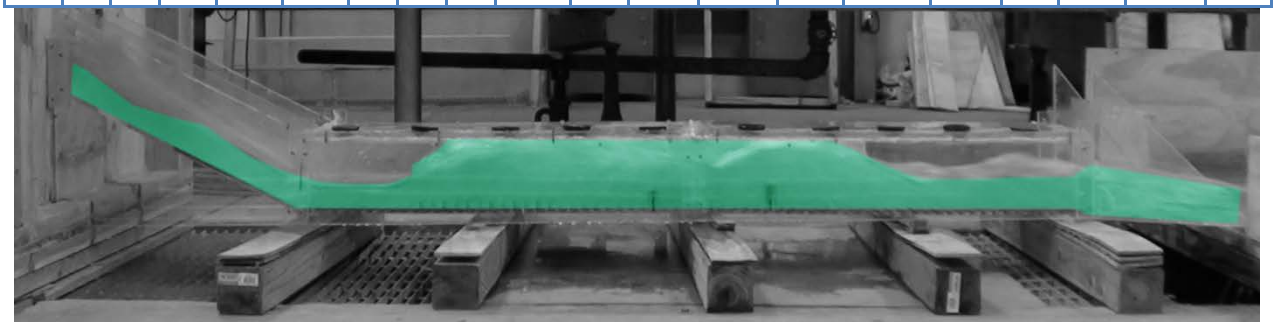

Figure A92. Experiment 31A for 0.6% slope.

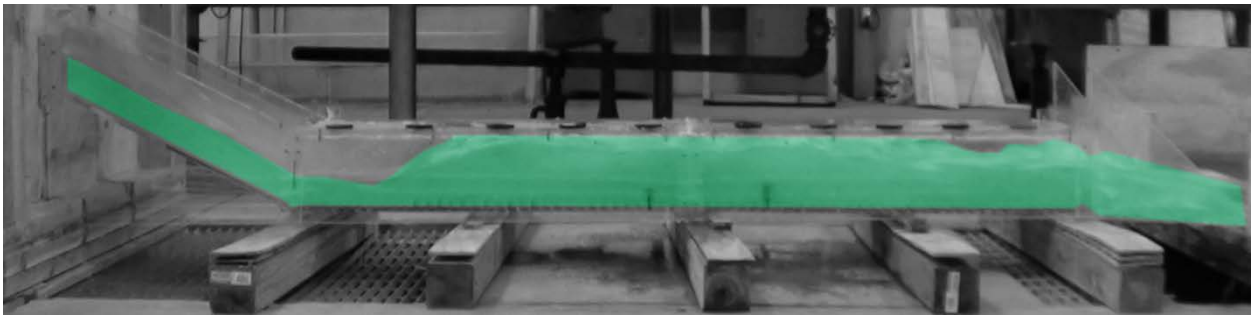

Figure A93. Experiment 31B for 0.6% slope.

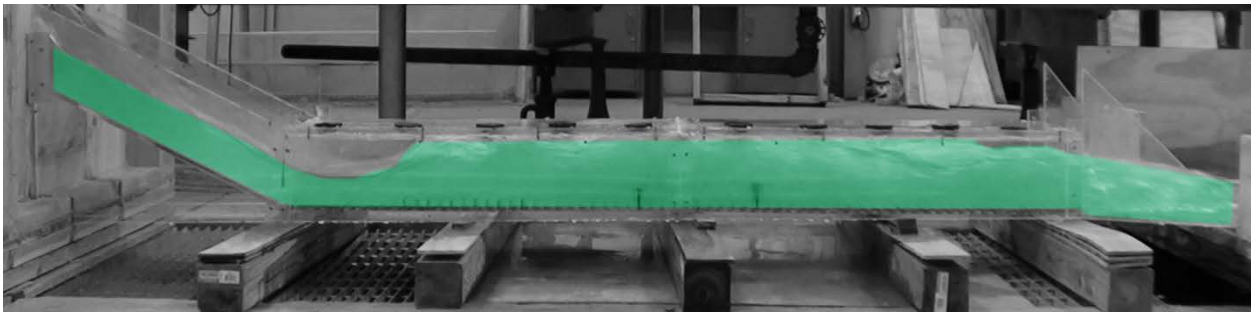

Figure A94. Experiment 31C for 0.6% slope.

Table A31. Experiment 31 for 0.6% slope using Pressure Flow Condition with 30 flat faced friction blocks and a 1.5''sill at 37'' from the end and a 2'' sill at 27'' from the end.

H.J.	Run	H	W_{temp}	Q	$V_{u/s}$	Y_s	Y_{toe}	Y_1	Y_2	$Y_{d/s}$	Fr1	V_1	V_2	$V_{d/s}$	L	X	ΔE	THL	E_2/E_1
Y	31A	0.8d	-	0.9648	2.4120	1.85	1.75	1.75	8.8854	2.75	3.9	8.5118 P-tube	4.1763	3.4749 P-tube	8.00	34.00	5.8409	11.6841	0.6170
Y	31B	1.0d	-	1.2524	2.4850	2.75	2.25	2.13	9.9587	3.50	3.6	8.7081 P-tube	5.2470	5.3583 P-tube	9.00	34.00	5.6549	9.1007	0.6522
Y	31C	1.2d	-	1.5635	2.6058	3.50	2.75	2.75	10.2577	4.25	3.0	8.0683 P-tube	5.3080	6.1292 P-tube	12.00	41.40	3.7504	8.0153	0.7480

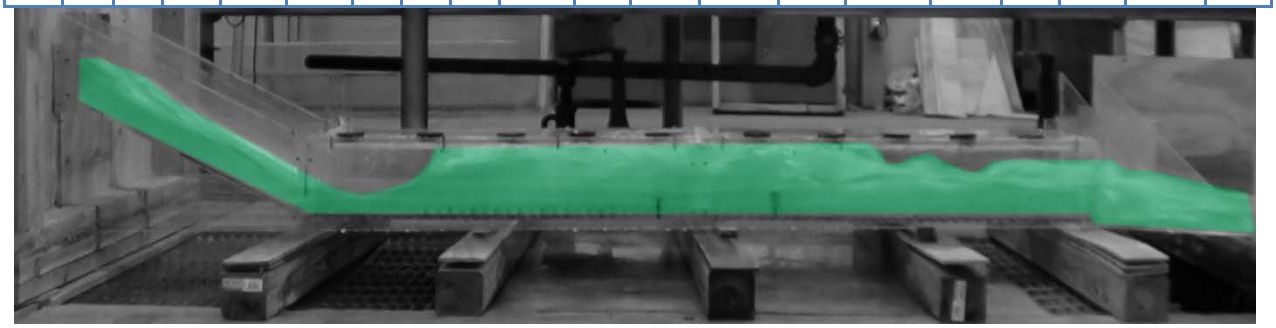

Figure A95. Experiment 32A for 0.6% slope.

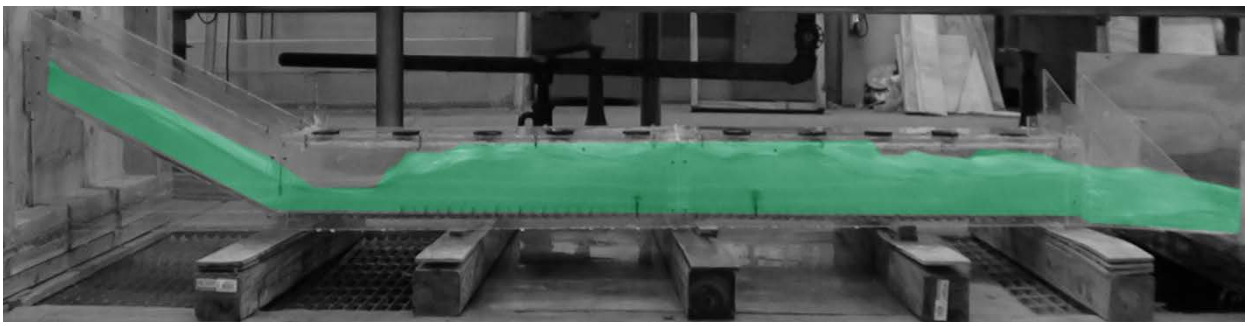

Figure A96. Experiment 32B for 0.6% slope.

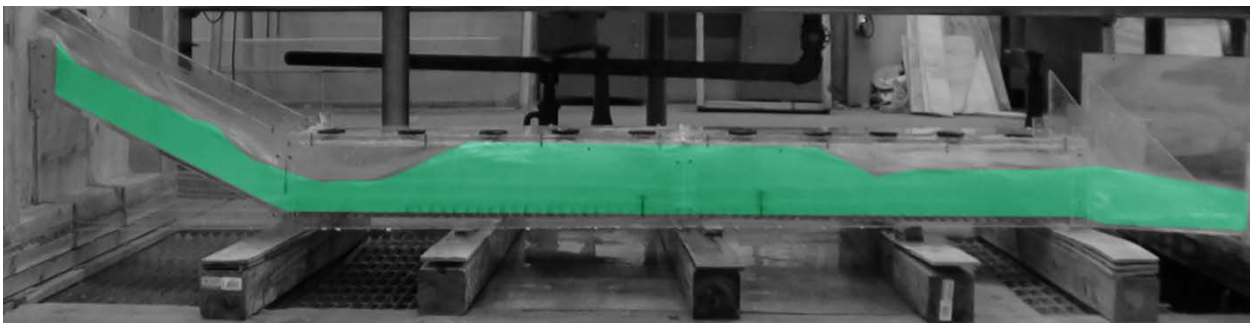

Figure A97. Experiment 32C for 0.6% slope.

Table A32. Experiment 32 for 0.6% slope using Pressure Flow Condition with 45 flat faced friction blocks and a 1.5''sill at 37'' from the end and a 2'' sill at 27'' from the end.

H.J.	Run	H	W_{temp}	Q	$V_{u/s}$	Y_s	Y_{toe}	Y_1	Y_2	$Y_{d/s}$	Fr1	V_1	V_2	$V_{d/s}$	L	X	ΔE	THL	E_2/E_1
Y	32A	0.8d	-	0.9648	2.4120	1.85	1.85	1.75	8.83	2.75	3.9	8.4643 P-tube	3.7712	4.7758 P-tube	8.00	33.00	5.7443	9.6841	0.6169
Y	32B	1.0d	-	1.2524	2.5048	2.75	2.13	2.00	9.44	3.25	3.7	8.5118 P-tube	4.3340	5.5550 P-tube	9.00	33.00	5.4538	8.9691	0.6481
Y	32C	1.2d	-	1.5937	2.6562	3.35	2.65	2.50	10.00	4.00	3.2	8.1904 P-tube	6.4492	6.3443 P-tube	11.00	34.00	4.2188	7.8146	0.7188

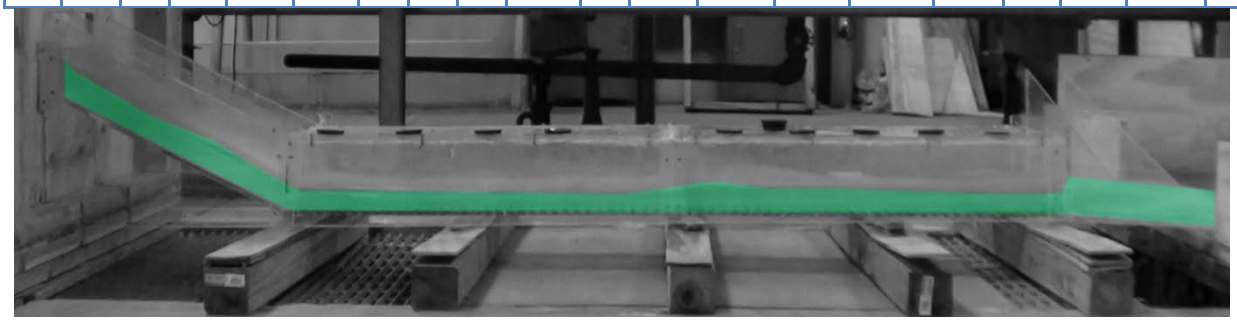

Figure A98. Experiment 33A for 0.3% slope.

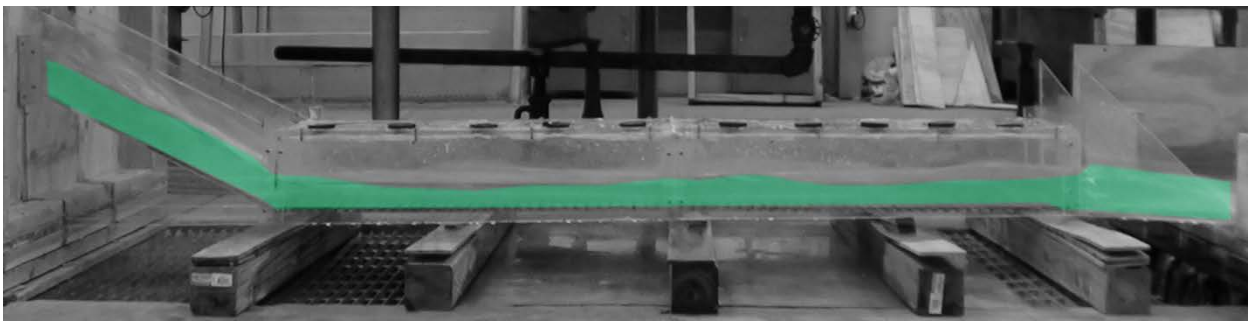

Figure A99. Experiment 33B for 0.3% slope.

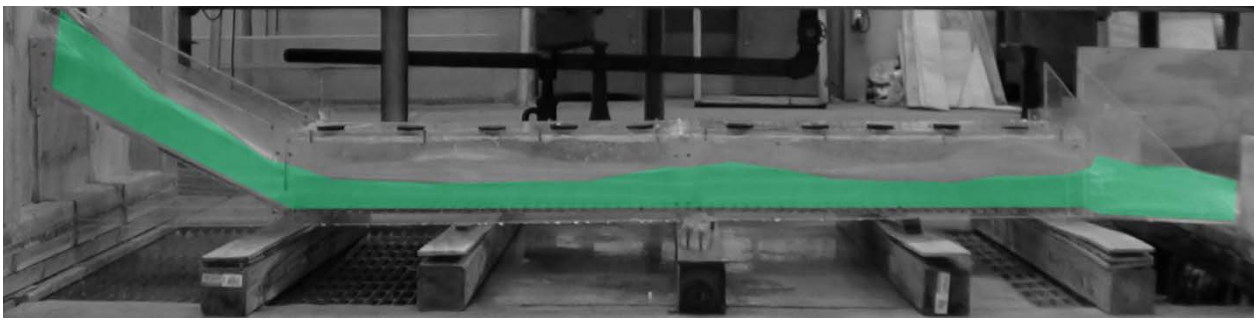

Figure A100. Experiment 33C for 0.3% slope.

Table A33. Experiment 33 for 0.3% slope horizontal channel using Pressure Flow Condition without any friction blocks.

H.J.	Run	H	W_{temp}	Q	$V_{u/s}$	Y_s	Y_{toe}	Y_1	Y_2	$Y_{d/s}$	Fr1	V_1	V_2	$V_{d/s}$	L	X	ΔE	THL	E_2/E_1
N	33A	0.8d	-	0.9648	2.4120	1.85	1.75	1.50	1.50	1.65	4.3	8.5902 P-tube	8.4326	7.6833 P-tube	-	-	-	4.0341	-
N	33B	1.0d	-	1.2524	2.5048	2.85	2.13	1.85	1.85	2.13	4.0	8.8214 P-tube	8.5118	8.0250 P-tube	-	-	-	3.8391	-
N	33C	1.2d	-	1.5962	2.6603	3.25	2.75	2.50	2.25	2.35	3.5	9.0466 P-tube	8.8971	8.4326 P-tube	-	-	-	3.7188	-

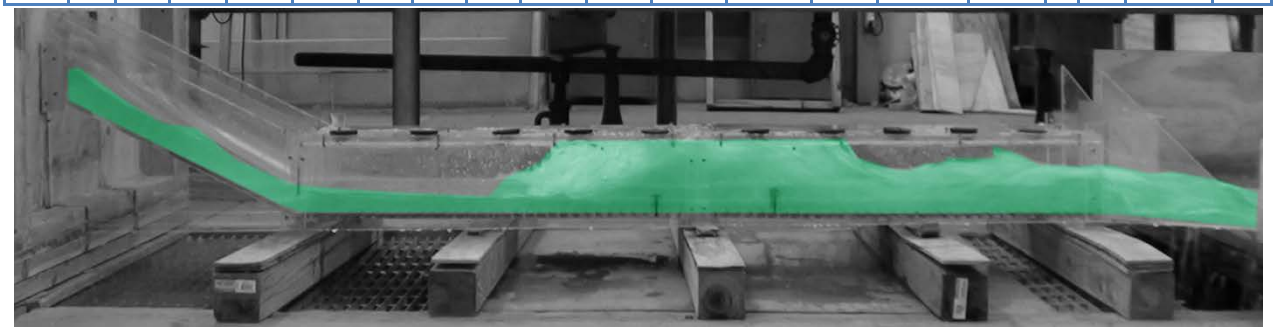

Figure A101. Experiment 34A for 0.3% slope.

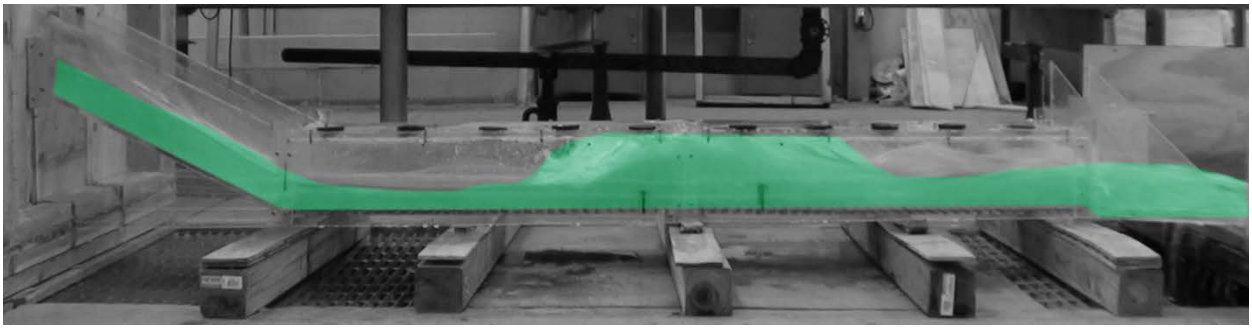

Figure A102. Experiment 34B for 0.3% slope.

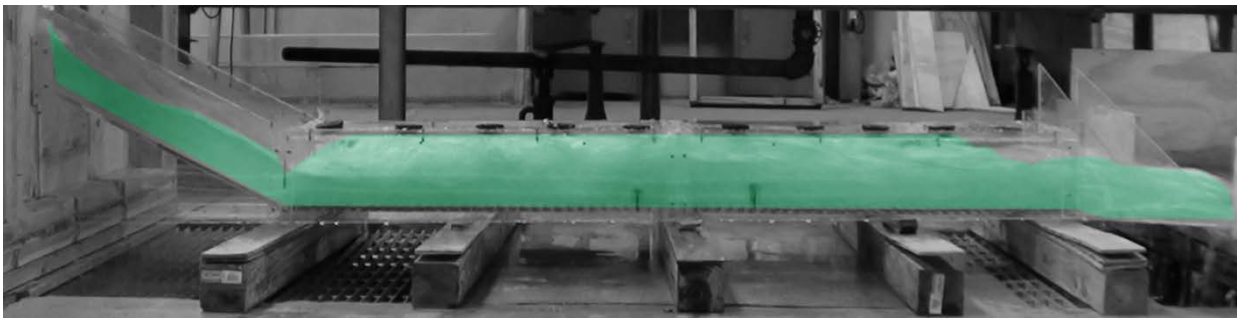

Figure A103. Experiment 34C for 0.3% slope.

Table A34. Experiment 34 for 0.3% slope using Pressure Flow Condition and a 1.5''sill at 37'' from the end and a 2'' sill at 27'' from the end.

H.J.	Run	H	W_{temp}	Q	$V_{u/s}$	Y_s	Y_{toe}	Y_1	Y_2	$Y_{d/s}$	Fr1	V_1	V_2	$V_{d/s}$	L	X	ΔE	THL	E_2/E_1
Y	34A	0.8d	-	0.9565	2.3913	1.85	1.75	1.50	8.28	2.75	4.2	8.5118 P-tube	5.7915	5.1801 P-tube	8.00	24.00	6.2759	8.9155	0.5816
Y	34B	1.0d	-	1.2460	2.4920	2.65	3.25	2.00	9.76	3.25	3.8	8.7756 P-tube	6.7540	6.1292 P-tube	9.00	23.00	5.9865	7.7072	0.6339
Y	34C	1.2d	-	1.6012	2.6687	3.25	2.85	2.50	10.44	4.25	3.3	8.5118 P-tube	4.3340	6.0187 P-tube	15.00	39.00	4.7893	8.3270	0.7007

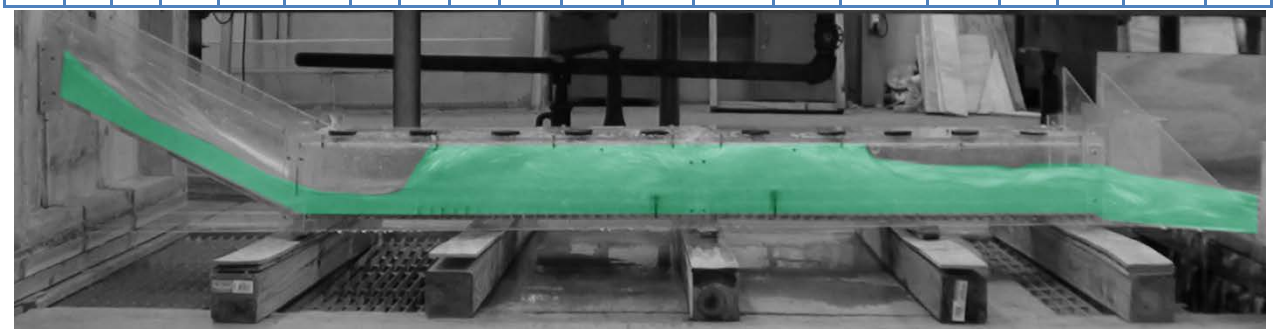

Figure A104. Experiment 35A for 0.3% slope.

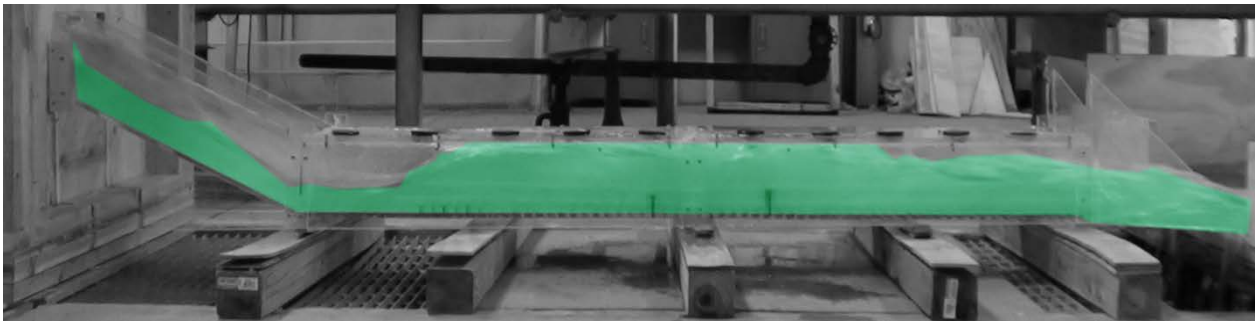

Figure A105. Experiment 35B for 0.3% slope.

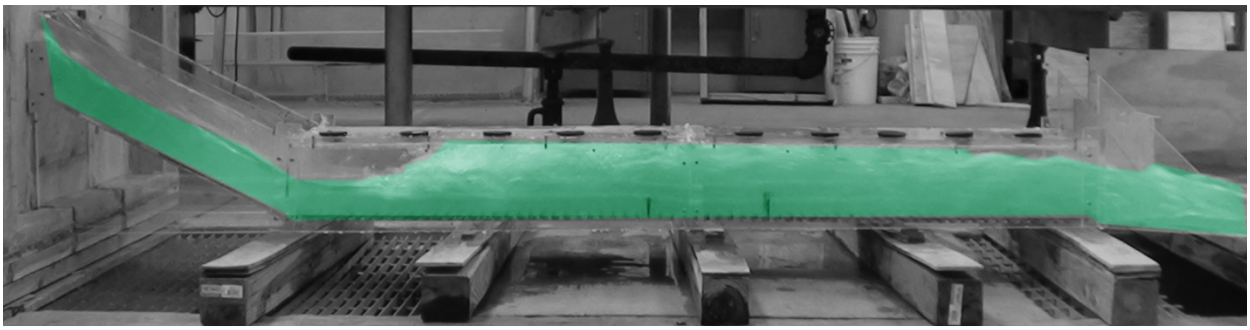

Figure A106. Experiment 35C for 0.3% slope.

Table A35. Experiment 35 for 0.3% slope using Pressure Flow Condition with 15 flat faced friction blocks and a 1.5''sill at 37'' from the end and a 2'' sill at 27'' from the end.

H.J.	Run	H	W_{temp}	Q	$V_{u/s}$	Y_s	Y_{toe}	Y_1	Y_2	$Y_{d/s}$	Fr1	V_1	V_2	$V_{d/s}$	L	X	ΔE	THL	E_2/E_1
Y	35A	0.8d	-	0.9565	2.3913	1.85	1.75	1.75	8.89	2.75	3.9	8.5118 P-tube	3.2762	4.7079 P-tube	7.00	34.00	5.8409	9.7855	0.6170
Y	35B	1.0d	-	1.2524	2.5048	2.75	2.25	2.13	9.96	3.75	3.6	8.7081 P-tube	5.3080	5.3080 P-tube	9.00	37.00	5.6549	8.9691	0.6522
Y	35C	1.2d	-	1.5837	2.6395	3.25	3.00	3.00	10.84	4.25	2.9	8.1904 P-tube	7.0457	6.1292 P-tube	12.00	41.40	3.7035	8.0482	0.7611

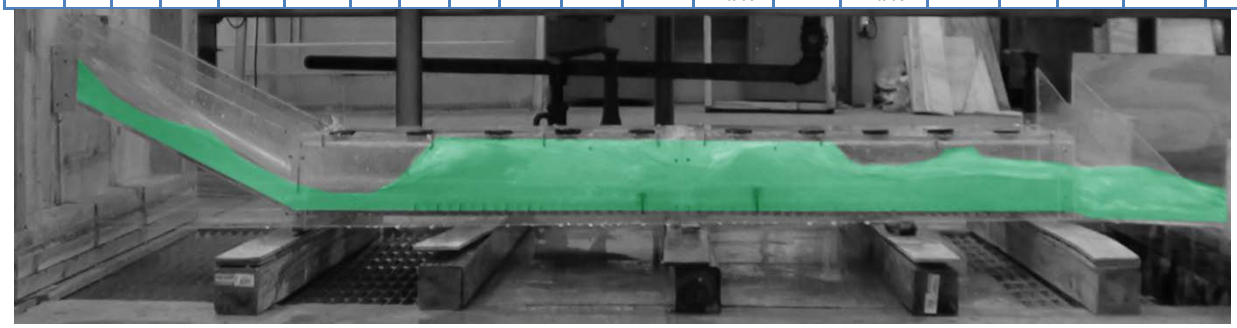

Figure A107. Experiment 36A for 0.3% slope.

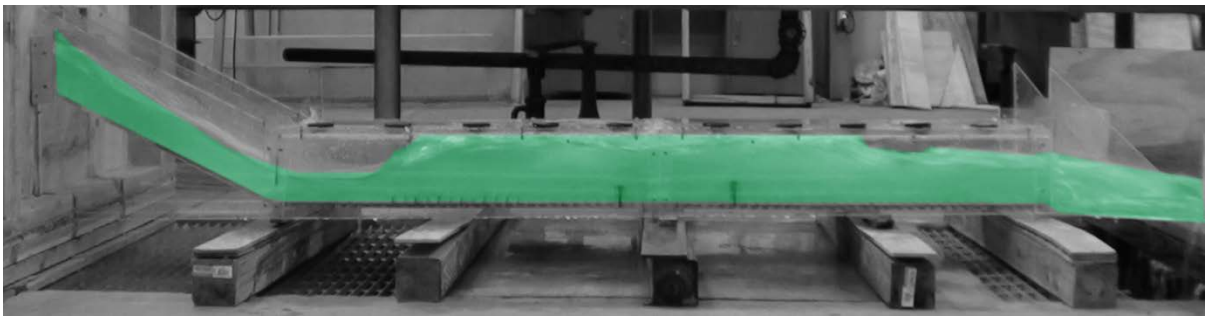

Figure A108. Experiment 36B for 0.3% slope.

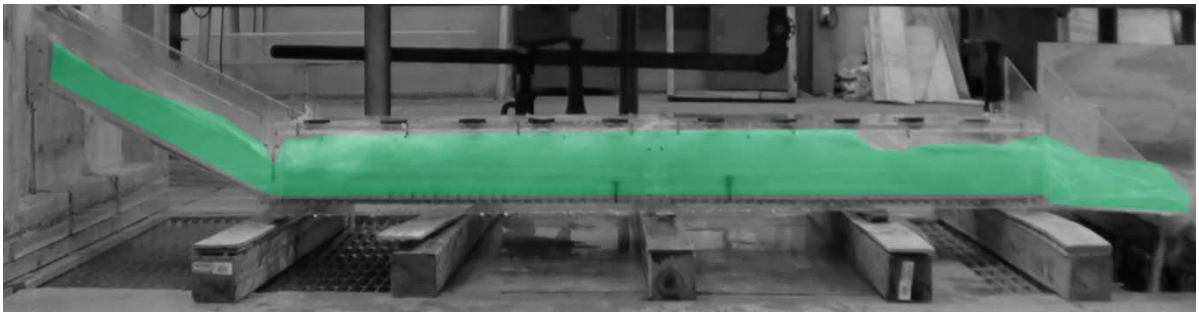

Figure A109. Experiment 36C for 0.3% slope.

Table A36. Experiment 36 for 0.3% slope using Pressure Flow Condition with 30 flat faced friction blocks and a 1.5''sill at 37'' from the end and a 2'' sill at 27'' from the end.

H.J.	Run	H	W_{temp}	Q	$V_{u/s}$	Y_s	Y_{toe}	Y_1	Y_2	$Y_{d/s}$	Fr1	V_1	V_2	$V_{d/s}$	L	X	ΔE	THL	E_2/E_1
Y	36A	0.8d	-	0.9648	2.4120	1.85	1.75	1.75	7.74	3.25	3.5	7.5067 P-tube	3.2762	4.7758 P-tube	8.00	33.00	3.9709	9.1841	0.6758
Y	36B	1.0d	-	1.2460	2.4920	2.75	1.25	2.00	9.57	3.50	3.7	8.6214 P-tube	4.3340	5.4329 P-tube	9.00	34.00	5.6720	8.9572	0.6421
Y	36C	1.2d	-	1.5987	2.6645	3.35	3.00	3.00	10.59	4.25	2.8	8.0250 P-tube	5.4329	6.2377 P-tube	12.00	41.40	3.4442	7.8229	0.7704

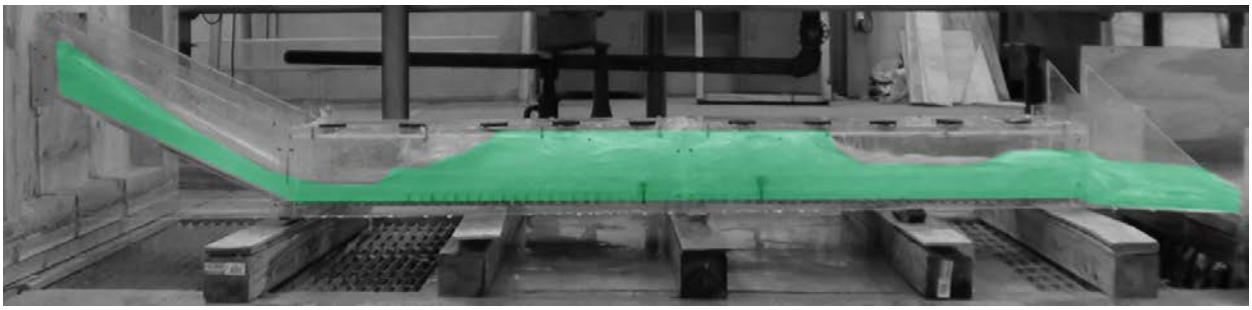

Figure A110. Experiment 37A for 0.3% slope.

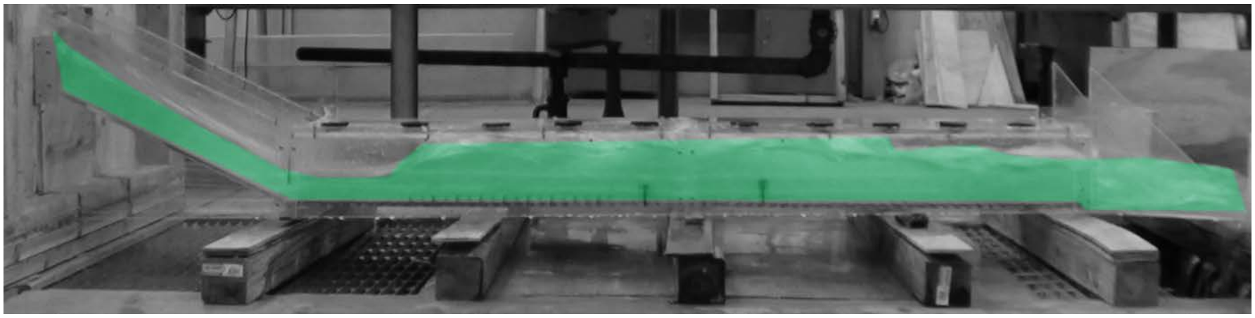

Figure A111. Experiment 37B for 0.3% slope.

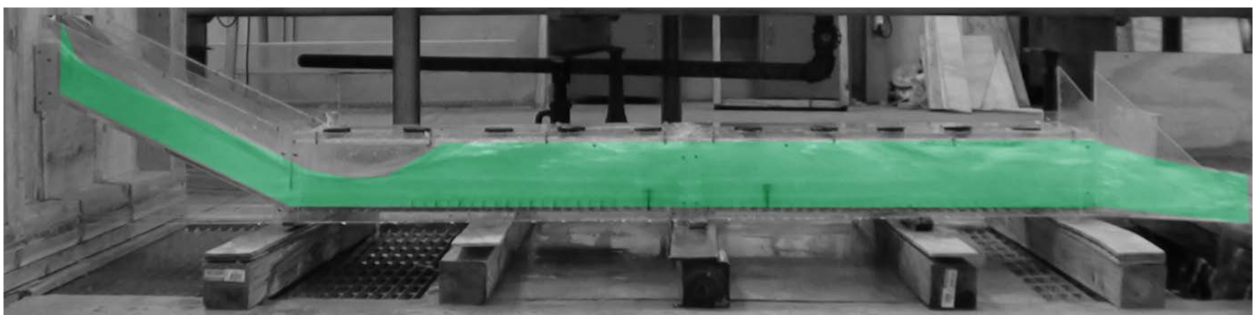

Figure A112. Experiment 37C for 0.3% slope.

Table A37. Experiment 37 for 0.3% slope using Pressure Flow Condition with 45 flat faced friction blocks and a 1.5''sill at 37'' from the end and a 2'' sill at 27'' from the end.

0.8d	0.8d	0.8d	0.8d	0.8d	0.8d	0.8d	0.8d	0.8d	0.8d	0.8d	0.8d	0.8d	0.8d	0.8d	0.8d	0.8d	0.8d	0.8d	0.8d
0.8d	0.8d	0.8d	0.8d	0.8d	0.8d	0.8d	0.8d	0.8d	0.8d	0.8d	0.8d	0.8d	0.8d	0.8d	0.8d	0.8d	0.8d	0.8d	0.8d
0.8d	0.8d	0.8d	0.8d	0.8d	0.8d	0.8d	0.8d	0.8d	0.8d	0.8d	0.8d	0.8d	0.8d	0.8d	0.8d	0.8d	0.8d	0.8d	0.8d
0.8d	0.8d	0.8d	0.8d	0.8d	0.8d	0.8d	0.8d	0.8d	0.8d	0.8d	0.8d	0.8d	0.8d	0.8d	0.8d	0.8d	0.8d	0.8d	0.8d

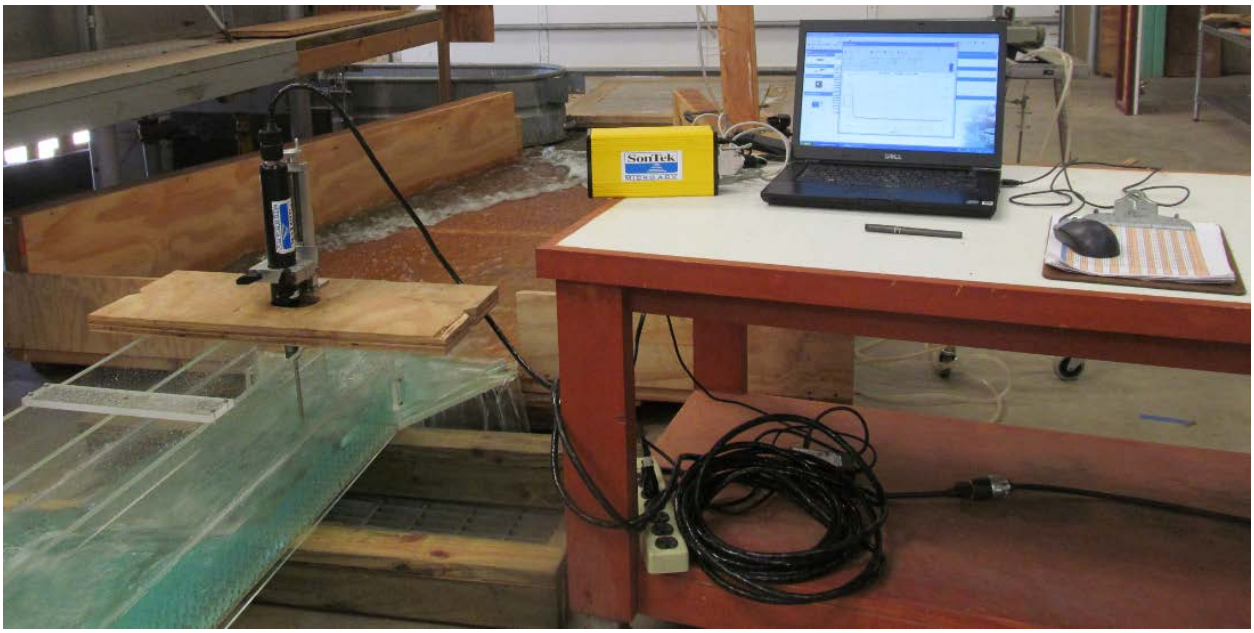

Figure A113. ADV plugged to measure the downstream velocity $V_{d/s}$

Figure A114. ADV instrument.

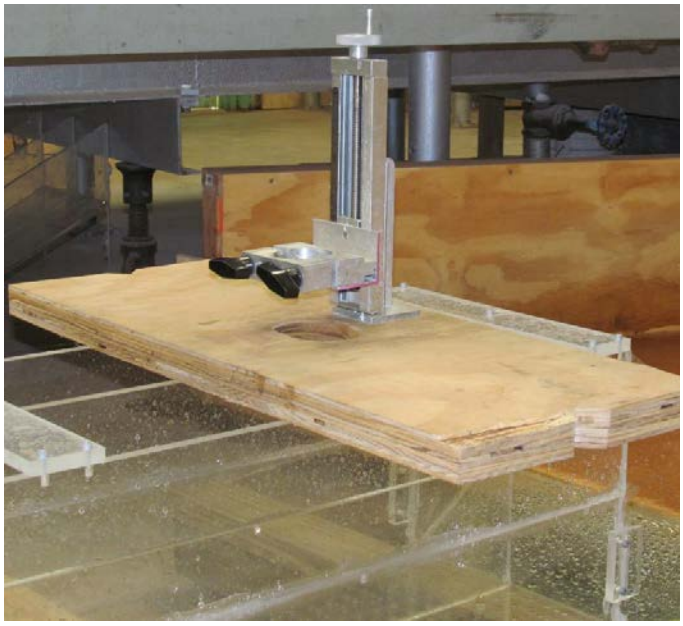

Figure A115. ADV Mount over Flume

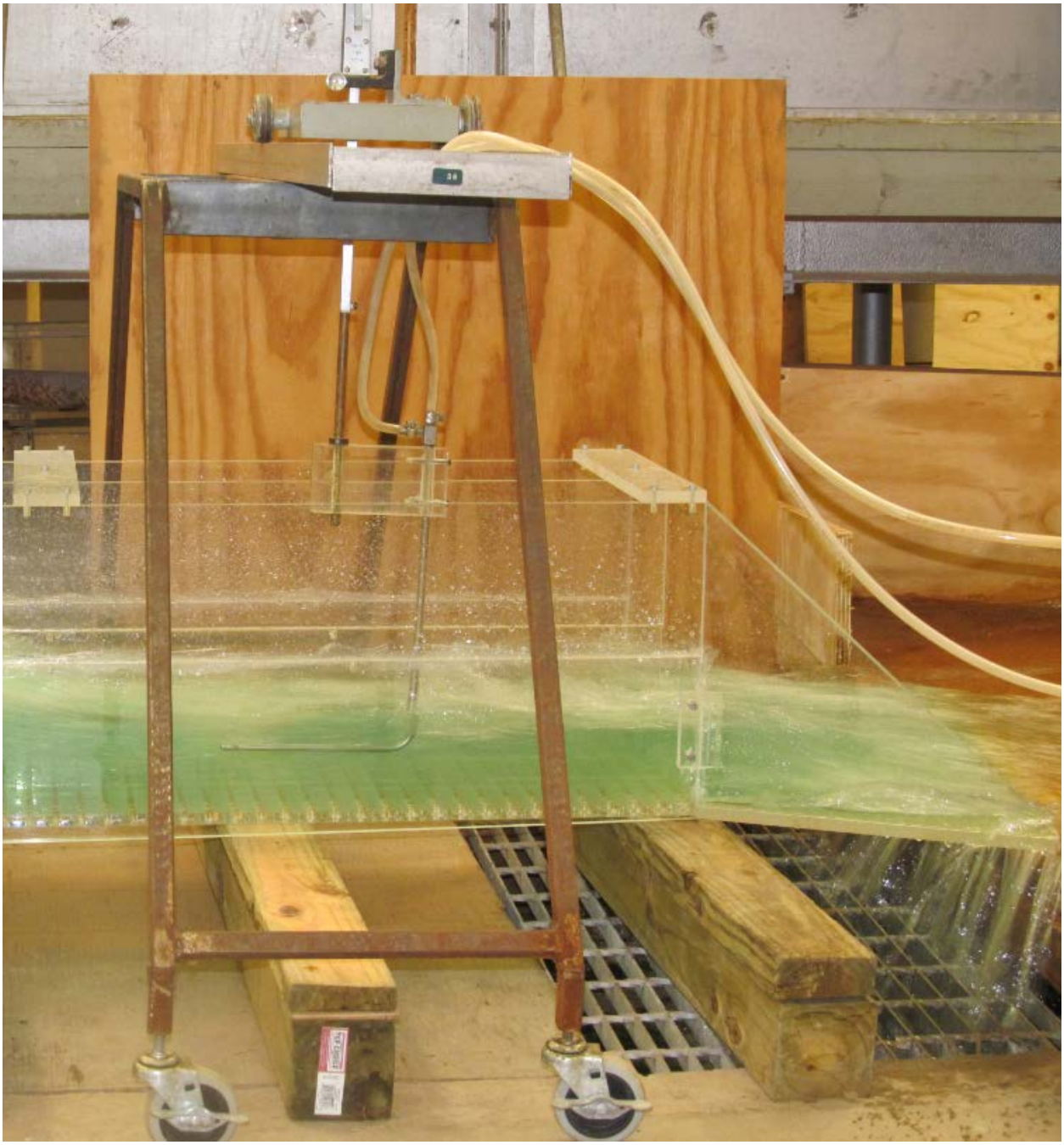

Figure A116. Pitot Tube plugged in culverts downstream to $V_{d/s}$

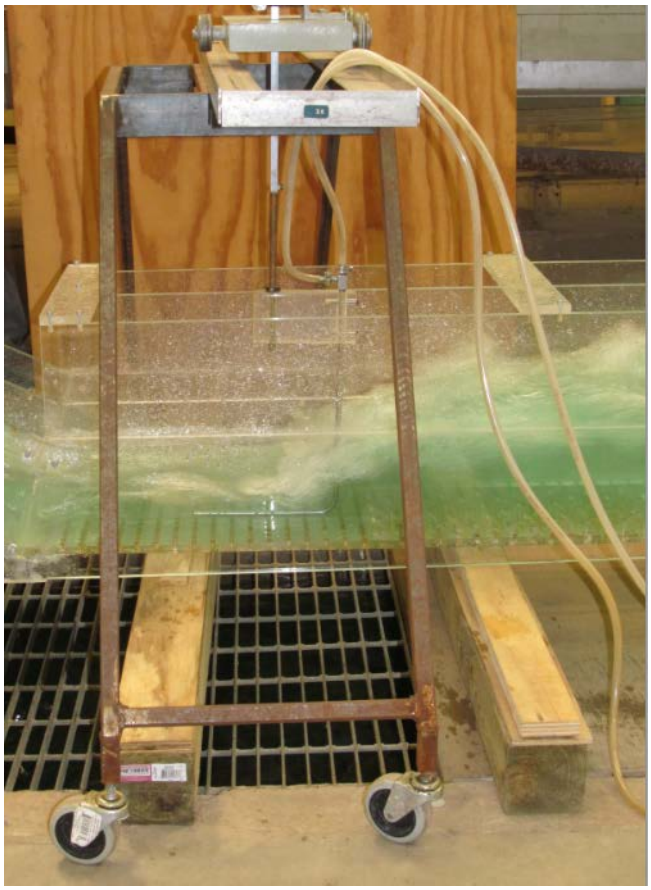

Figure A117. Pitot Tube plugged in culverts upstream to $V_{u/s}$

Figure A118. Pitot Tube.